Supporting Information

Controlling Alkyne Dimerization and Trimerization with Ruthenium(II) Arene Isocyanide Catalysts

Hugo M. Lapa,[a, b, c] Mattia del Rosso,[d] Stefano Zacchini,[e] Greta Giarola,[d,#] Elisabete C.B.A. Alegria,[a,c] Anna M. Trzeciak,[f] Fabio Marchetti,[d] Luísa M.D.R.S. Martins,[a,b,*] Lorenzo Biancalana [d,*]

[a] *Centro de Química Estrutural, Institute of Molecular Sciences, Instituto Superior Técnico, Universidade de Lisboa, Av. Rovisco Pais 1, 1049-001 Lisboa, Portugal*

[b] *Chemical Engineering Department of Instituto Superior Técnico, Universidade de Lisboa, Av. Rovisco Pais, 1049-001 Lisboa, Portugal*

[c] *Chemical Engineering Department of Instituto Superior de Engenharia de Lisboa Instituto Politécnico de Lisboa, R. Conselheiro Emídio Navarro 1, 1959-007 Lisboa, Portugal*

[d] *Università di Pisa, Dipartimento di Chimica e Chimica Industriale, Via Giuseppe Moruzzi 13, I-56124 Pisa, Italy.*

[e] *Università di Bologna, Dipartimento di Chimica Industriale "Toso Montanari", Via Piero Gobetti 85, 40129 Bologna, Italy*

[e] *Faculty of Chemistry, University of Wrocław, 14 F. Joliot-Curie, 50-383 Wroclaw, Poland*

[#] *Current address: Department of Energy Conversion and Storage, Technical University of Denmark, Fysikvej, 2800, Kgs. Lyngby, Denmark*

Table of contents	**Page(s)**
Synthesis and characterization of $[RuCl_2(L)(\eta^6\text{-}C_6H_6)]$ (L = Py, SMe_2), $[RuCl_2(CO)(\eta^6\text{-arene})]$ (arene = *p*-cymene, C_6Me_6) and $[RuCl(OAc)(\eta^6\text{-p-cymene})]$ (**Charts S1-S5**)	S3-S7
IR, NMR and X-ray characterization of Ru arene bis-halide isocyanide complexes (**Figures S1-S56, Tables S1-S2**)	S8-S36
IR, NMR and X-ray characterization of acetylide-isocyanide and acetonitrile-isocyanide complexes (**Figures S57-S74, Table S3**)	S37-S46
Catalytic studies (**Figure S75**)	S47-S48
Reactivity with phenylacetylene and Na_2CO_3 in catalytically relevant conditions (**Figures S76-S92, Tables S4-S11**)	S49-S59
References	S60-S61

Synthesis and characterization of $[RuCl_2(L)(\eta^6\text{-}C_6H_6)]$ (L = Py, SMe_2), $[RuCl_2(CO)(\eta^6\text{-arene})]$ (arene = *p*-cymene, C_6Me_6) and $[RuCl(OAc)(\eta^6\text{-}p\text{-cymene})]$

$[RuCl_2(Py)(\eta^6\text{-}C_6H_6)]$ (Chart S1).

Chart S1. Structure of $[RuCl_2(Py)(\eta^6\text{-}C_6H_6)]$.

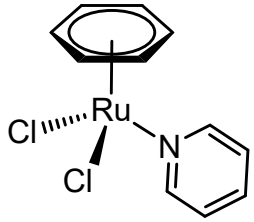

The title compound was previously prepared from $[RuCl_2(\eta^6\text{-}C_6H_6)]_2$ in neat pyridine and was isolated in 65 % yield after "*several days*" at room temperature.[1] An alternative preparation involves the reaction of $Cs[RuCl_3(\eta^6\text{-}C_6H_6)]$ with pyridine (*ca*. 50 eq.) in methanol at room temperature (86 % yield).[2] Herein we describe a more convenient and higher-yielding synthetic procedure.

In a 50 mL Schlenk flask, a brick-red suspension of $[RuCl_2(\eta^6\text{-}C_6H_6)]_2$ (316 mg, 1.26 mmol Ru) in THF (10 mL) was treated with pyridine (0.30 mL, 3.7 mmol). After 2 h under reflux, an orange solid and a pale-yellow solution were obtained. The suspension was filtered (G4) and the resulting solid was washed with acetone and dried under vacuum (40 °C). Yield: 384 mg, 92 %. Soluble in DMSO, poorly soluble in DMF, insoluble in THF, acetone, MeOH, CH_2Cl_2. IR (solid state): $\tilde{\upsilon}/cm^{-1}$ = 3070w-sh, 3055m, 3037w-sh, 2999w, 1061m, 1505w, 1476w, 1445s-sh, 1434s, 1357w, 1232w, 1216m, 1154w, 1142w, 106m, 1044w, 1008w, 978w, 966w, 936w, 835m-sh, 830s, 770m-sh, 760s, 702m-sh, 690s.

$[RuCl_2(SMe_2)(\eta^6\text{-}C_6H_6)]$ (Chart S2).

Chart S2. Structure of $[RuCl_2(SMe_2)(\eta^6\text{-}C_6H_6)]$.

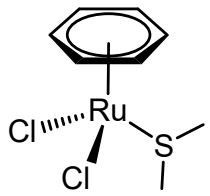

An optimized version of the literature preparation is described below.[3] In a 100 mL Schlenk flask, a brick-red suspension of $[RuCl_2(\eta^6\text{-}C_6H_6)]_2$ (628 mg, 2.51 mmol Ru) in anhydrous CH_2Cl_2 (15 mL) was treated with dimethyl sulfide (0.65 mL, 8.8 mmol) and stirred at room temperature overnight. The resulting suspension (orange-red solution + solid) was allowed to settle. The saturated solution was filtered over a celite pad (h 2 cm). The solid was repeatedly stirred with fresh aliquots of CH_2Cl_2 (tot. *ca*. 150 mL) until all the orange product was collected in the filtrate and thus separated from a minor amount of a brown, insoluble residue. The filtrate solution was taken to dryness under vacuum (room temperature) and the residue was triturated in petroleum ether. The suspension was filtered and the resulting brown-red, microcrystalline solid was washed with petroleum ether, dried under vacuum (room temperature) and stored under N_2. Yield: 714 mg, 93 %. Moderately soluble in CH_2Cl_2, poorly soluble in $CHCl_3$, insoluble in Et_2O and hexane. Anal. calcd. for $C_8H_{12}Cl_2RuS$: C, 30.78; H, 3.87; S, 10.27. Found: C, 30.34; H, 3.87; S; 10.16. IR (solid state): $\tilde{\upsilon}/cm^{-1}$ = 3061w, 1433m-sh, 1248m, 1411w-sh, 1325w, 1156w, 1148w, 1135w, 1034w, 1028w, 1006w, 994m, 986m, 968w, 957w, 913w, 907w, 844m-sh, 835s. ^1H NMR ($CDCl_3$) δ/ppm = 5.71 (s, 6H, C_6H_6), 2.32 (s, 6H, SMe_2). $^{13}C\{^1H\}$ NMR ($CDCl_3$): δ/ppm = 85.5 (C_6H_6), 23.0 (SMe_2). Compound $[RuCl_2(SMe_2)(\eta^6\text{-}C_6H_6)]$ is stable in the solid state for several months but much less so in solution of organic solvents. Traces of free C_6H_6 (δ_H = 7.36 ppm) and SMe_2 (δ_H = 2.12 ppm) are already present in the ^1H NMR spectrum of the freshly-prepared solution.

[$RuCl_2(CO)(\eta^6$-*p*-cymene)] (Chart S3).

Chart S3. Structure of [$RuCl_2(CO)(\eta^6$-*p*-cymene)].

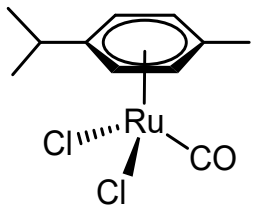

The title compound was previously prepared from $[RuCl_2(\eta^6$-*p*-cymene)$]_2$ in hot hexane (50°C) under 10 atm of carbon monoxide (56 % yield)[4] on in CH_2Cl_2 at room temperature by bubbling CO at ambient pressure (60-70 % yield).[5] An improved version of this latter method is described below.

In a 25 mL round bottom flask, a brick-red solution of $[RuCl_2(\eta^6$-*p*-cymene)$]_2$ (111 mg, 0.363 mmol Ru) in anhydrous CH_2Cl_2 (8 mL) was placed under 1 atm of carbon monoxide via a T-junction connected to a 2 L gas balloon. The mixture was stirred for 30' at room temperature, affording a dark blood-red solution. Argon was flushed into the system and the conversion was checked by IR (CH_2Cl_2). Next, volatiles were removed under vacuum. The residue was dissolved in CH_2Cl_2 and filtered over celite. The filtrate solution was taken to dryness under vacuum, affording a raspberry red solid. The solid was washed with hexane, dried under vacuum (room temperature) and stored under N_2 at 4 °C. Yield: 110 mg, 92 %. Soluble in CH_2Cl_2, insoluble in Et_2O and hexane. IR (solid state): $\tilde{\upsilon}/cm^{-1}$ = 3036w, 2973w, 2956w, 2016s (CO), 1977w-sh, 1504w, 1473w, 1463w, 1447w, 1392w, 1323w, 1281w, 1202w, 1167w, 1113w, 1096w, 1056w, 1037w, 849m, 797w, 737w, 683w. IR (CH_2Cl_2): $\tilde{\upsilon}/cm^{-1}$ = 2052 (CO). ^{1}H NMR ($CDCl_3$): δ/ppm = 5.96 (d, $^3J_{HH}$ = 6.3 Hz, 2H), 5.80 (d, $^3J_{HH}$ = 6.2 Hz, 2H) (C_6H_4); 2.89 (hept, $^3J_{HH}$ = 6.8 Hz, 1H, $\underline{CH}Me_2$); 2.37 (s, 3H C$\underline{Me}$); 1.33 (d, $^3J_{HH}$ = 6.9 Hz, 6H. CH$\underline{Me_2}$).

The reaction time is crucial: after 1 h under a CO atmosphere the blood-red solution becomes turbid and after 2.5 h an abundant brown precipitate is present. The formation of soluble carbonyl by-products was assessed by IR ($\tilde{\upsilon}/cm^{-1}$ = 1986, 1957).

$[RuCl_2(CO)(\eta^6\text{-}C_6Me_6)]$ (Chart S4).

Chart S4. Structure of $[RuCl_2(CO)(\eta^6\text{-}C_6Me_6)]$.

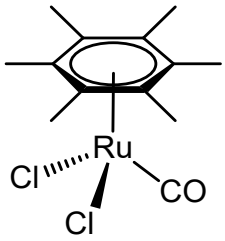

The title compound was previously prepared from $[RuCl_2(\eta^6\text{-}C_6Me_6)]_2$ in CH_2Cl_2 at room temperature by bubbling CO at ambient pressure (60-70 % yield).[5,6] An improved version of this latter method is described below.

In a 25 mL round bottom flask, an orange suspension of $[RuCl_2(\eta^6\text{-}C_6Me_6)]_2$ (99 mg, 0.296 mmol Ru) in anhydrous CH_2Cl_2 (6 mL) was placed under 1 atm of carbon monoxide via a T-junction connected to a 2 L gas balloon. The mixture was stirred for 2 h at room temperature, affording a dark blood-red solution. Argon was flushed into the system and the conversion was checked by IR (CH_2Cl_2). Next, volatiles were removed under vacuum. The residue was dissolved in CH_2Cl_2 and filtered over celite to remove a dark brown solid. The filtrate solution was taken to dryness under vacuum and the residue was triturated in a Et_2O/hexane 1:1 *V*/*V* solution. The suspension was filtered and the resulting red-purple solid was washed with hexane, dried under vacuum and stored under N_2. Yield: 95 mg, 93 %. Moderately soluble in CH_2Cl_2, poorly soluble in acetone, $CHCl_3$, MeOH, insoluble in Et_2O and hexane. IR (solid state): $\tilde{\upsilon}/cm^{-1}$ = 2922w, 1986s (CO), 1536w, 1506w, 1435m, 1377m, 1277w, 1263w, 1069m, 1021w-sh, 1003m, 786w, 738w. IR (CH_2Cl_2): $\tilde{\upsilon}/cm^{-1}$ = 2026 (CO). ^1H NMR (acetone-d_6) δ/ppm = 2.19 (s).

[RuCl(OAc)(η^6-*p*-cymene)] (Chart S5).

Chart S5. Structure of [RuCl(OAc)(η^6-*p*-cymene)].

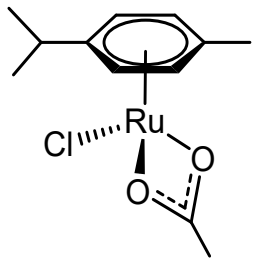

Despite being mentioned various times in the literature, a convenient and high-yielding synthetic procedure has not been reported for the title compound.[7]

In a round-bottom flask, a mixture of $[RuCl_2(\eta^6\text{-}p\text{-cymene})]_2$ (150 mg, 0.49 mmol Ru) and sodium acetate trihydrate (67 mg, 0.49 mmol) in ^{i}PrOH (20 mL) was stirred at room temperature for 5 h. The resulting suspension was filtered over a celite pad and the filtrate was taken to dryness under vacuum. The residue was dissolved in CH_2Cl_2 and filtered again through celite to completely remove sodium salts. Volatiles were removed under vacuum, affording an orange solid. Yield: 129 mg, 80 %. IR (solid state): $\tilde{\upsilon}$/cm^{-1} = 3071w, 2961w, 2929w, 2878w; 1514m ($\nu_{asym,CO2}$); 1469s, 1417m ($\nu_{sym,CO2}$); 1386m, 1373m-sh, 1324w, 1298w, 1275w, 1262w, 1202w, 1162w, 1140w, 1117w, 1089w, 1055w, 1005w, 948w, 903w, 889w, 807w, 679s. ^{1}H NMR (acetone-d_6): δ/ppm = 5.75 (d, $^3J_{HH}$ = 6.1 Hz, 2H), 5.49 (d, $^3J_{HH}$ = 6.1 Hz, 2H) (C_6H_4); 2.88* (hept, $^3J_{HH}$ = 6.9 Hz, C<u>H</u>Me$_2$); 2.23 (s, 3H, C<u>Me</u>^{Cym}), 1.62 (s, 3H, O_2CMe); 1.36 (d, $^3J_{HH}$ = 6.1 Hz, 6H, CH<u>Me$_2$</u>); *over H_2O peak. ^{1}H NMR ($CDCl_3$): δ/ppm = 5.63 (d, $^3J_{HH}$ = 6.1 Hz, 2H), 5.41 (d, $^3J_{HH}$ = 6.0 Hz, 2H) (C_6H_4); 2.93 (hept, $^3J_{HH}$ = 7.0 Hz, C<u>H</u>Me$_2$), 2.31 (s, 3H, C<u>Me</u>^{Cym}), 1.82 (s, 3H, O_2CMe), 1.38 (d, $^3J_{HH}$ = 6.9 Hz, CH<u>Me$_2$</u>).

Figure S1. Solid-state IR spectra (650-4000 cm^{-1}) of pure [$RuCl_2$(CNMe)(η^6-*p*-cymene)], **1a** (top, blue line) and a mixture of **1a** and *trans*-[$RuCl_2(CNMe)_4$] (bottom, red line).

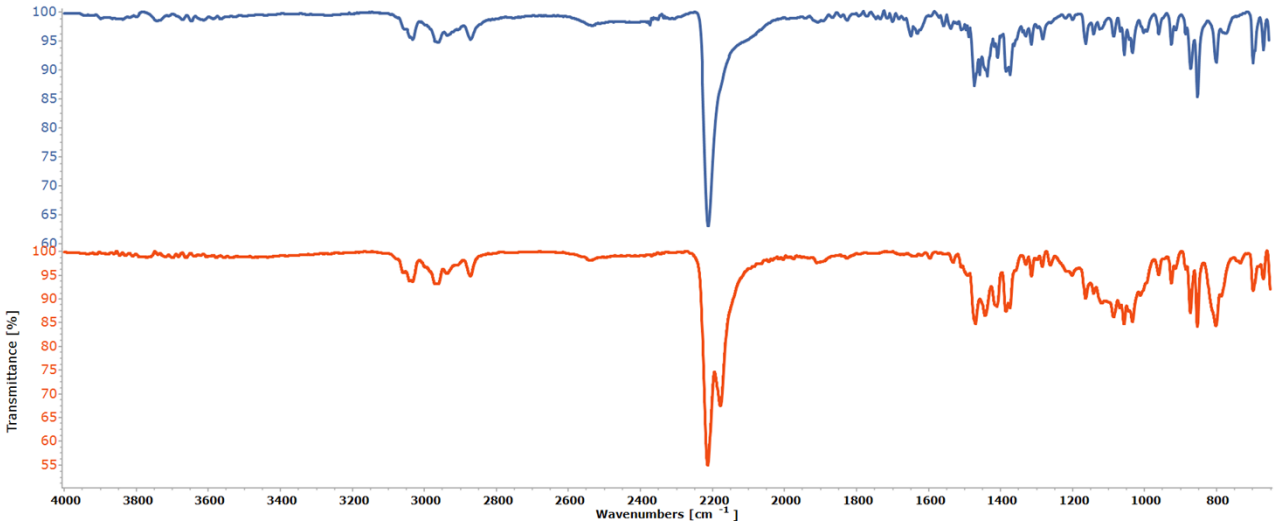

Figure S2. ^{1}H NMR spectrum (400 MHz, $CDCl_3$) of **1a**.

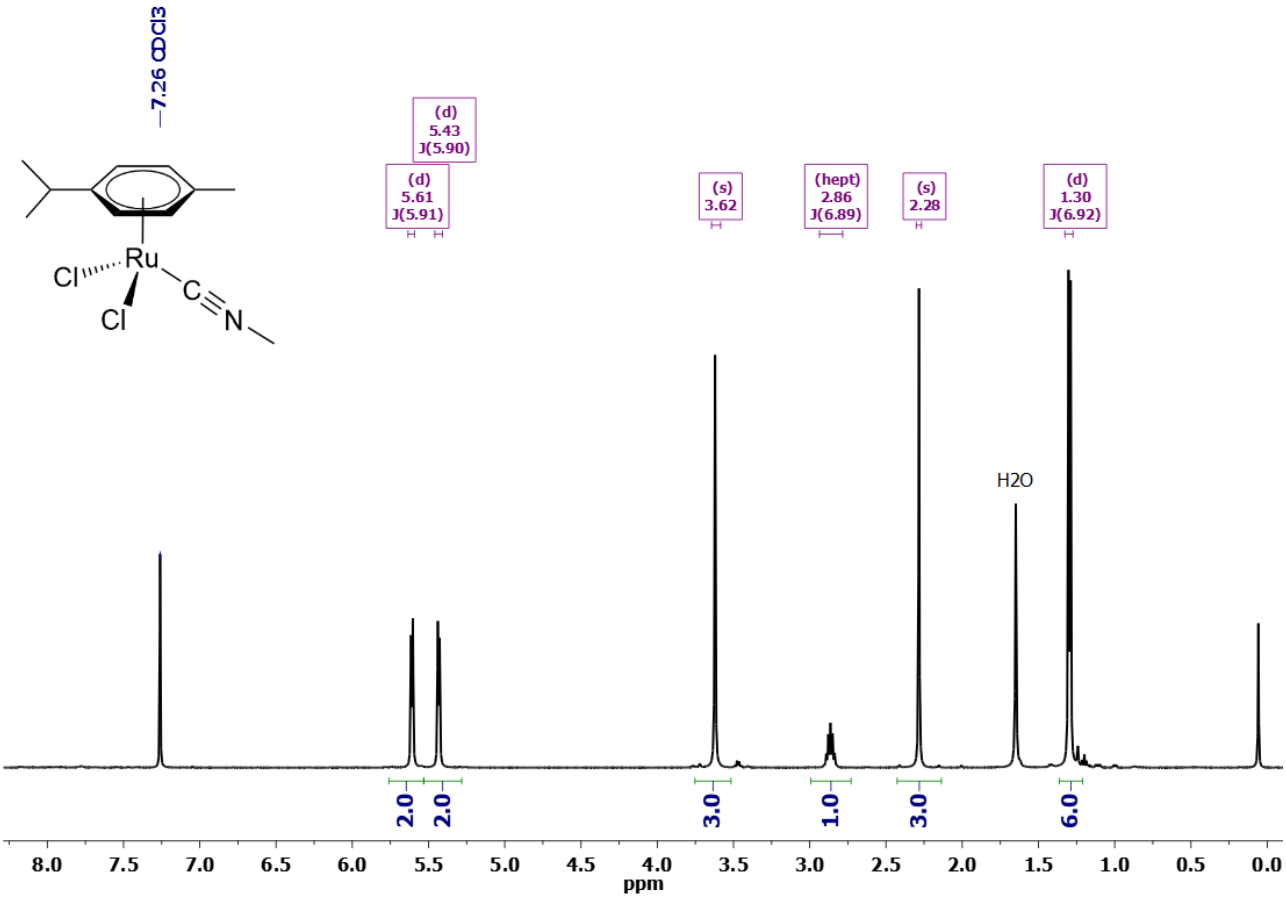

Figure S3. ^{1}H NMR spectrum (400 MHz, $CDCl_3$) of **1a** in admixture with *trans*-$[RuCl_2(CNMe)_4]$ (the related resonance is indicated by an asterisk *).

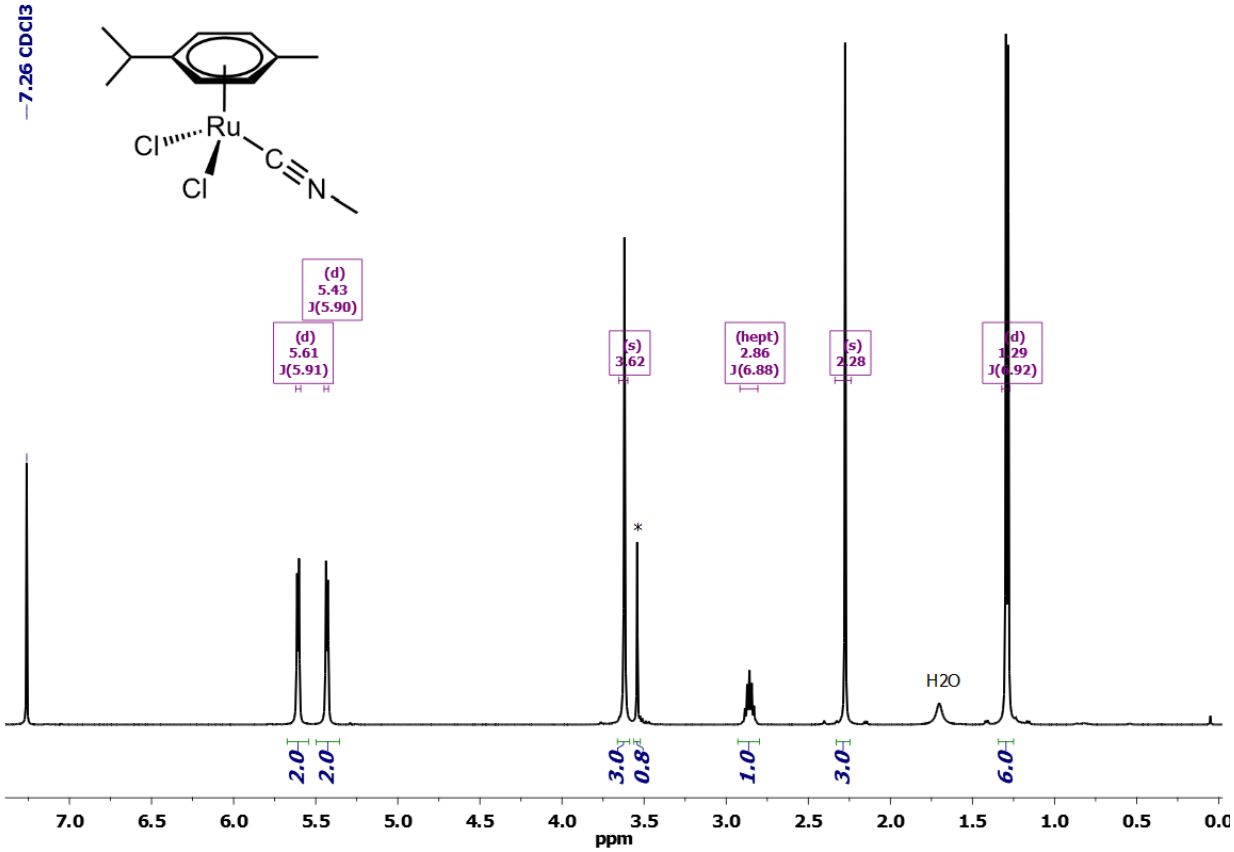

Figure S4. $^{13}C\{^{1}H\}$ NMR spectrum (100 MHz, $CDCl_3$) of **1a** in admixture with *trans*-$[RuCl_2(CNMe)_4]$ (the related methyl resonance is indicated by an asterisk *).

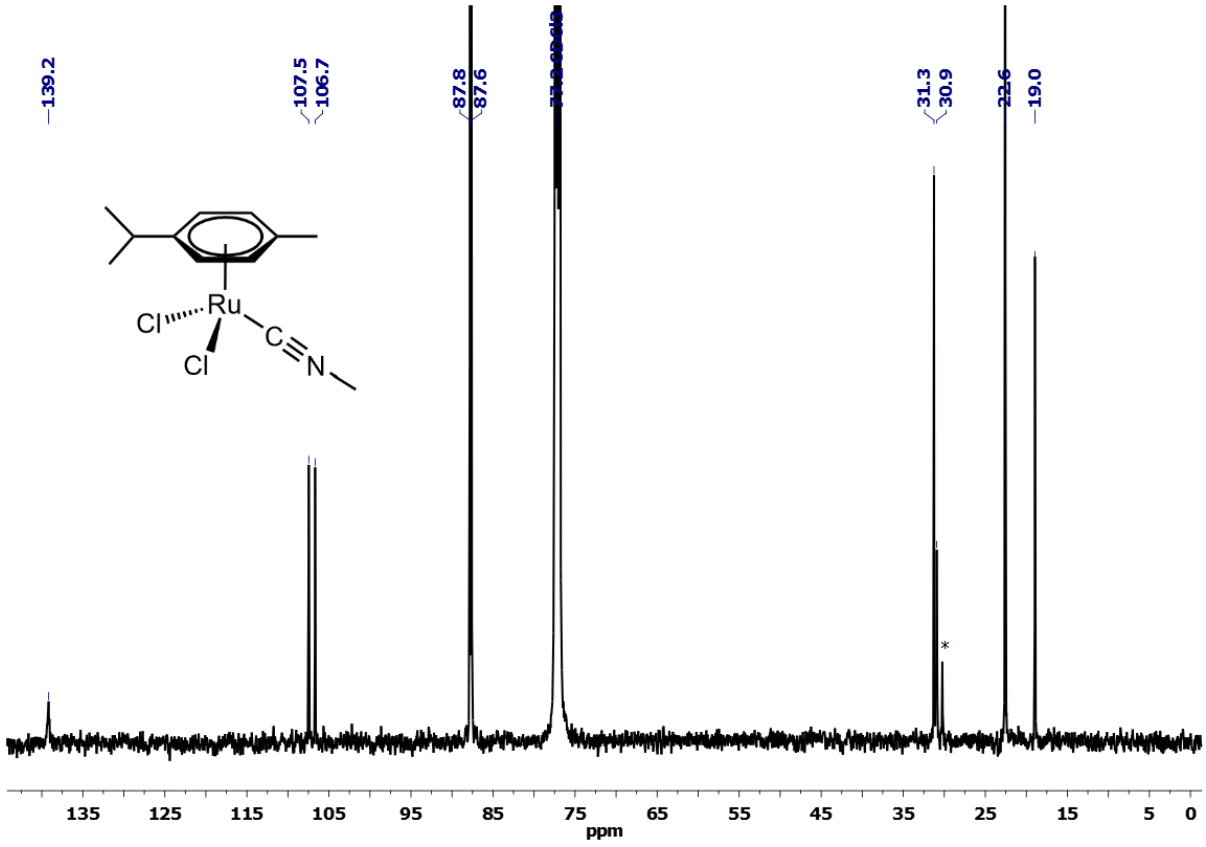

Figure S5. Solid-state IR spectrum (650-4000 cm^{-1}) of [$RuCl_2${*S*-CNCH(Me)Ph}(η^6-*p*-cymene)], **1c**.

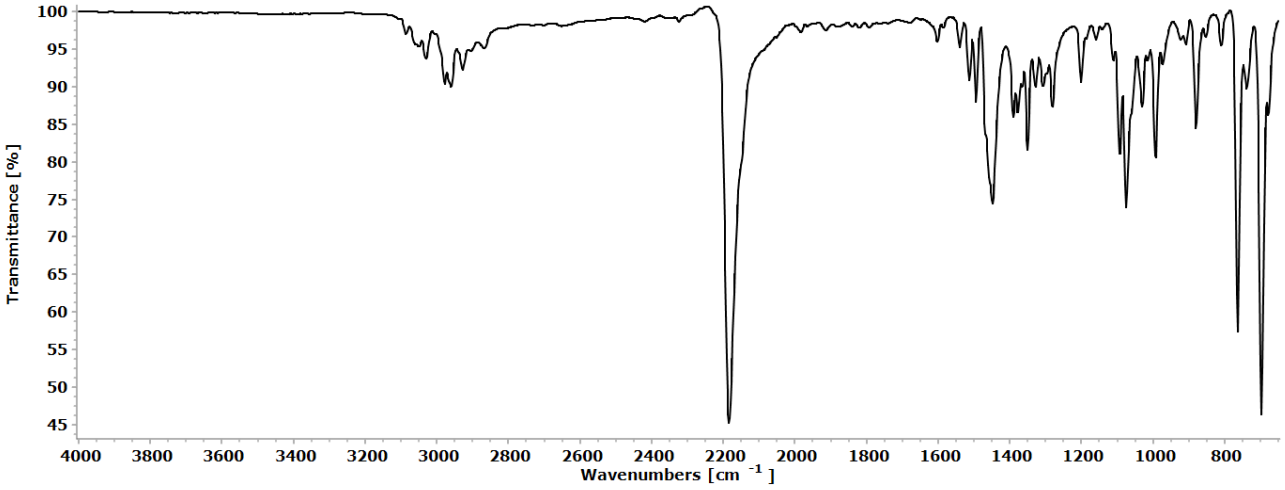

Figure S6. ^1H NMR spectrum (400 MHz, $CDCl_3$) of **1c**.

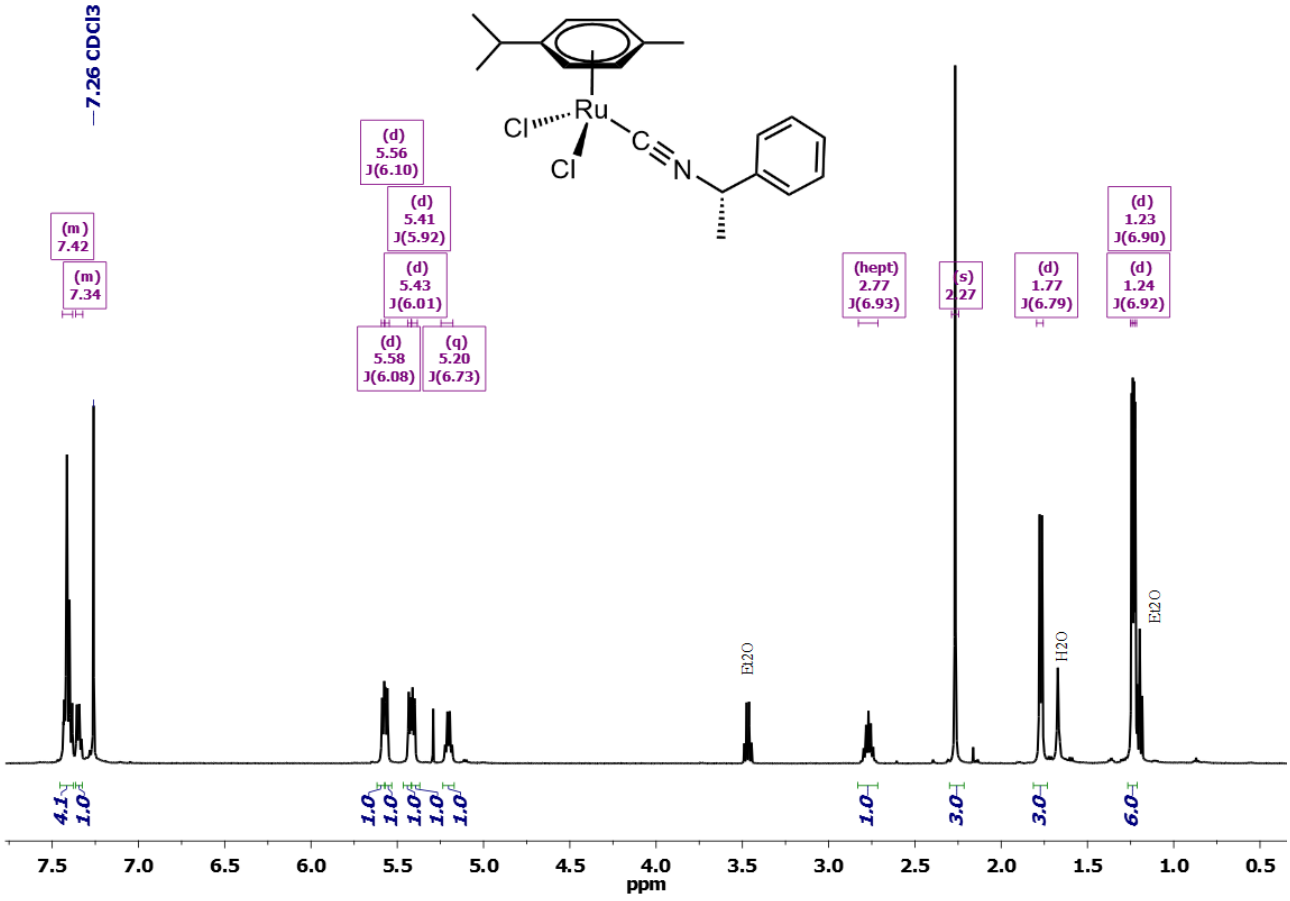

Figure S7. $^{13}C\{^{1}H\}$ NMR spectrum (100 MHz, $CDCl_3$) of **1c**.

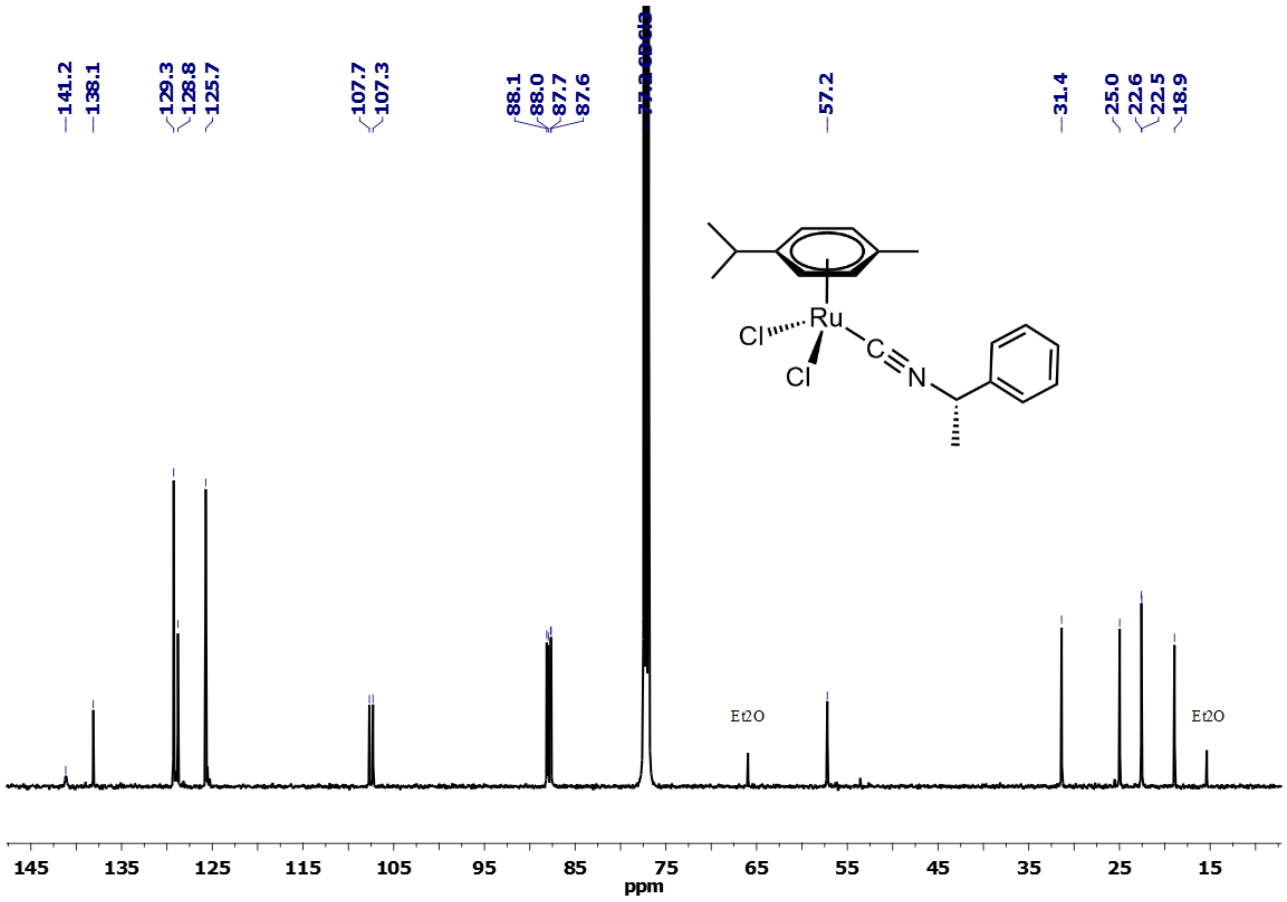

Figure S8. Solid-state IR spectrum (650-4000 cm^{-1}) of $[RuCl_2\{CNCH_2PO(OEt)_2\}(\eta^6\text{-}p\text{-cymene})]$, **1d**.

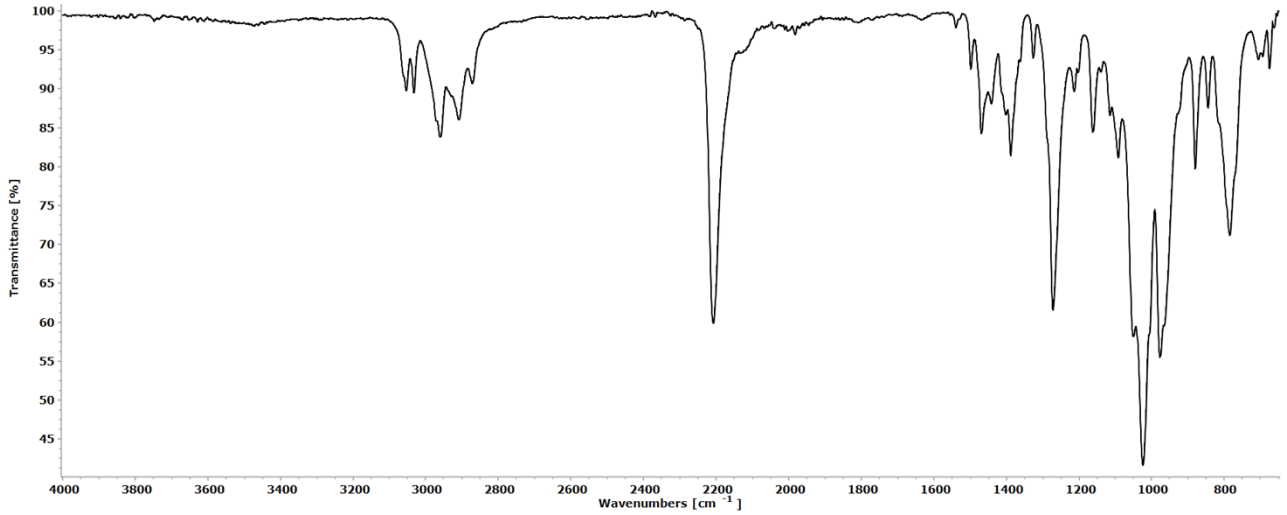

Figure S9. ^{1}H NMR spectrum (400 MHz, $CDCl_3$) of **1d**.

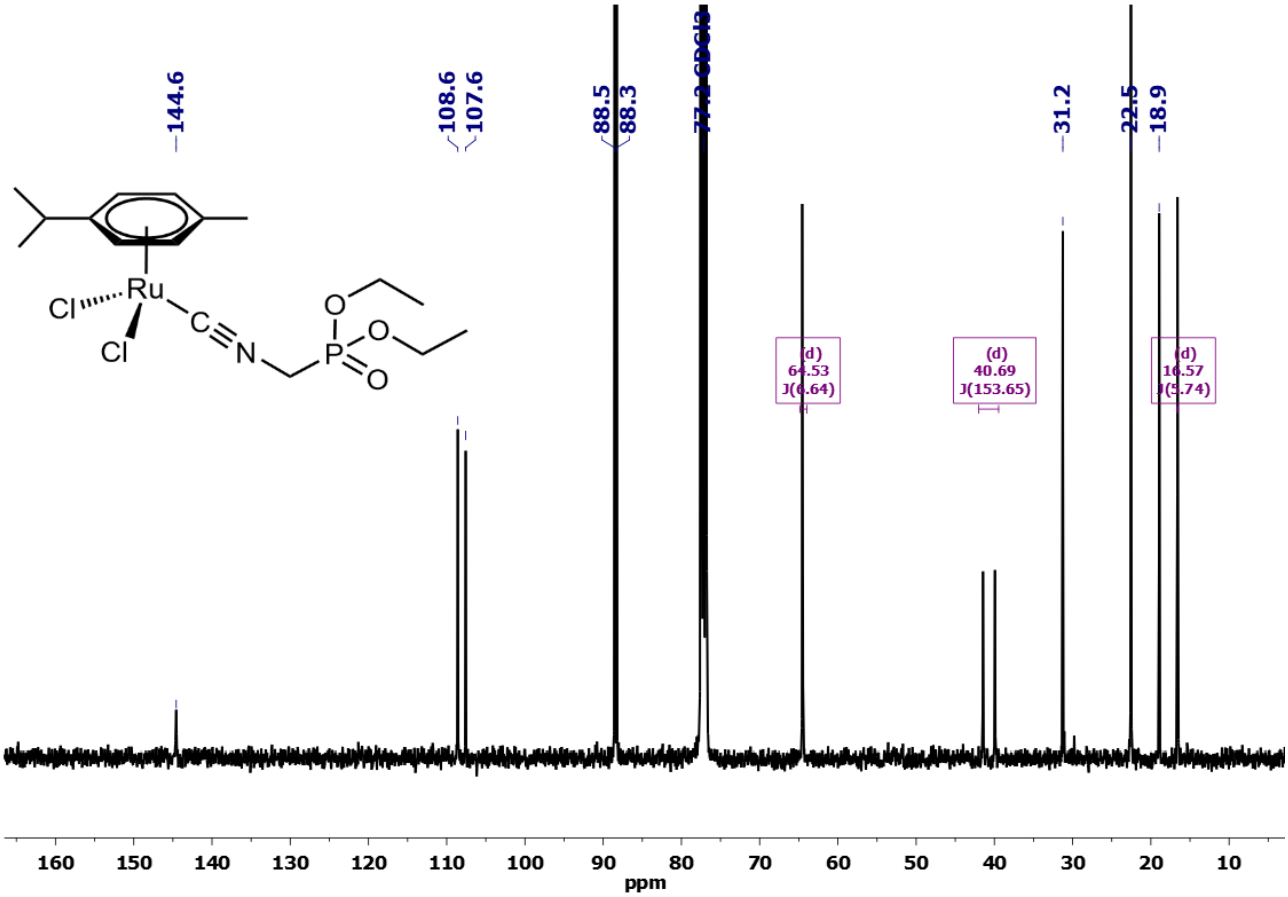

Figure S10. $^{13}C\{^{1}H\}$ NMR spectrum (100 MHz, $CDCl_3$) of **1d**.

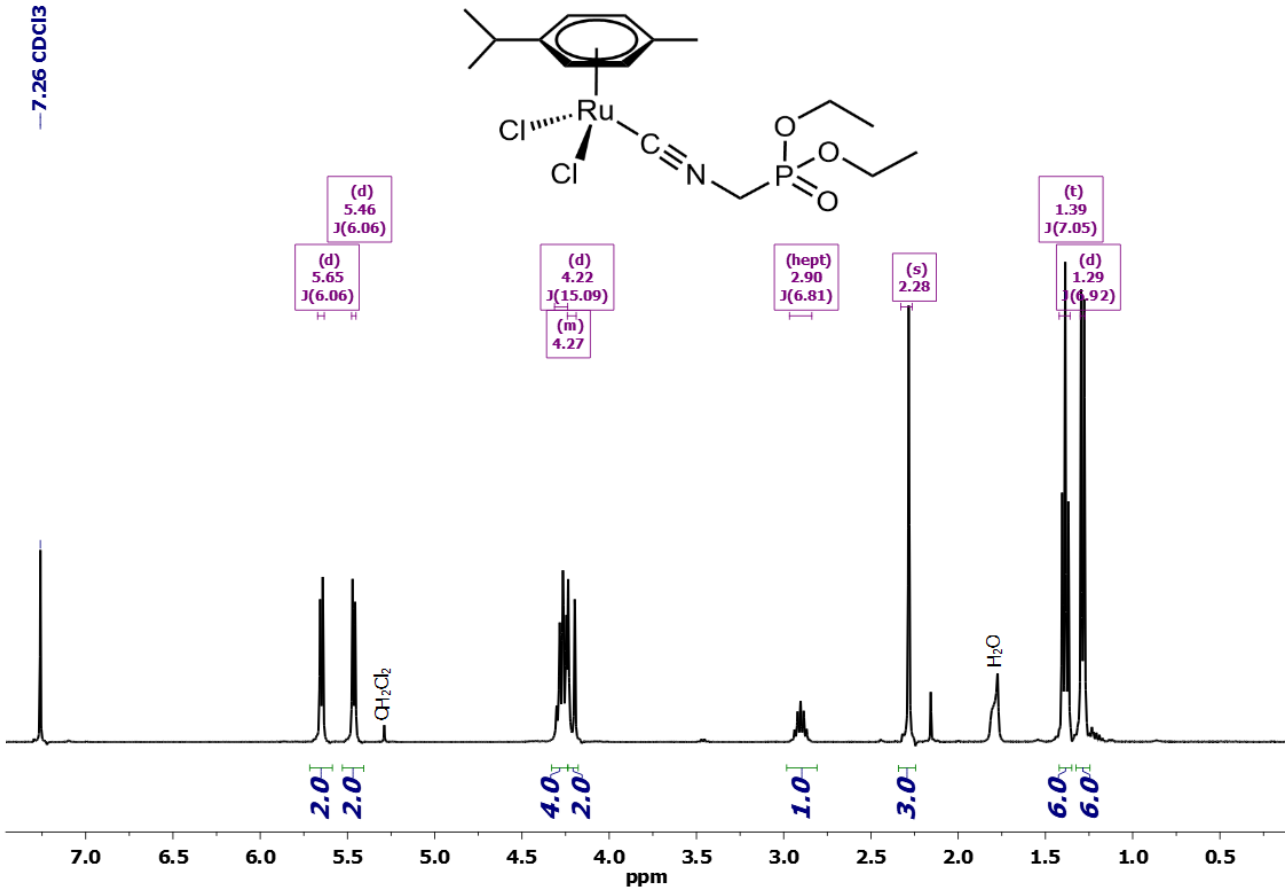

Figure S11. $^{31}P\{^{1}H\}$ NMR spectrum (162 MHz, $CDCl_3$) of **1d**.

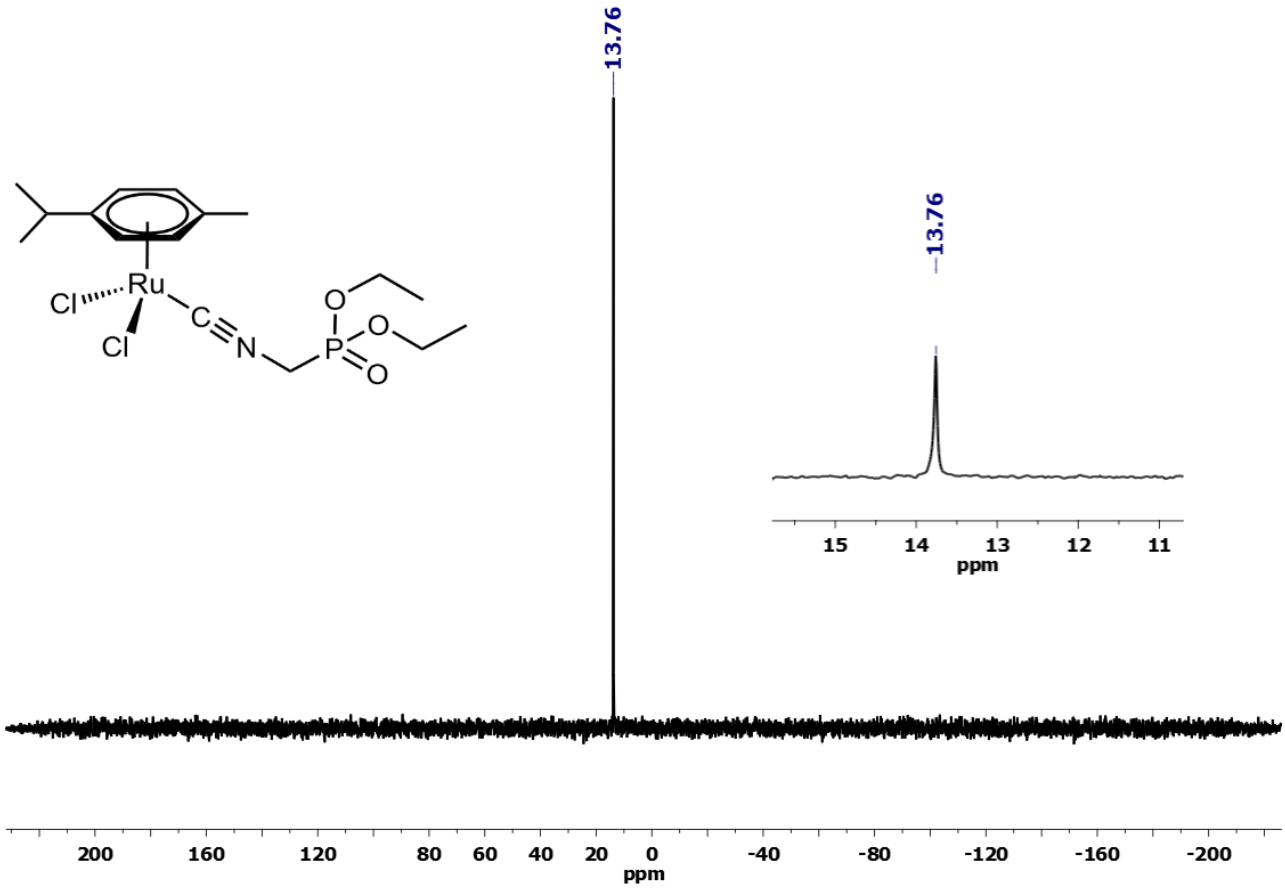

Figure S12. Solid-state IR spectrum (650-4000 cm^{-1}) of $[RuCl_2\{CNCH_2CO_2Et\}(\eta^6\text{-}p\text{-cymene})]$, **1e**.

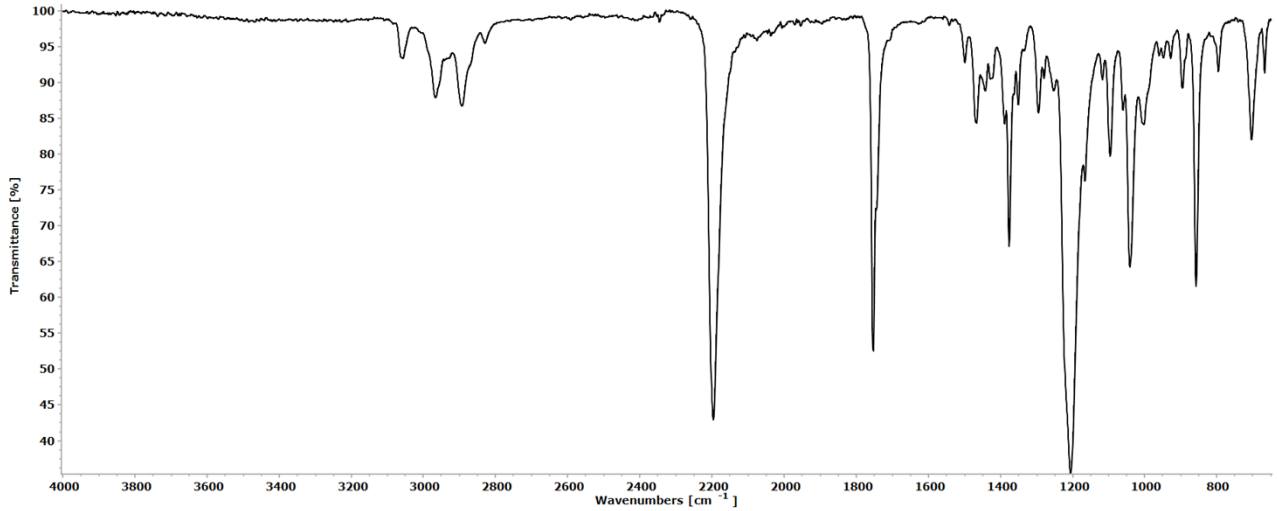

Figure S13. ^{1}H NMR spectrum (400 MHz, $CDCl_3$) of **1e.**

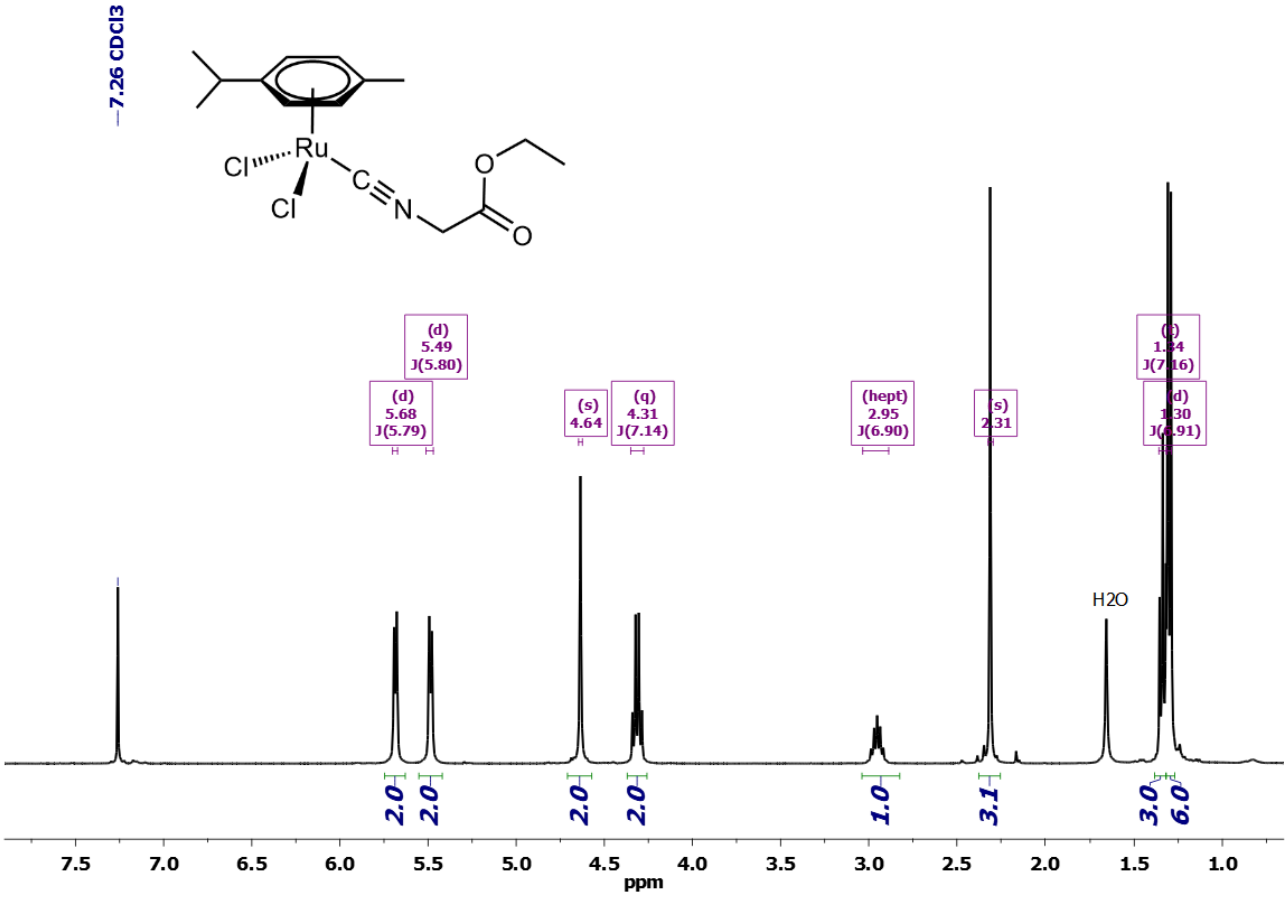

Figure S14. $^{13}C\{^{1}H\}$ NMR spectrum (100 MHz, $CDCl_3$) of **1e**.

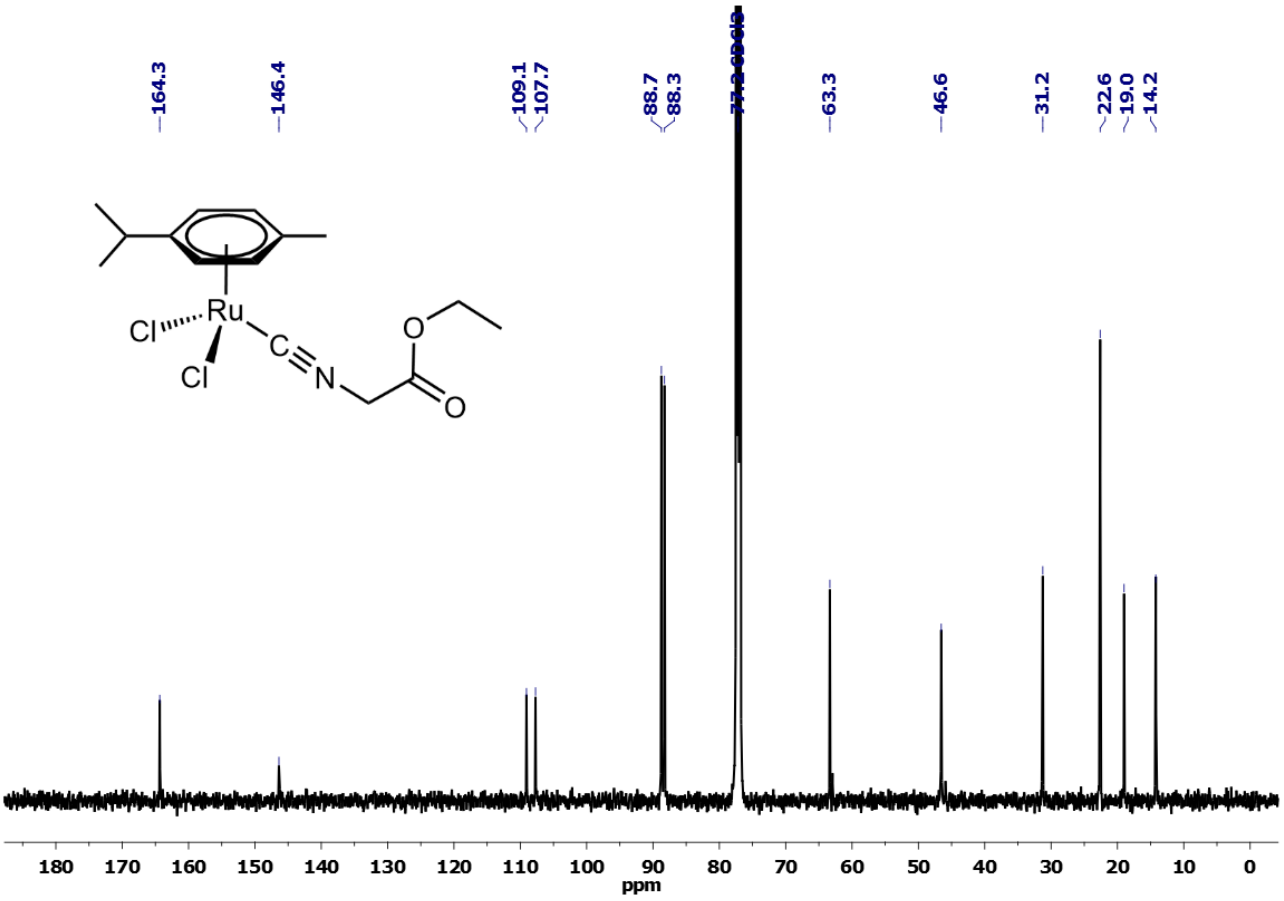

Figure S15. Solid-state IR spectrum (650-4000 cm^{-1}) of $[RuCl_2\{CN(4\text{-}C_6H_4OMe)\}(\eta^6\text{-}p\text{-cymene})]$, **1g**.

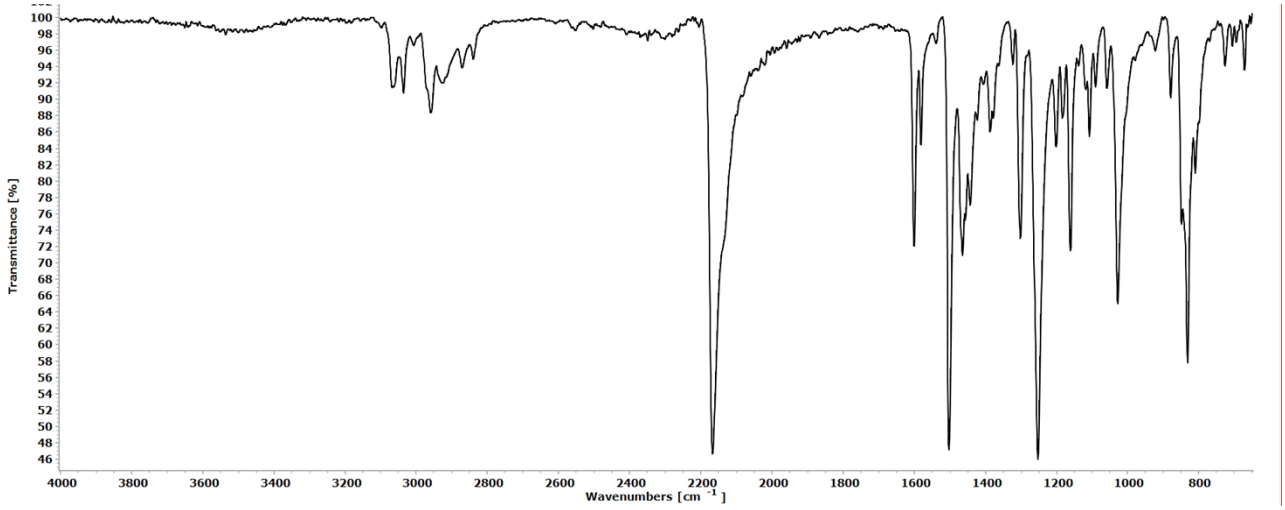

Figure S16. ^1H NMR spectrum (400 MHz, $CDCl_3$) of **1g**.

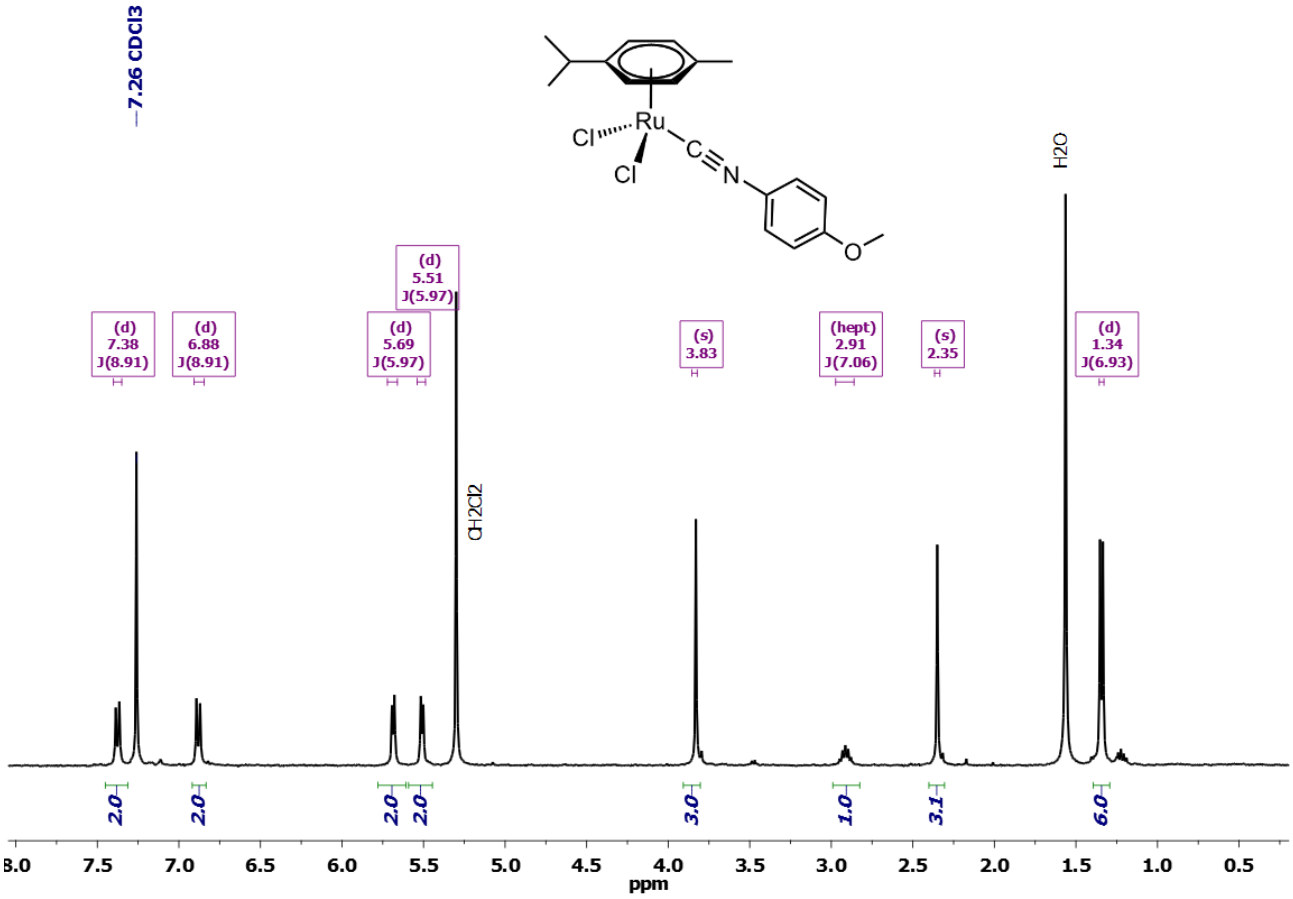

Figure S17. $^{13}C\{^{1}H\}$ NMR spectrum (100 MHz, $CDCl_3$) of **1g**.

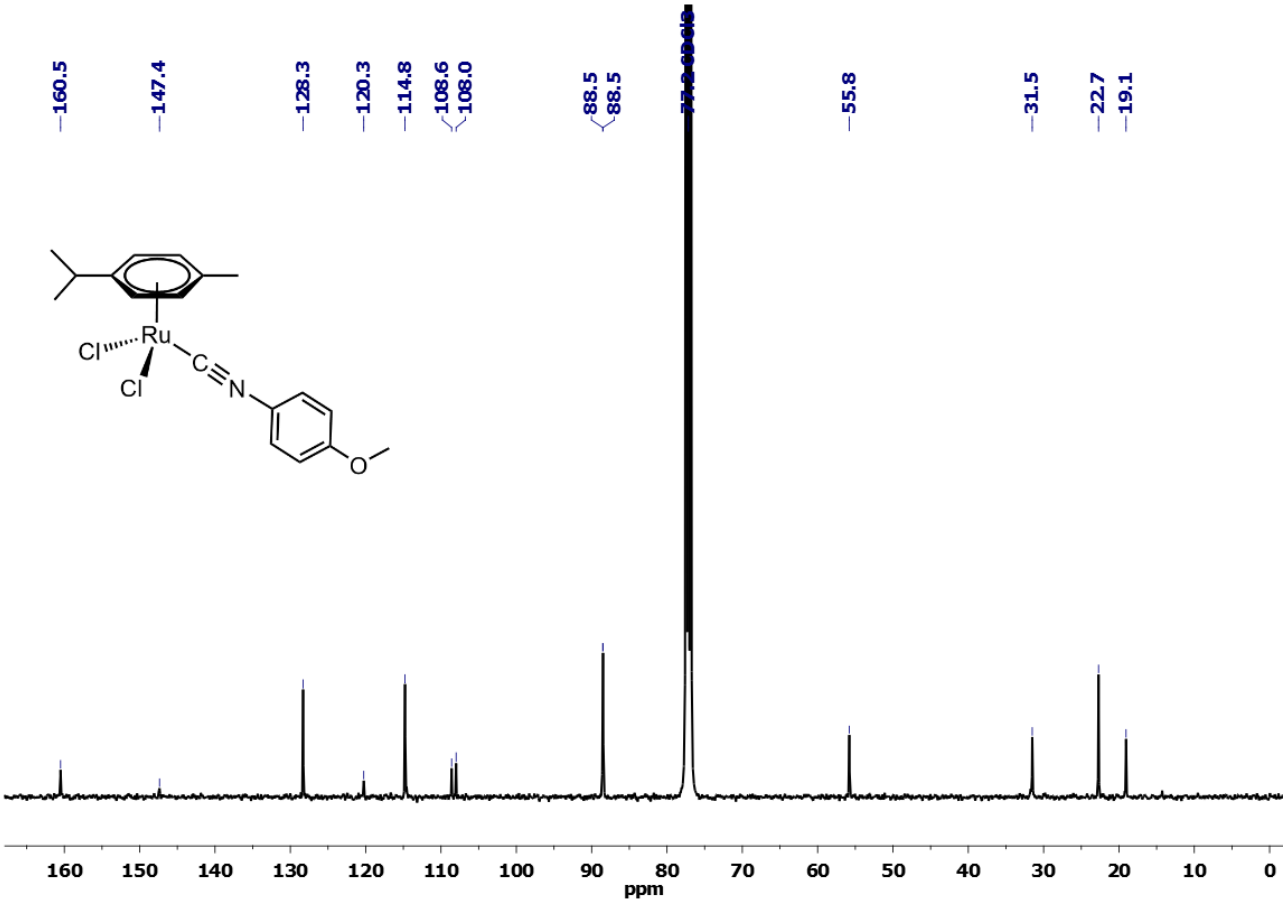

Figure S18. Solid-state IR spectrum (650-4000 cm^{-1}) of $[RuCl_2(CNMe)(\eta^6\text{-}C_6Me_6)]$, **2a.**

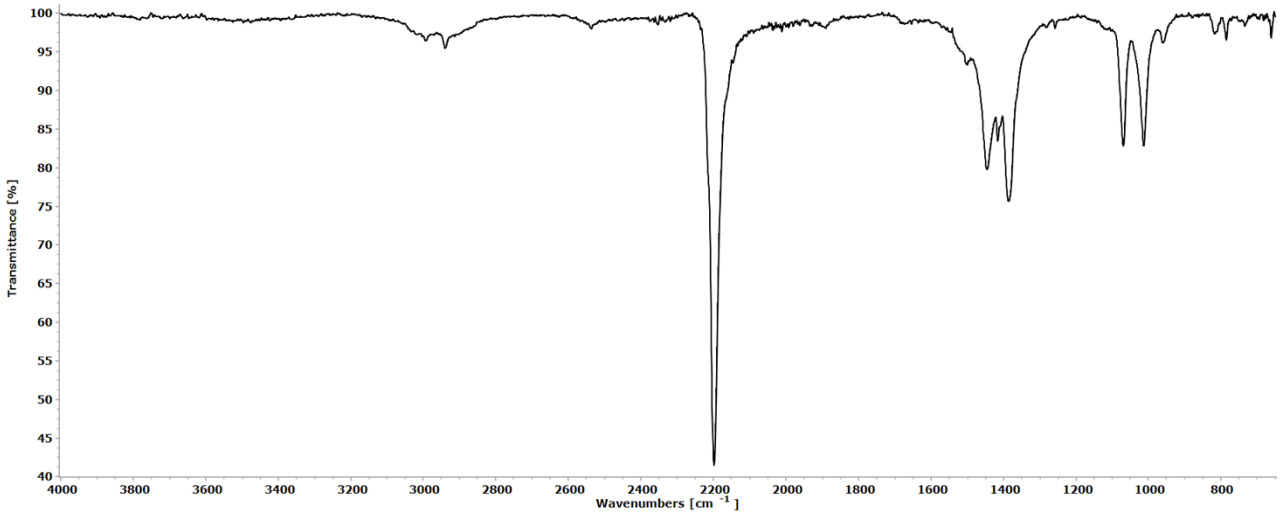

Figure S19. ^{1}H NMR spectrum (400 MHz, $CDCl_3$) of **2a.**

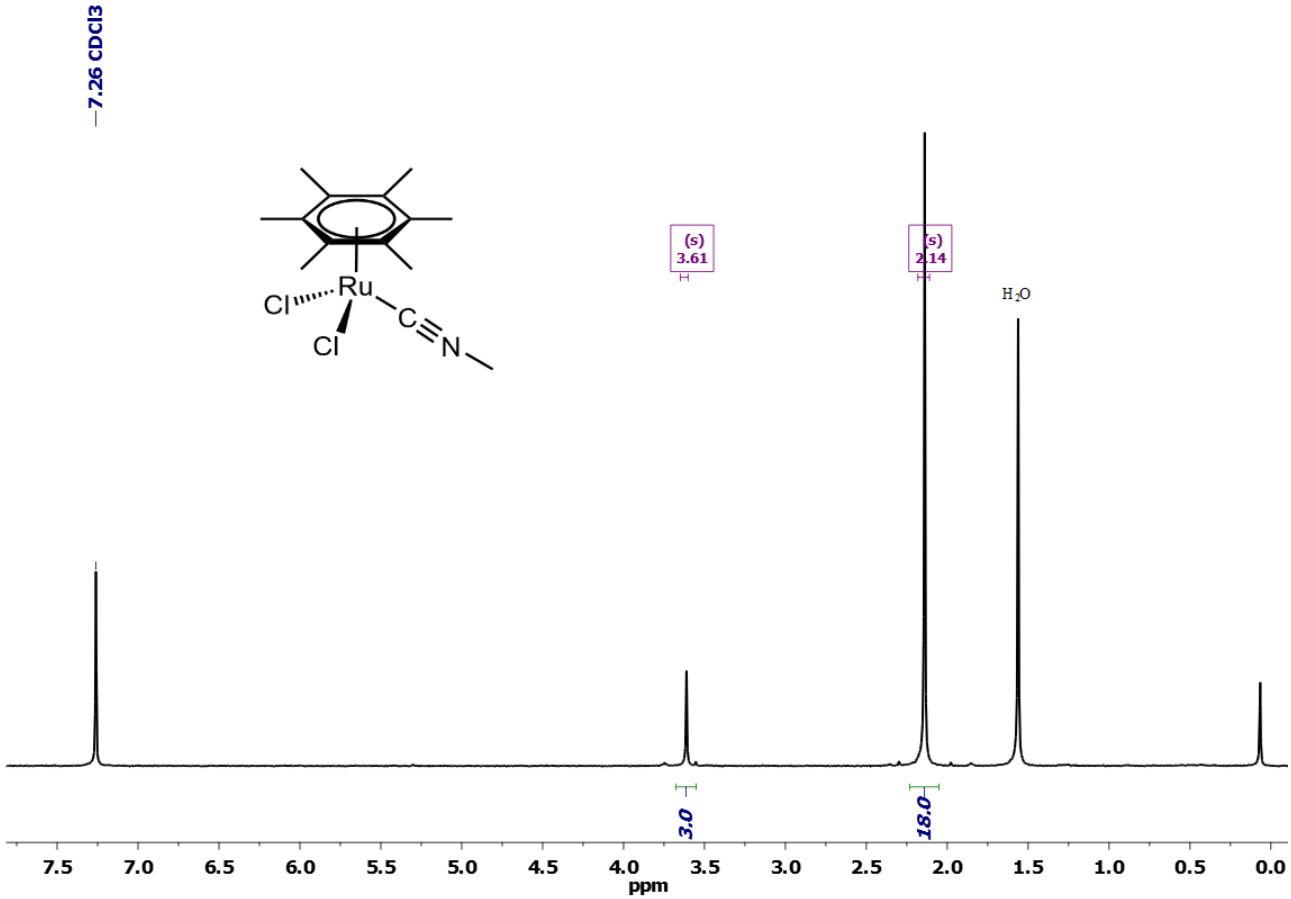

Figure S20. $^{13}C\{^{1}H\}$ NMR spectrum (100 MHz, $CDCl_3$) of **2a**.

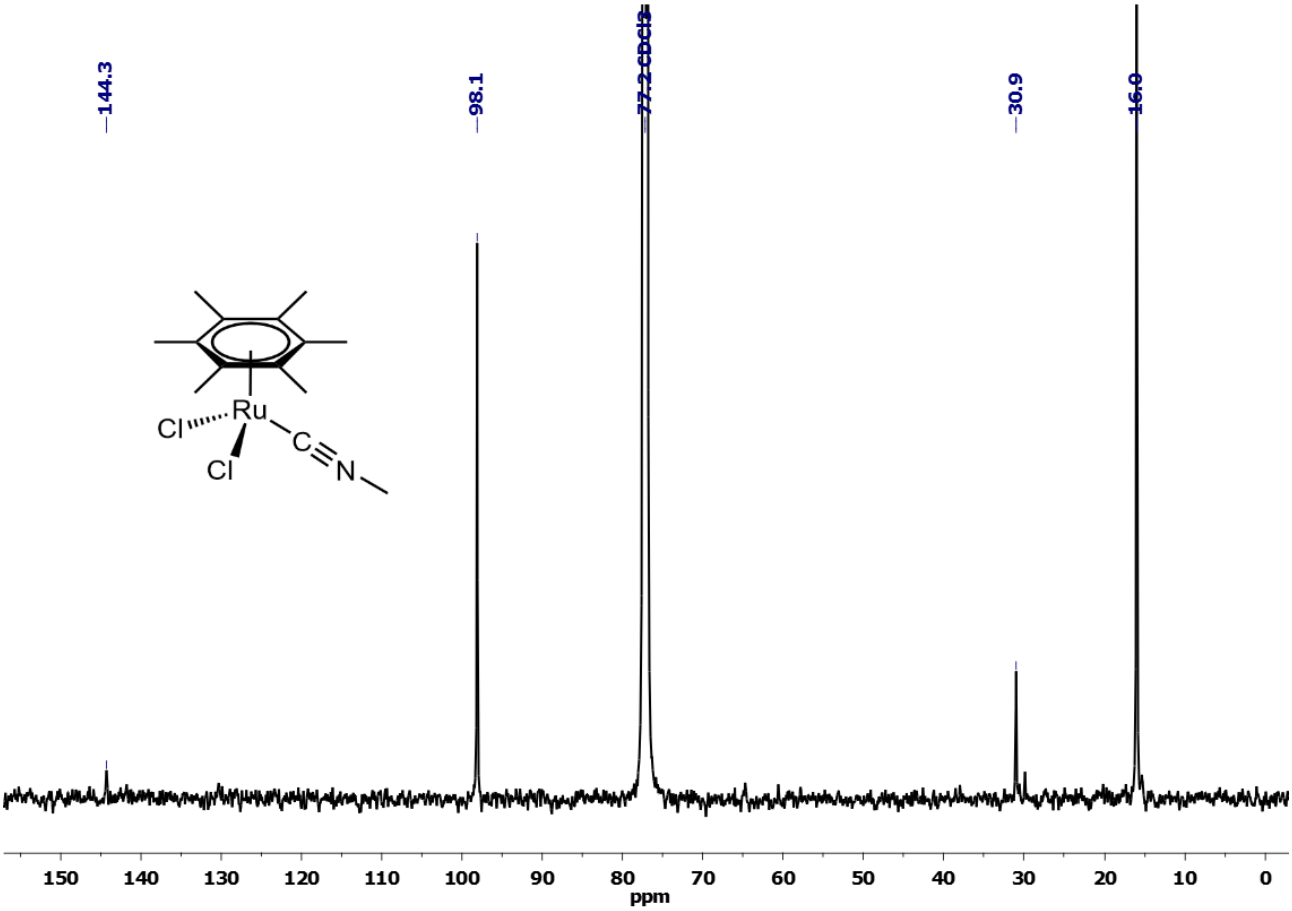

Figure S21. Solid-state IR spectrum (650-4000 cm^{-1}) of $[RuCl_2(CNCy)(\eta^6\text{-}C_6Me_6)]$, **2b**.

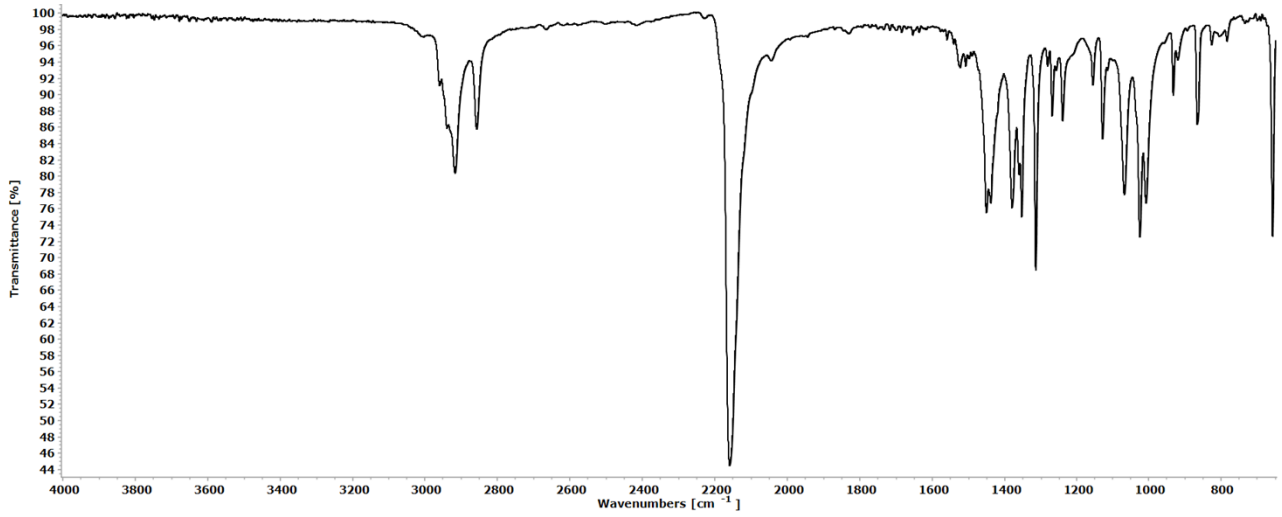

Figure S22. ^1H NMR spectrum (400 MHz, $CDCl_3$) of **2b.**

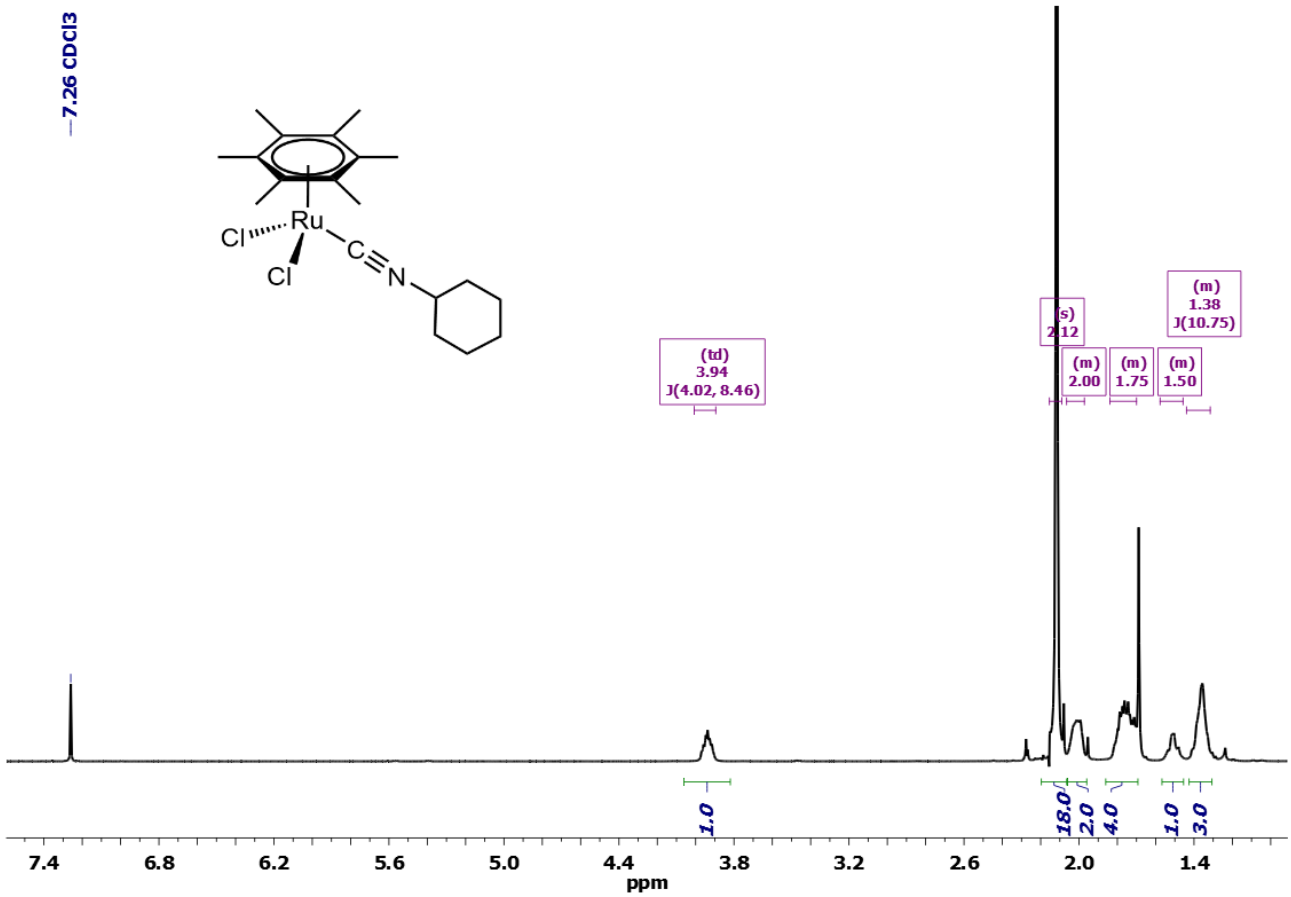

Figure S23. $^{13}C\{^{1}H\}$ NMR spectrum (100 MHz, $CDCl_3$) of **2b**.

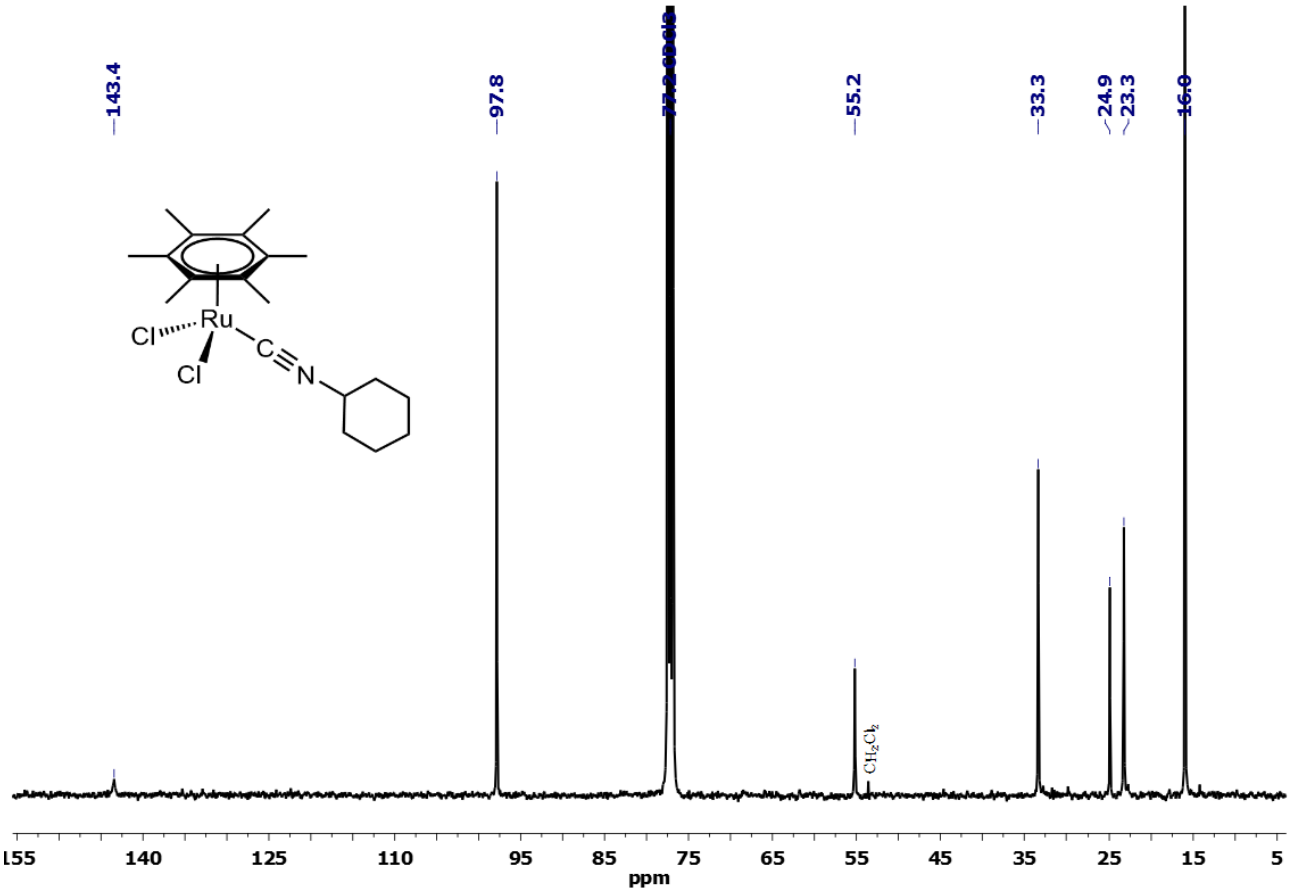

Figure S24. Solid-state IR spectrum (650-4000 cm^{-1}) of $[RuCl_2\{S\text{-}CNCH(Me)Ph\}(\eta^6\text{-}C_6Me_6)]$, **2c**.

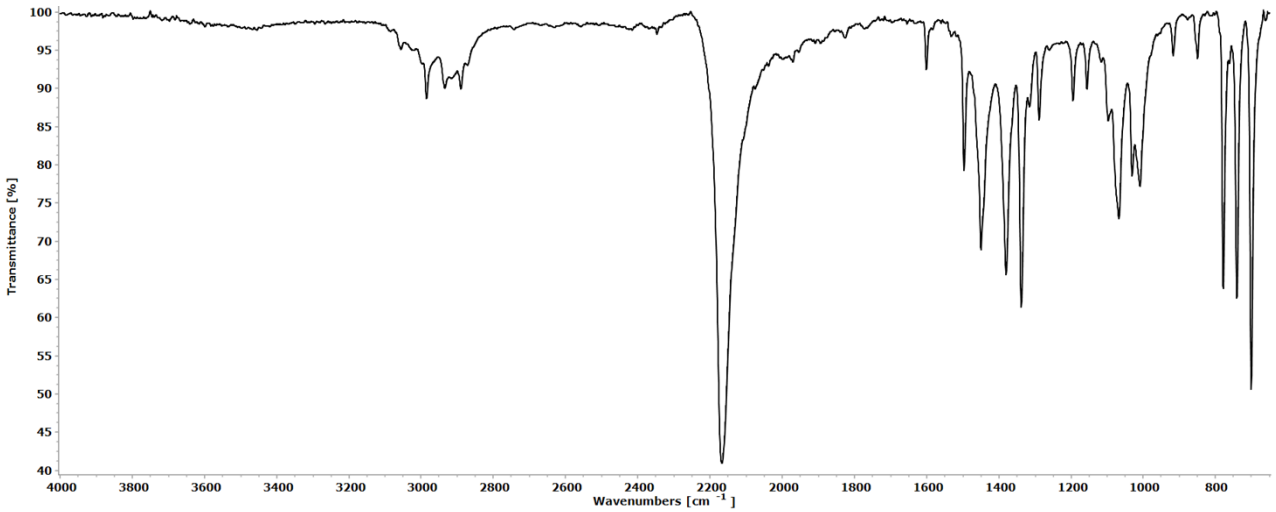

Figure S25. ^{1}H NMR spectrum (400 MHz, $CDCl_3$) of **2c.**

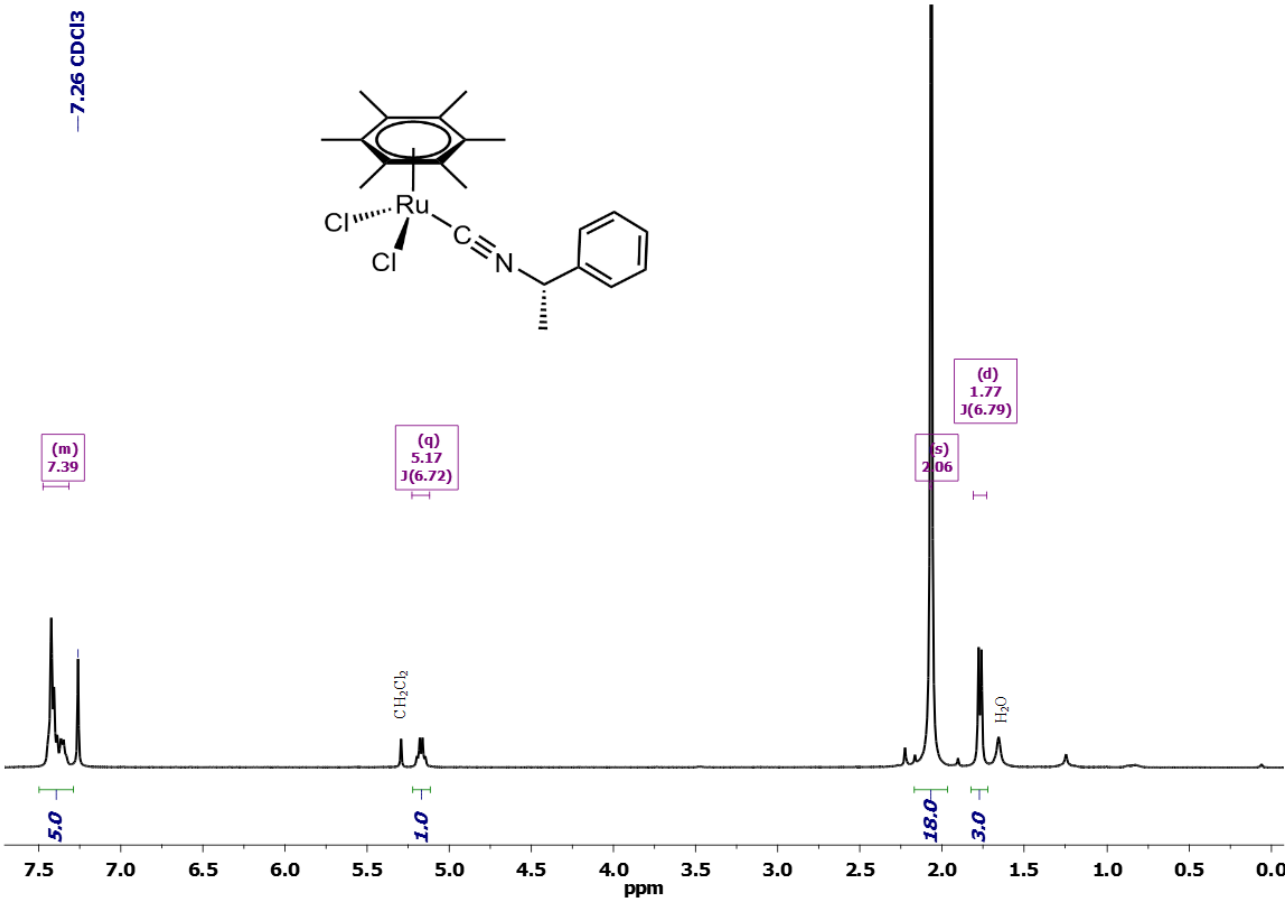

Figure S26. $^{13}C\{^{1}H\}$ NMR spectrum (100 MHz, $CDCl_3$) of **2c**.

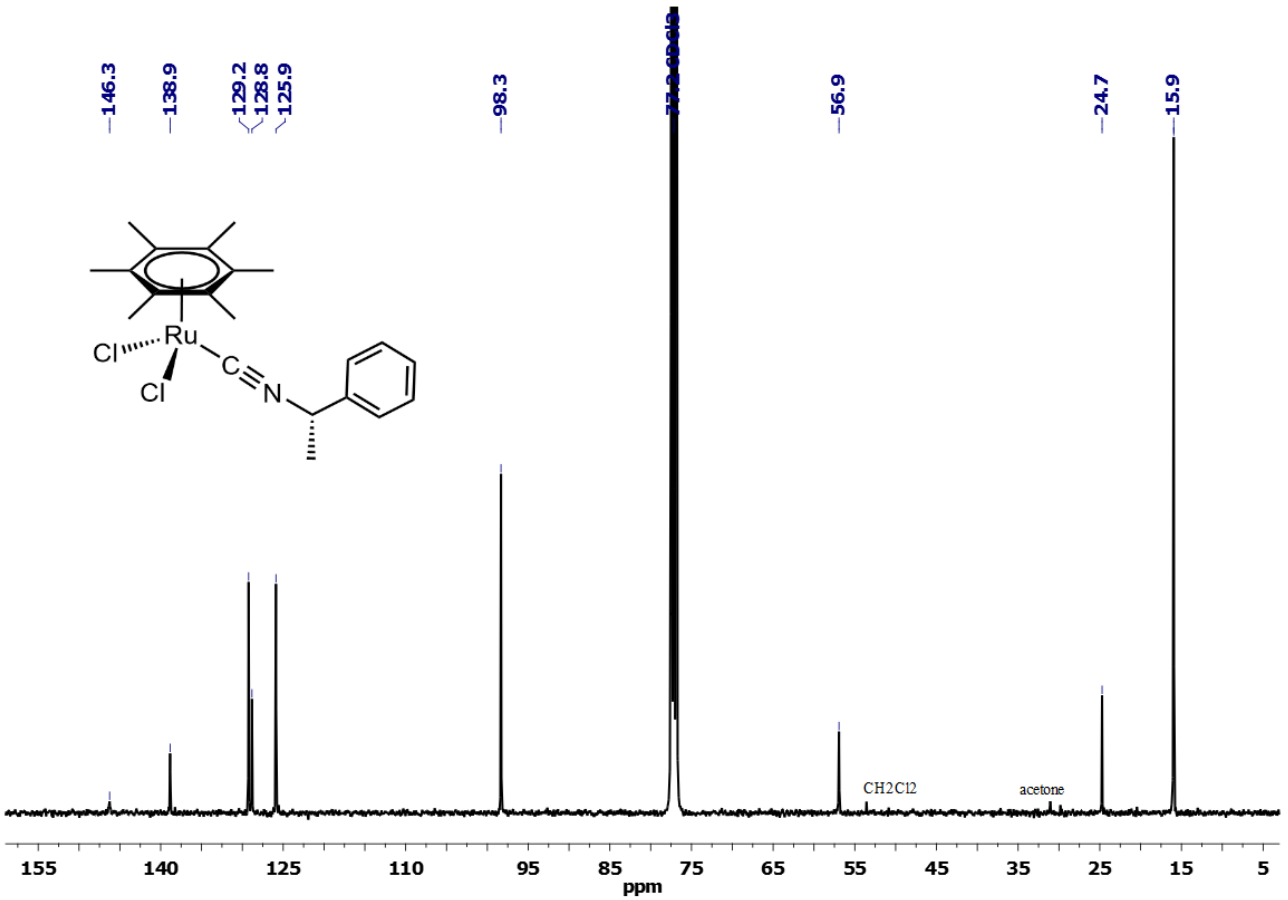

Figure S27. Solid-state IR spectrum (650-4000 cm^{-1}) of $[RuCl_2\{CNCH_2PO(OEt)_2\}(\eta^6\text{-}C_6Me_6)]$, **2d.**

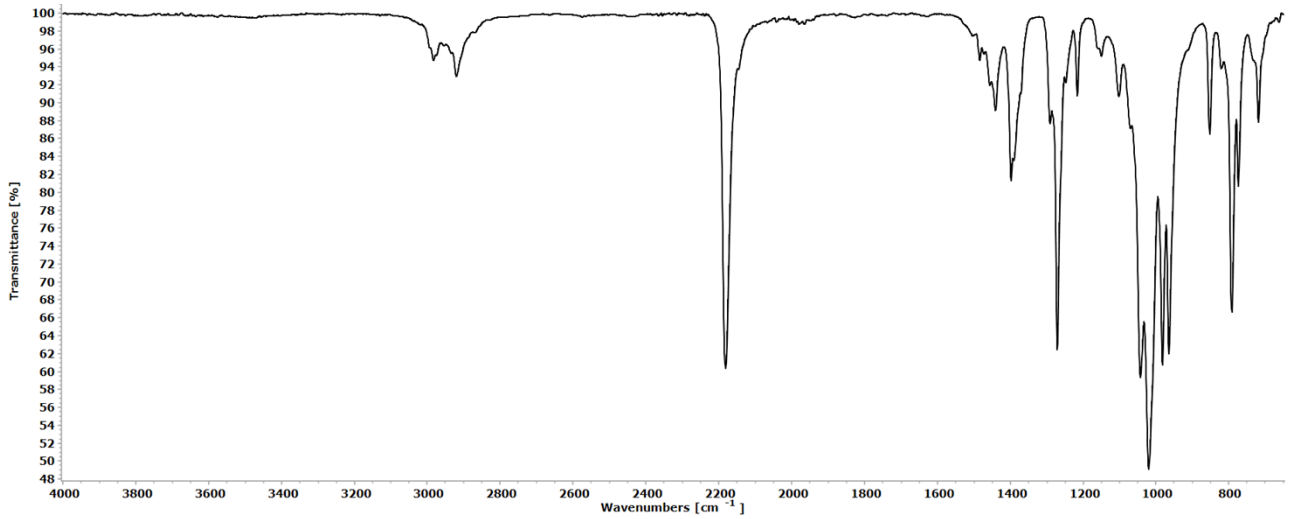

Figure S28. ^1H NMR spectrum (400 MHz, $CDCl_3$) of **2d.**

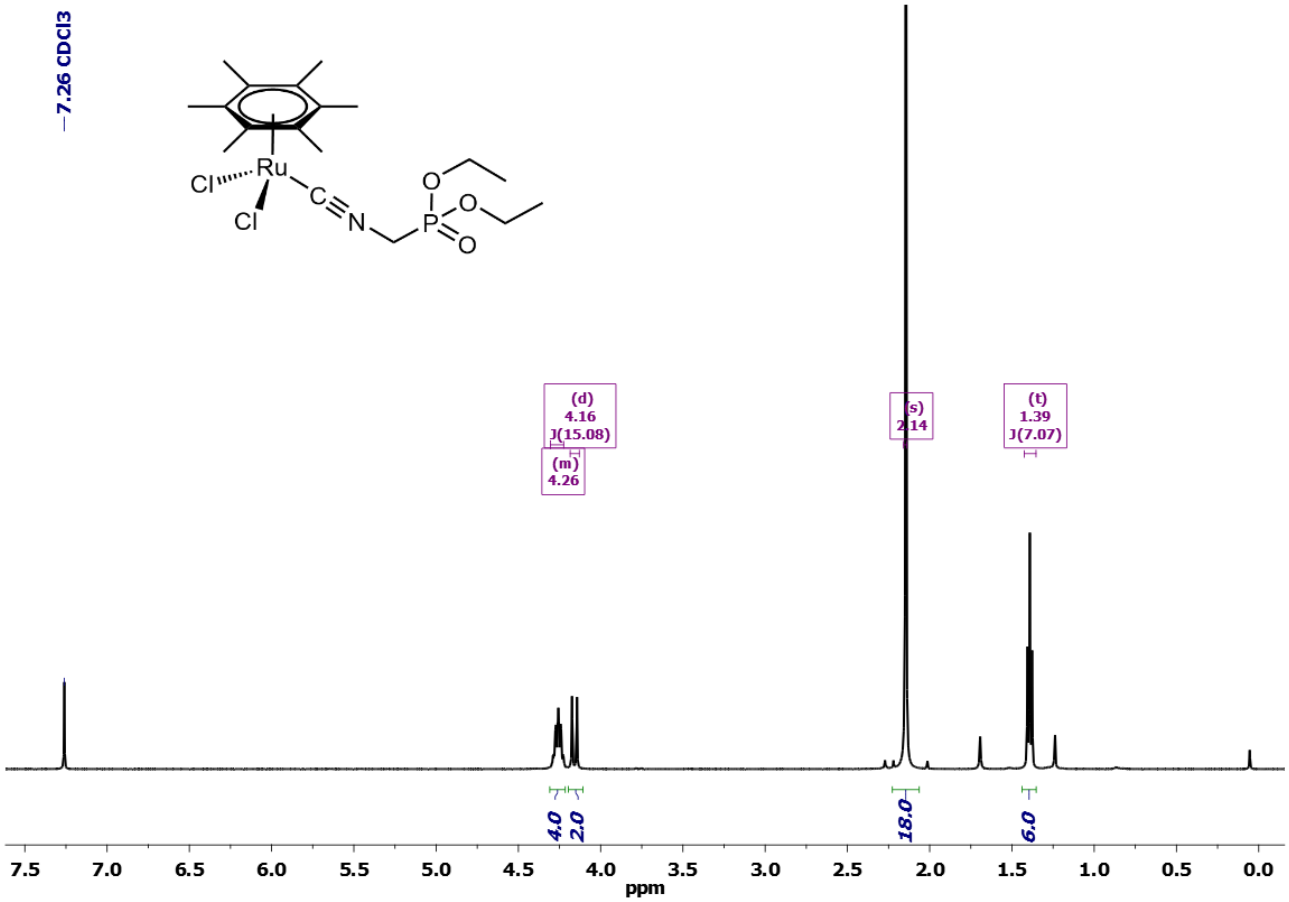

Figure S29. $^{13}C\{^{1}H\}$ NMR spectrum (100 MHz, $CDCl_3$) of **2d**.

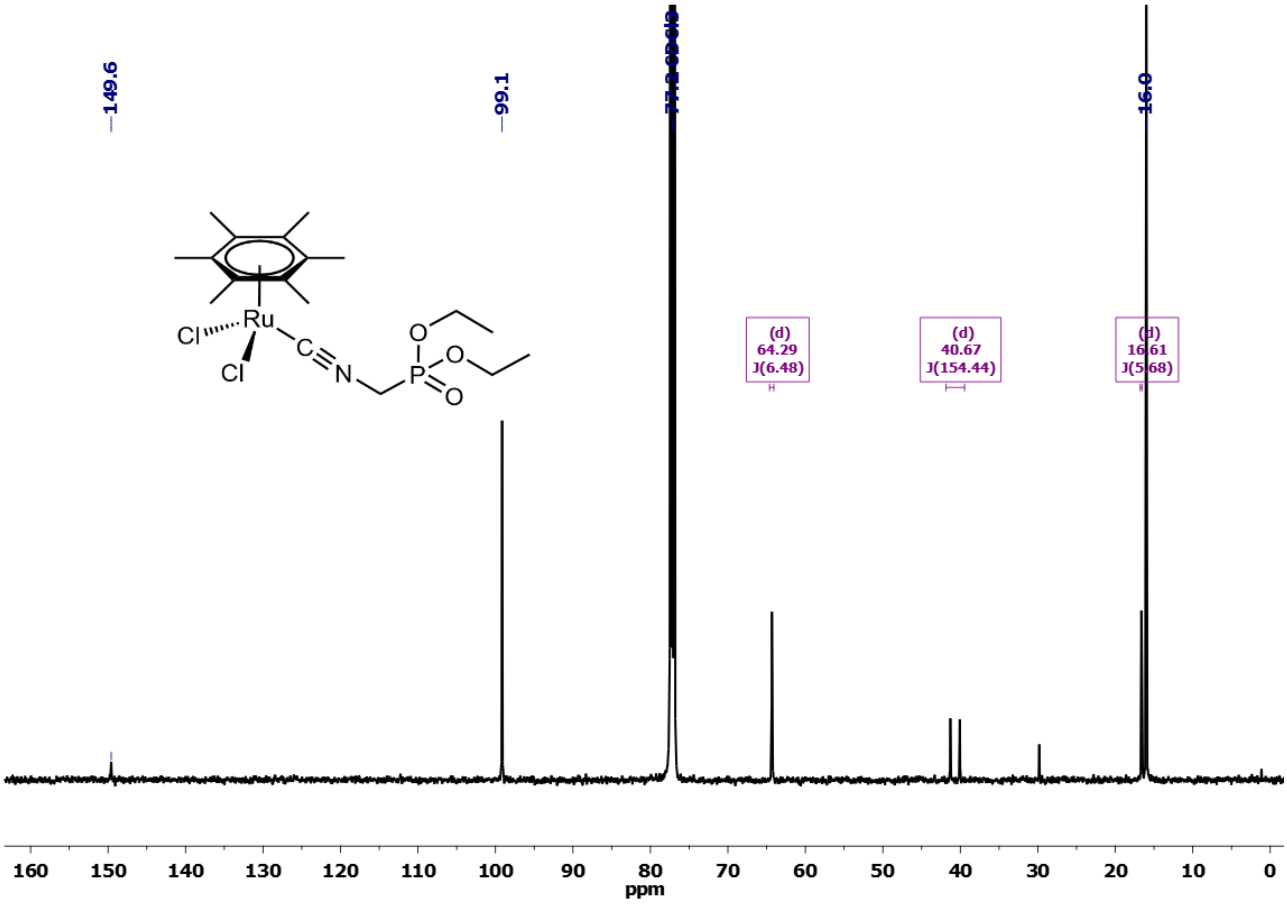

Figure S30. $^{31}P\{^{1}H\}$ NMR spectrum (162 MHz, $CDCl_3$) of **2d**.

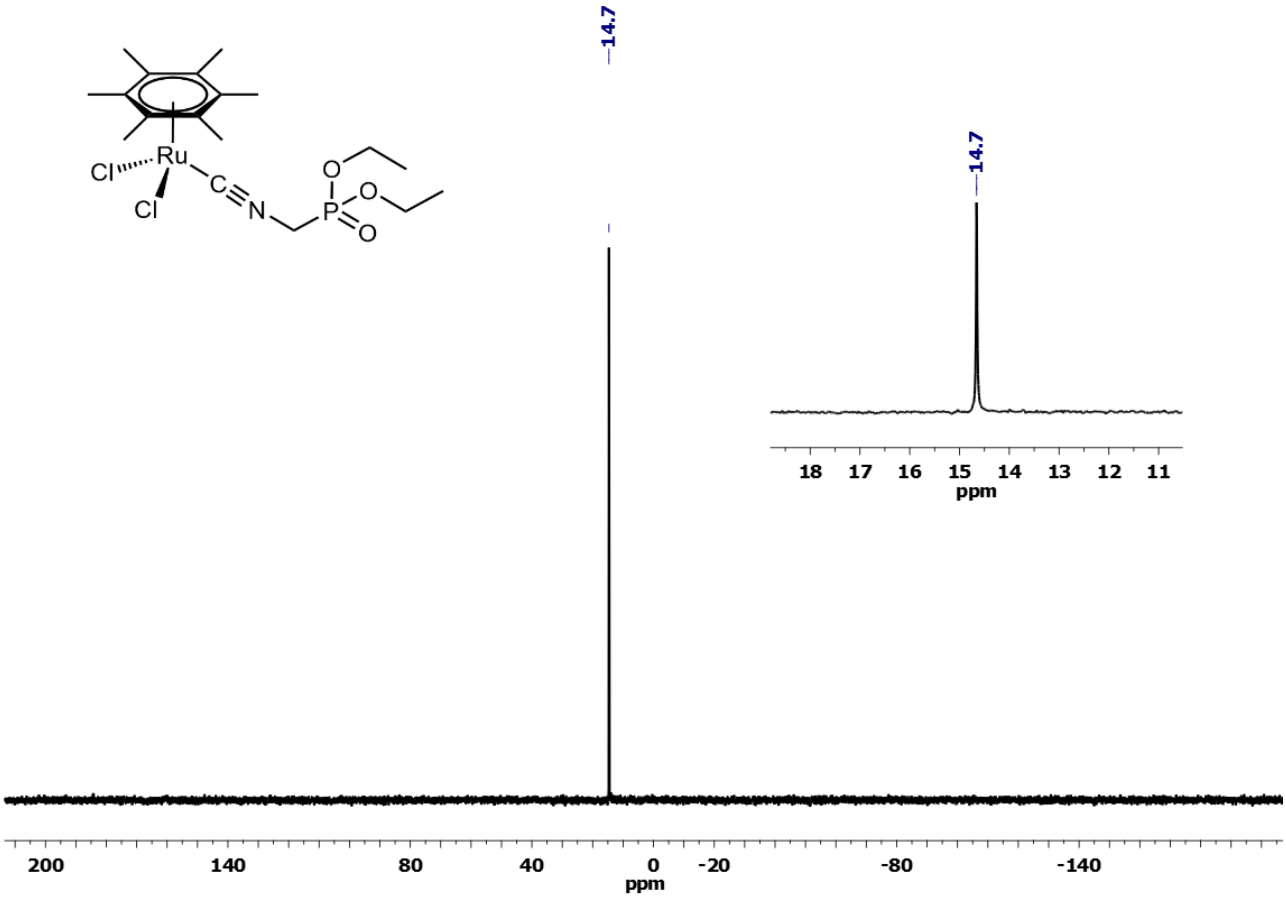

Figure S31. Solid-state IR spectrum (650-4000 cm^{-1}) of $[RuCl_2(CNXyl)(\eta^6\text{-}C_6Me_6)]$, **2f.**

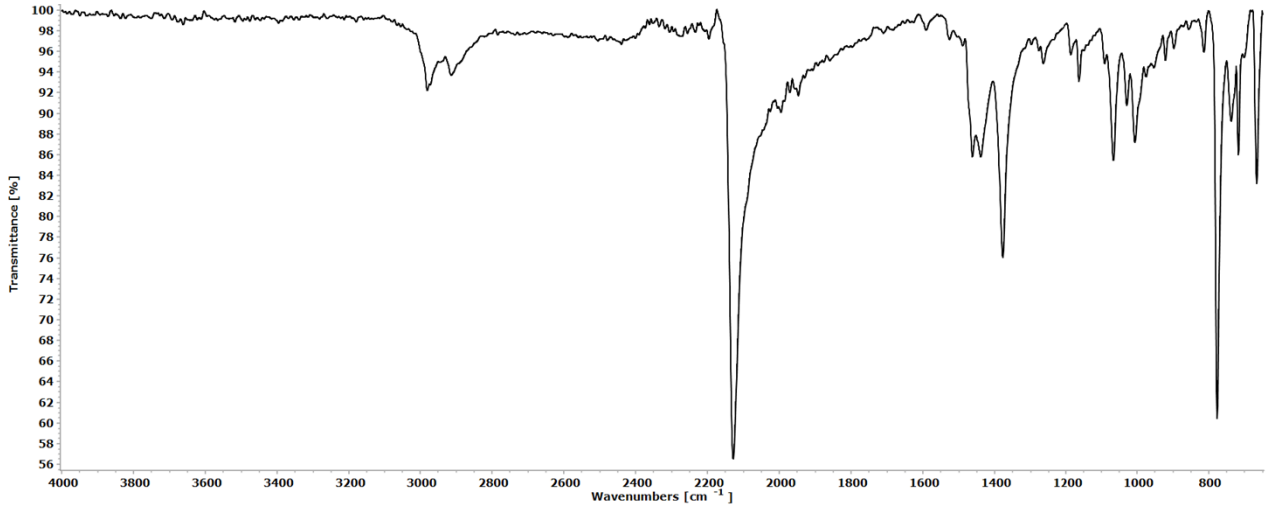

Figure S32. ^1H NMR spectrum (400 MHz, $CDCl_3$) of **2f.**

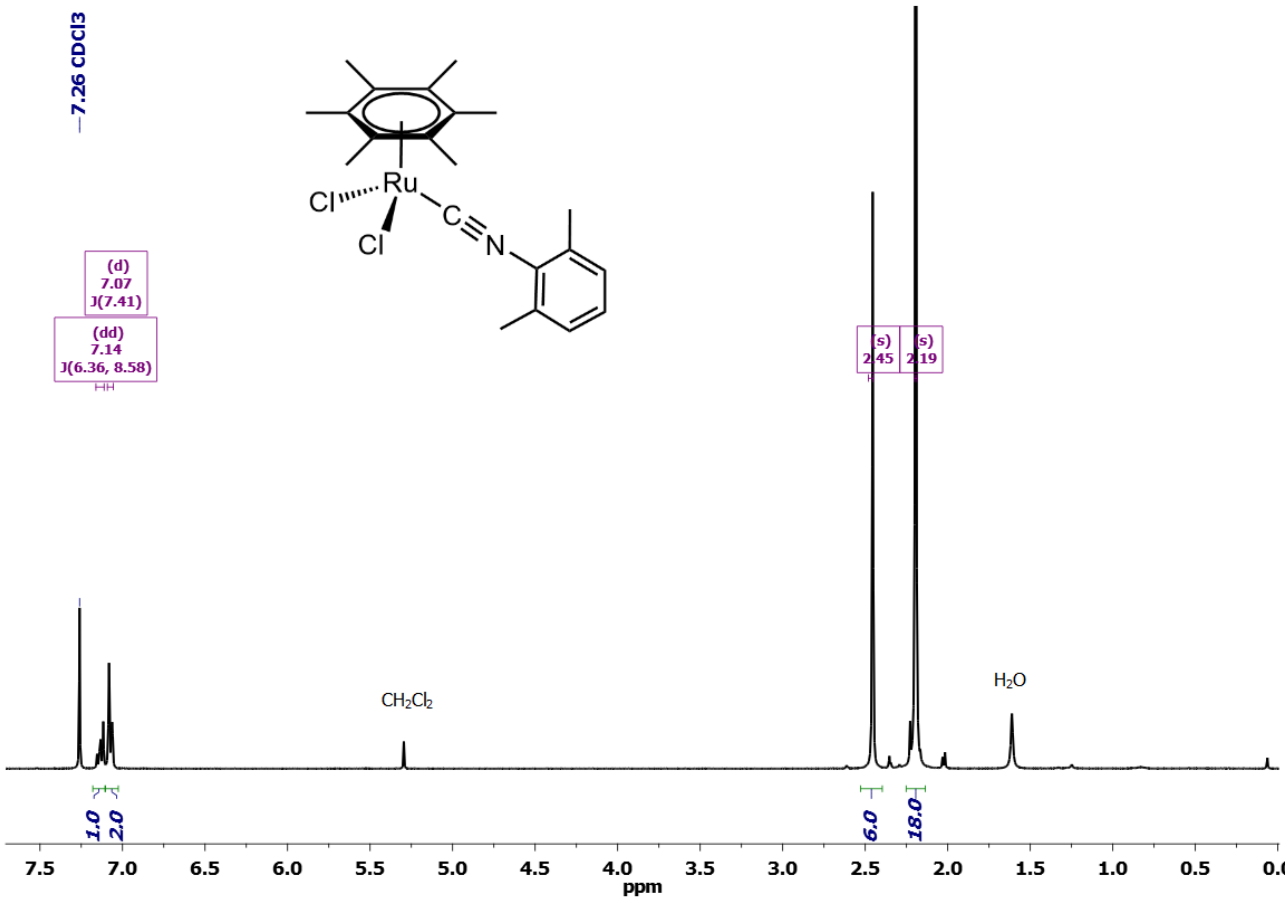

Figure S33. $^{13}C\{^{1}H\}$ NMR spectrum (100 MHz, $CDCl_3$) of **2f**.

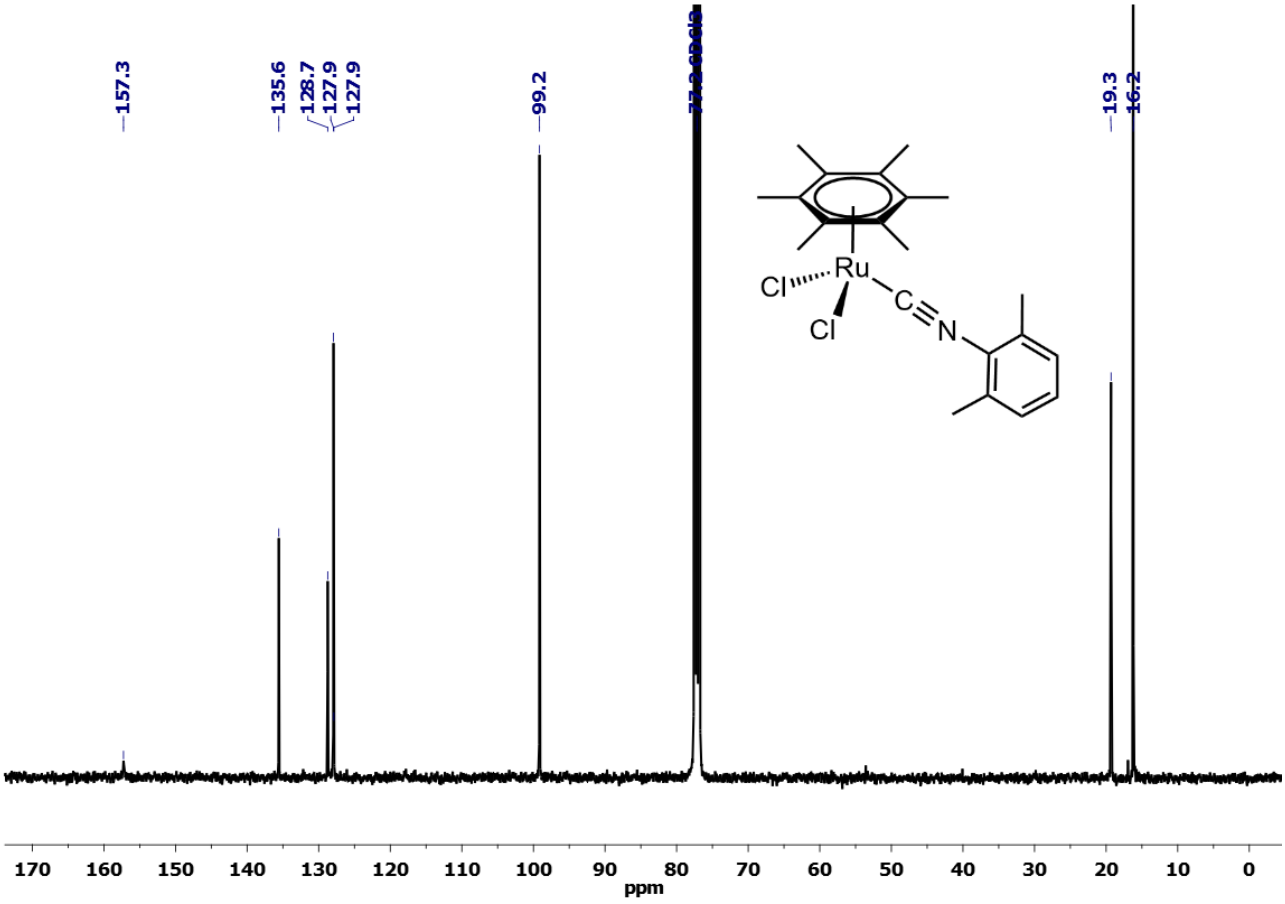

Figure S34. Solid-state IR spectrum (650-4000 cm^{-1}) of $[RuI_2(CNCy)(\eta^6\text{-}p\text{-cymene})]$, **1b-l**.

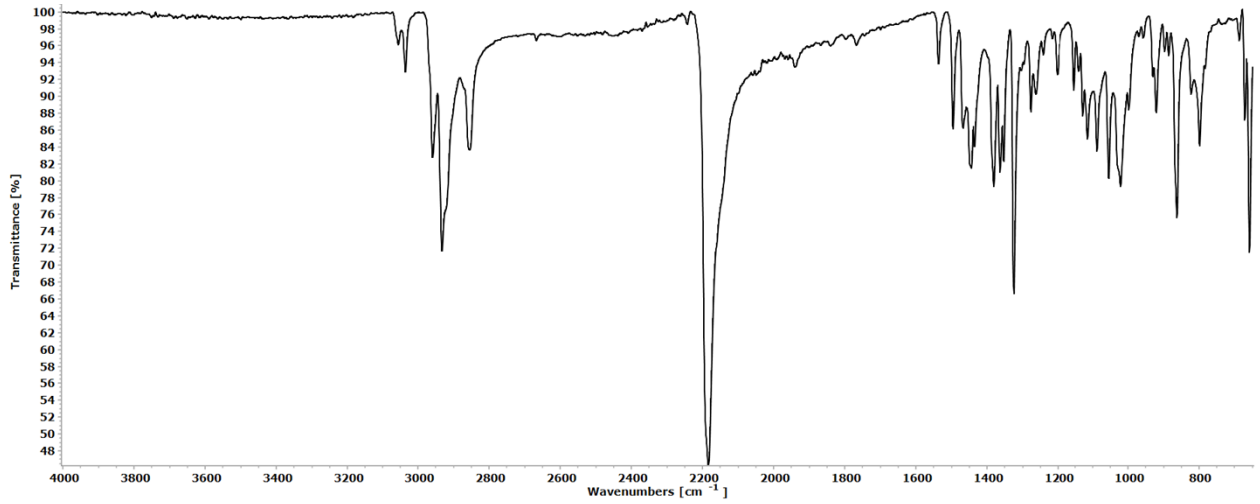

Figure S35. ^{1}H NMR spectrum (400 MHz, $CDCl_3$) of **1b-I.**

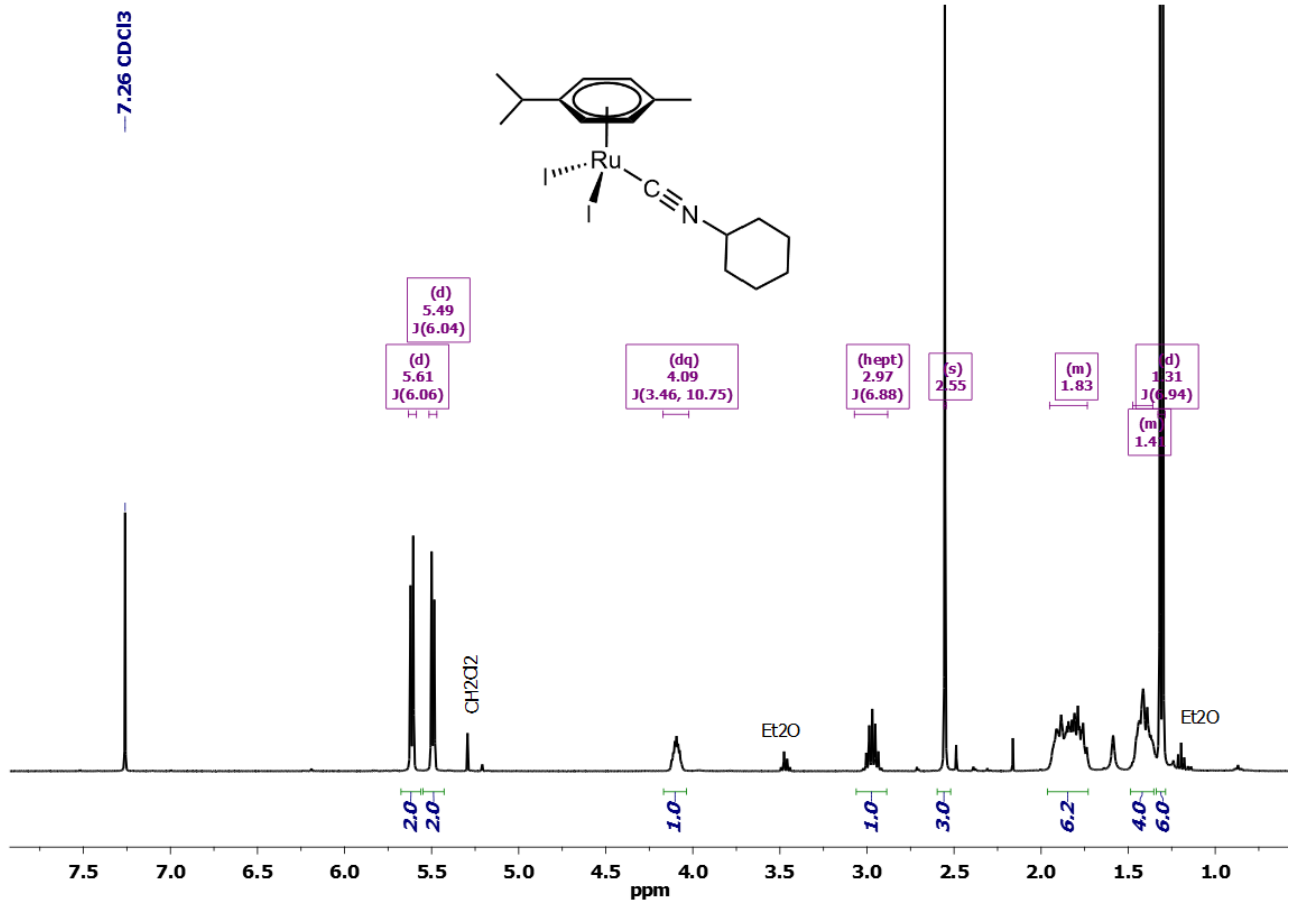

Figure S36. $^{13}C\{^{1}H\}$ NMR spectrum (100 MHz, $CDCl_3$) of **1b-I**.

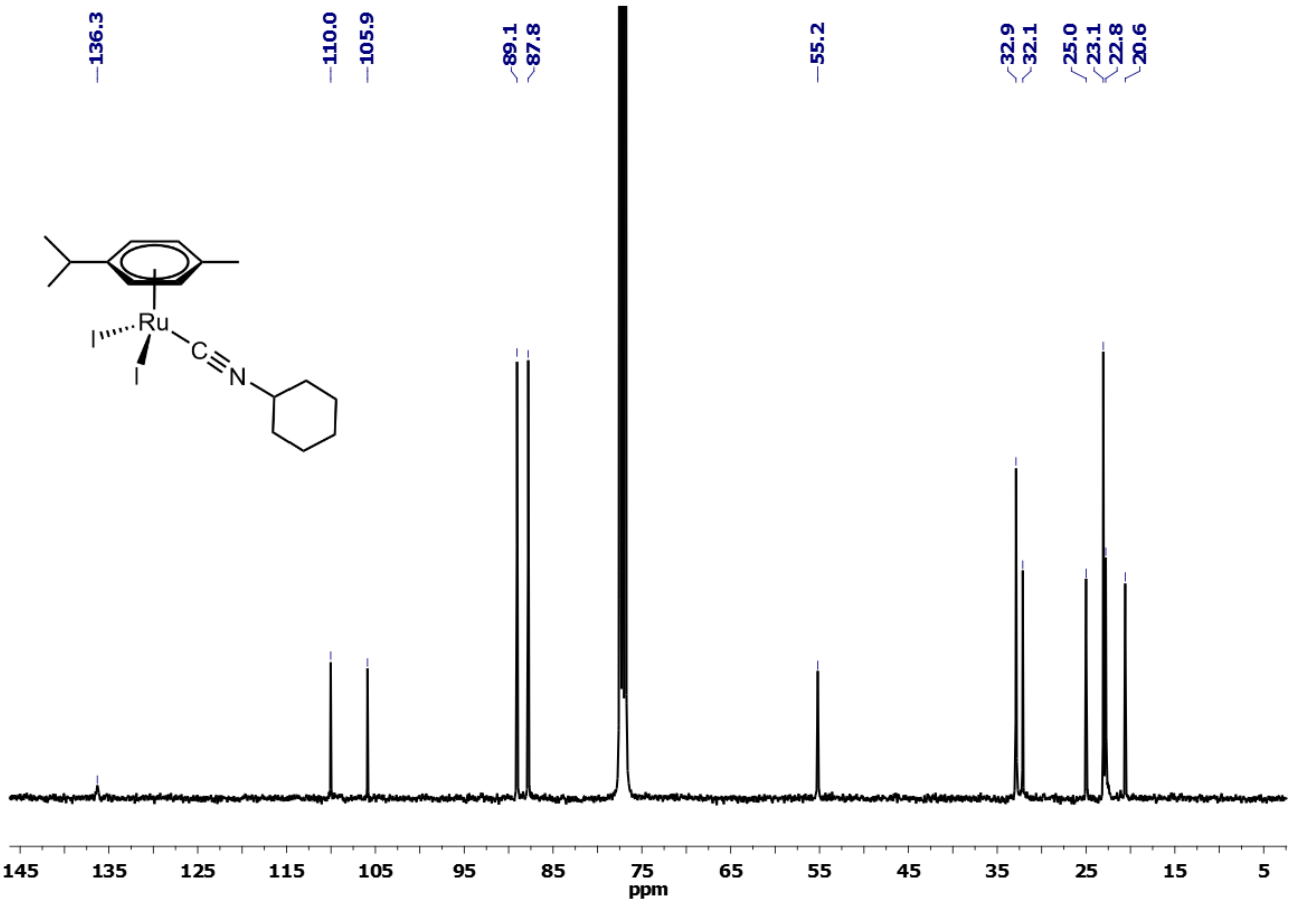

Figure S37. Solid-state IR spectrum (650-4000 cm^{-1}) of $[RuCl_2(CNCy)(\eta^6\text{-}C_6H_6)]$, **3b**.

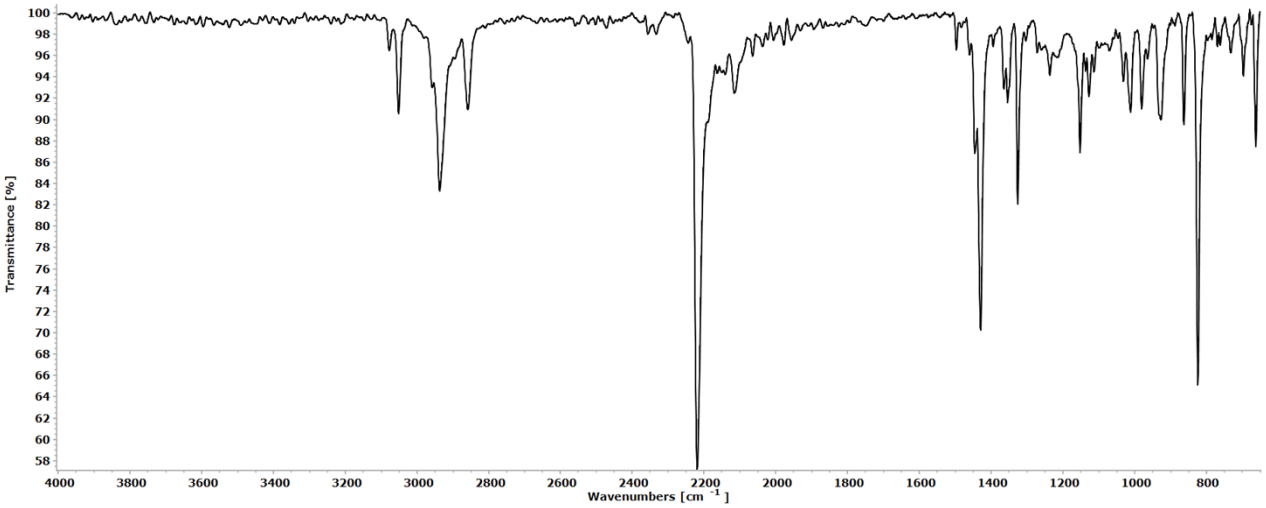

Figure S38. ^1H NMR spectrum (400 MHz, $CDCl_3$) of **3b.** The asterisk(*) indicates the signal of free C_6H_6.

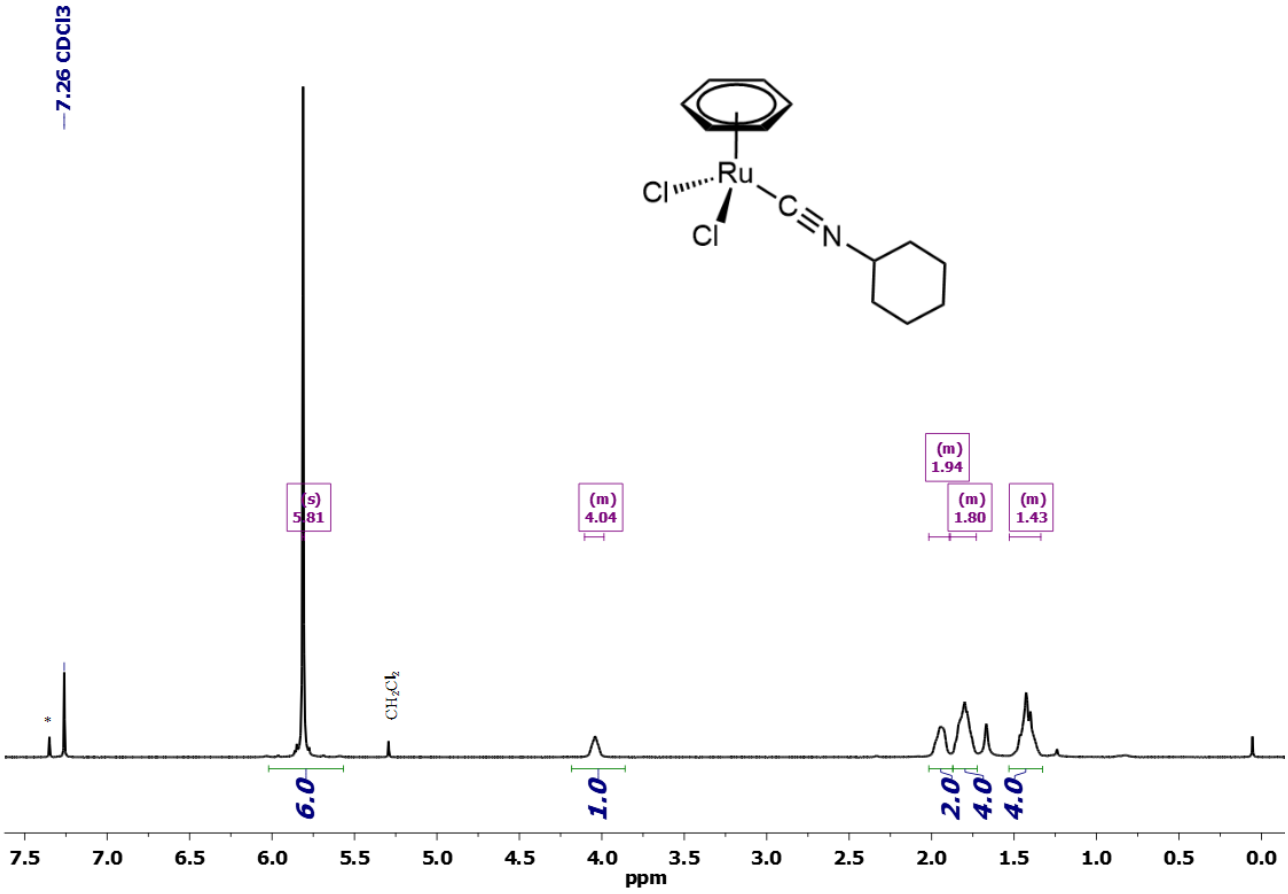

Figure S39. $^{13}C\{^{1}H\}$ NMR spectrum (100 MHz, $CDCl_3$) of **3b**. The asterisk(*) indicates the signal of free C_6H_6.

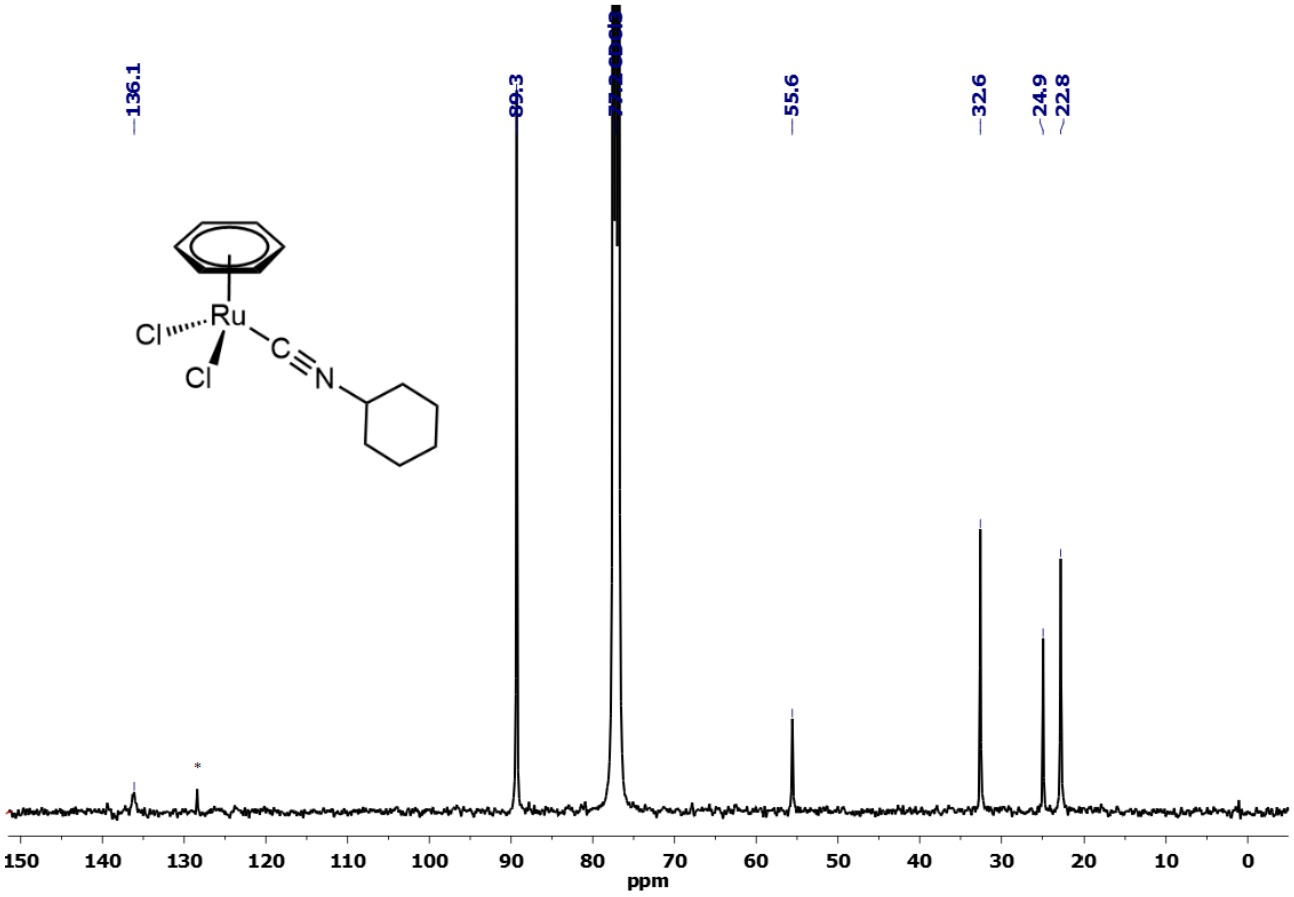

Figure S40. Solid-state IR spectrum (650-4000 cm^{-1}) of $[RuCl_2\{CNCH_2PO(OEt)_2\}(\eta^6\text{-}C_6H_6)]$, **3d**.

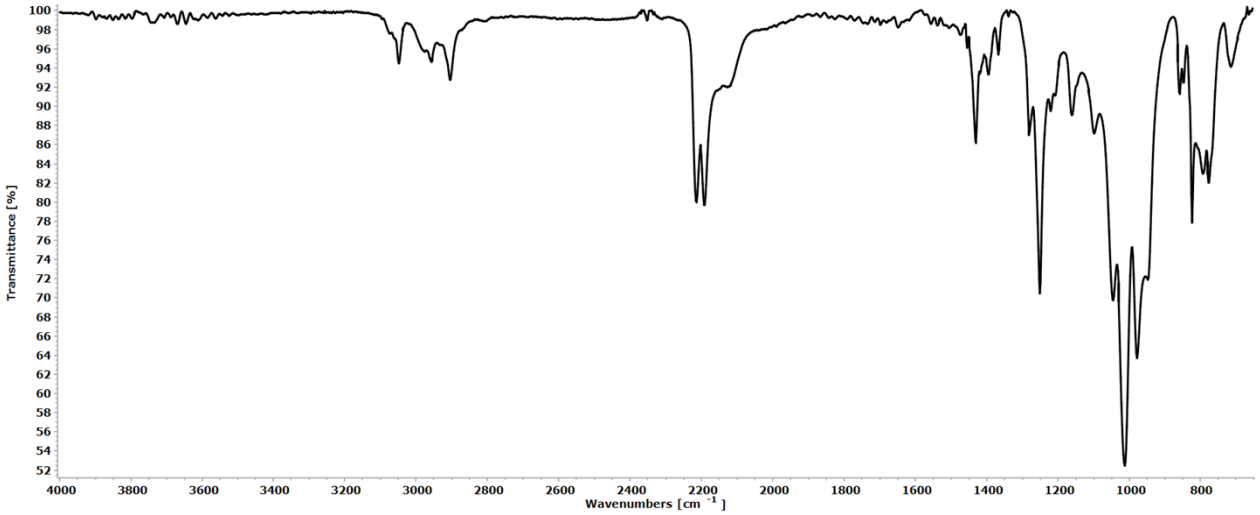

Figure S41. ^{1}H NMR spectrum (400 MHz, $CDCl_3$) of **3d.** The lower relative integral of C_6H_6 is probably due to an insufficient relaxation time of the experiment (d1 = 4s).

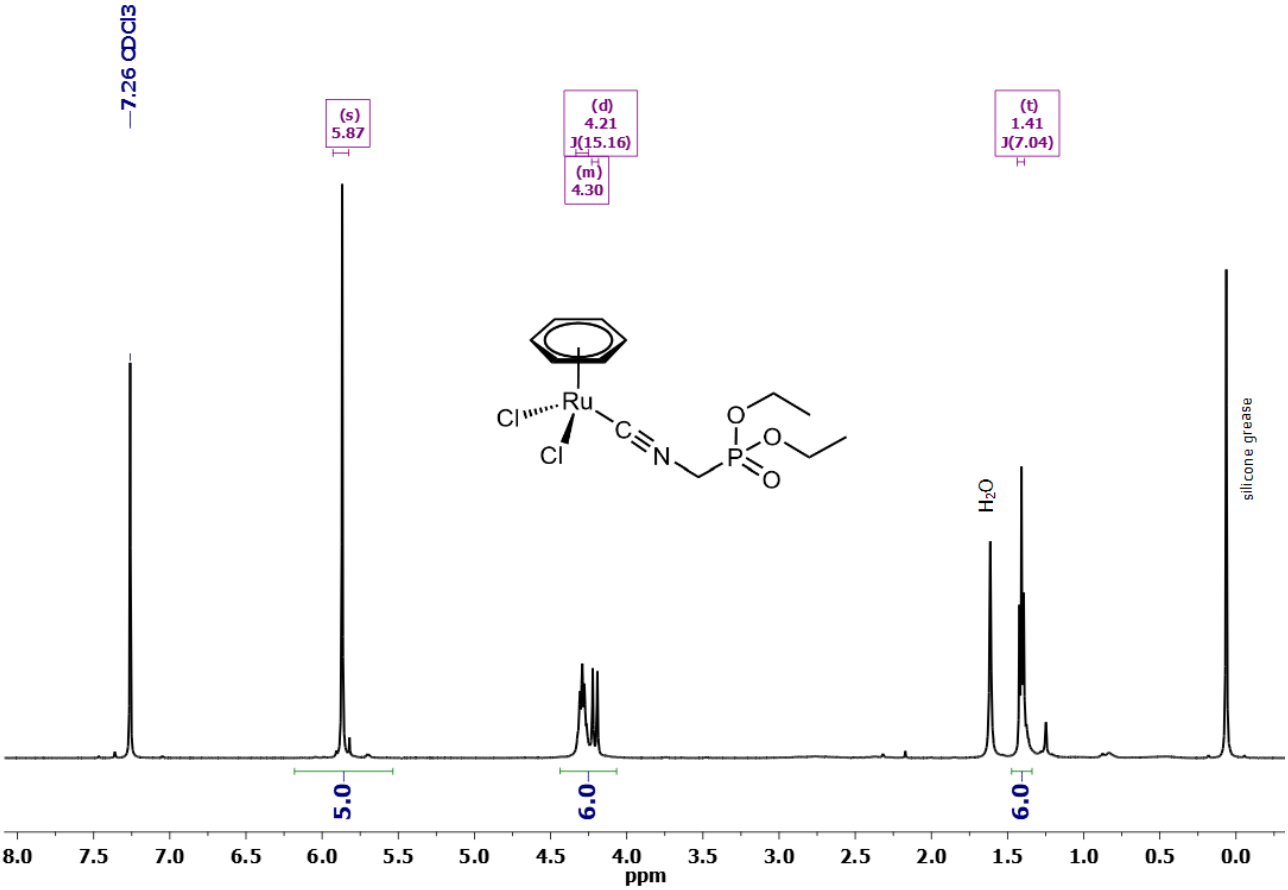

Figure S42. $^{31}P\{^{1}H\}$ NMR spectrum (162 MHz, $CDCl_3$) of **3d**.

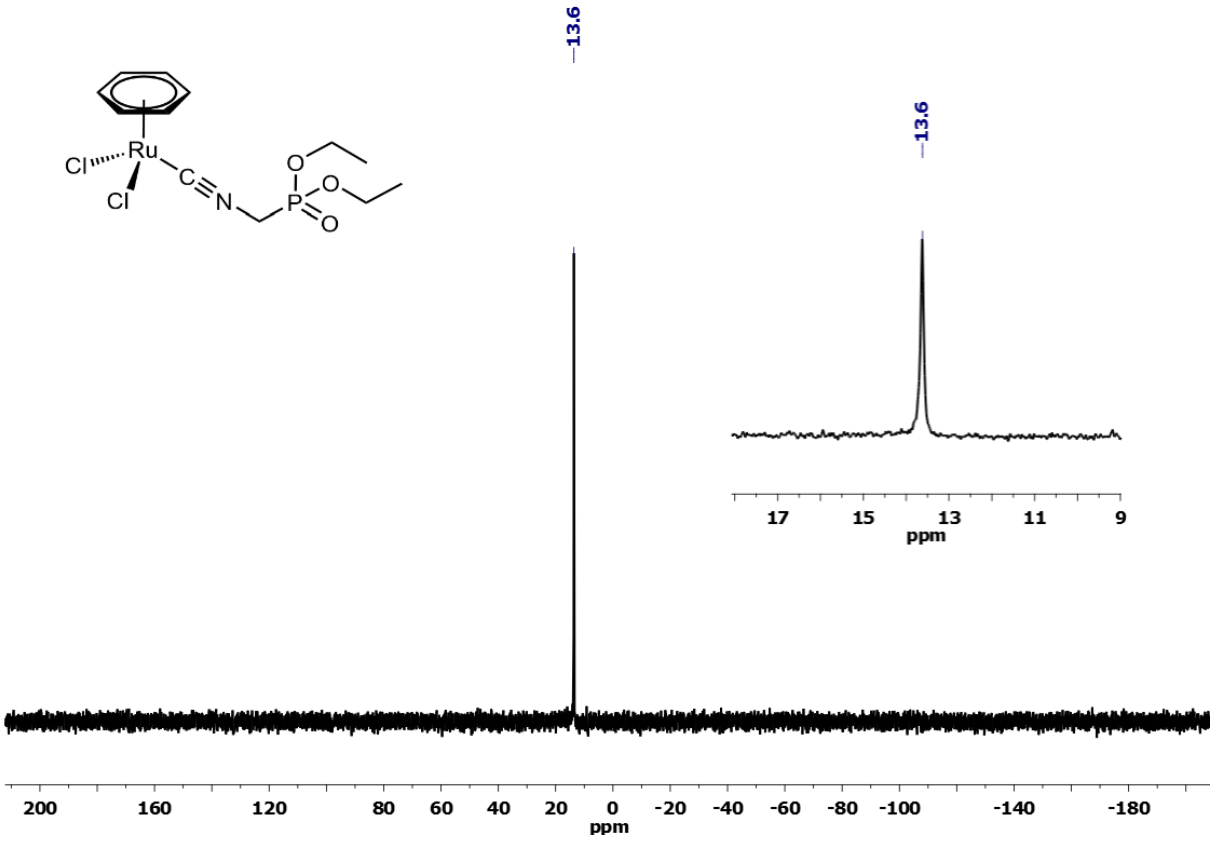

Figure S43. $^{13}C\{^{1}H\}$ NMR spectrum (100 MHz, $CDCl_3$) of **3d**. The asterisk(*) indicates free C_6H_6 and a $Ru(C_6H_6)$ decomposition product (see main text) arisen due to the long duration of the NMR experiment. Inset shows the 42 ppm resonance when a large apodization function is applied.

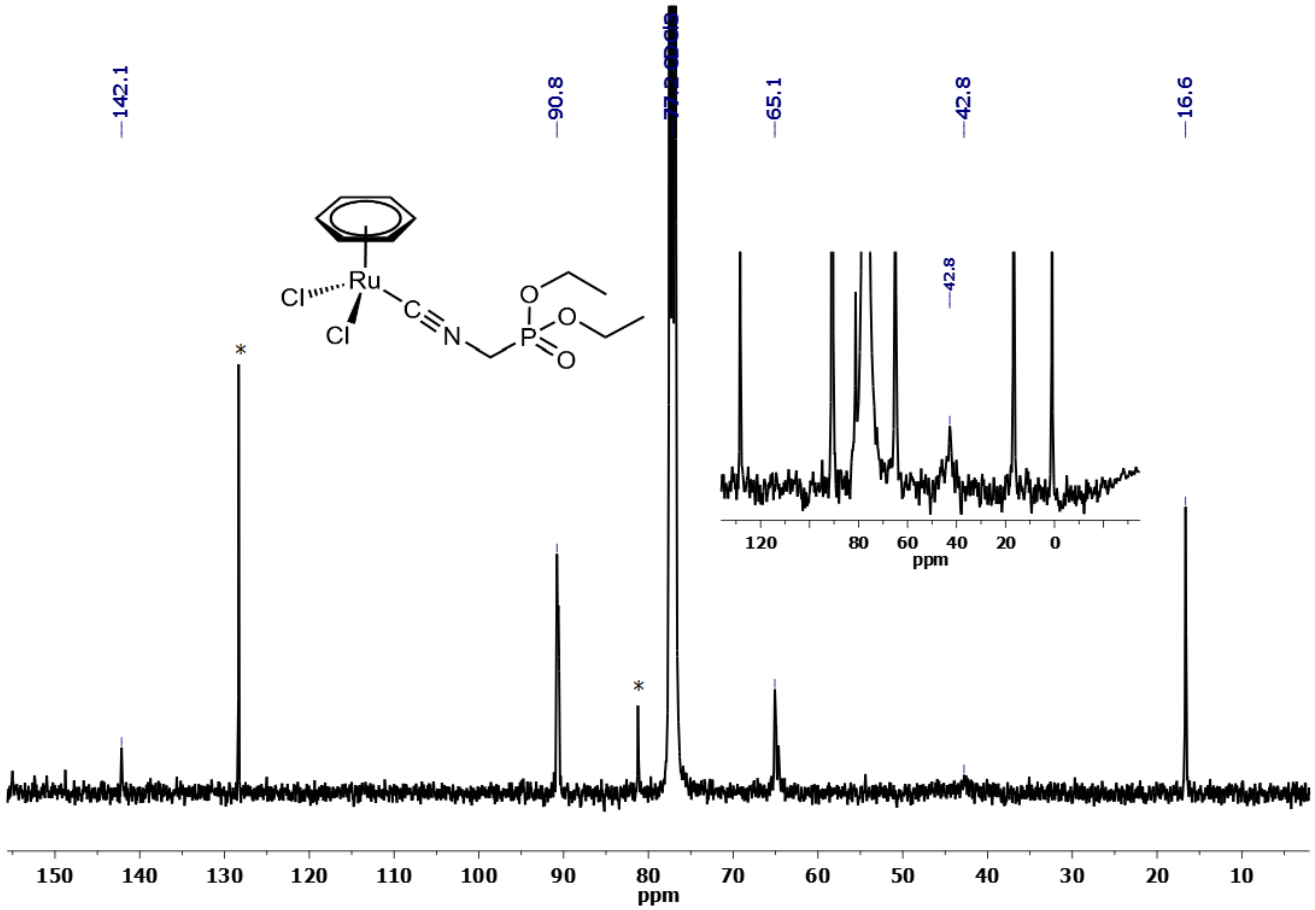

Figure S44. Solid-state IR spectrum (650-4000 cm^{-1}) of $[RuCl_2(CNXyl)(\eta^6\text{-}C_6H_6)]$, **3f**.

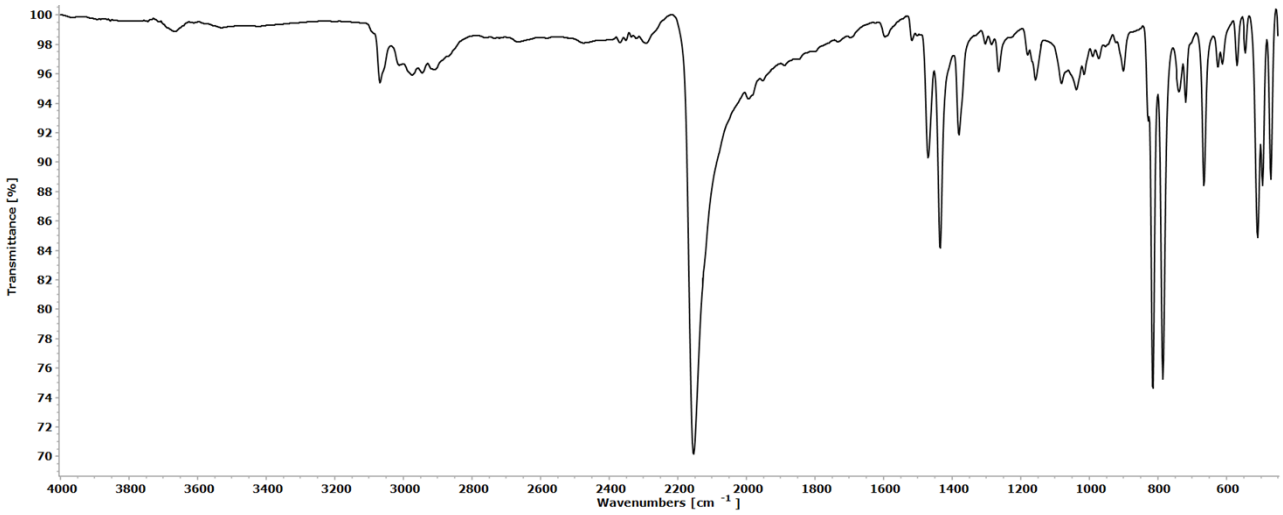

Figure S45. ^{1}H NMR spectrum (400 MHz, $CDCl_3$) of **3f.** The asterisk(*) indicates the signal of free C_6H_6.

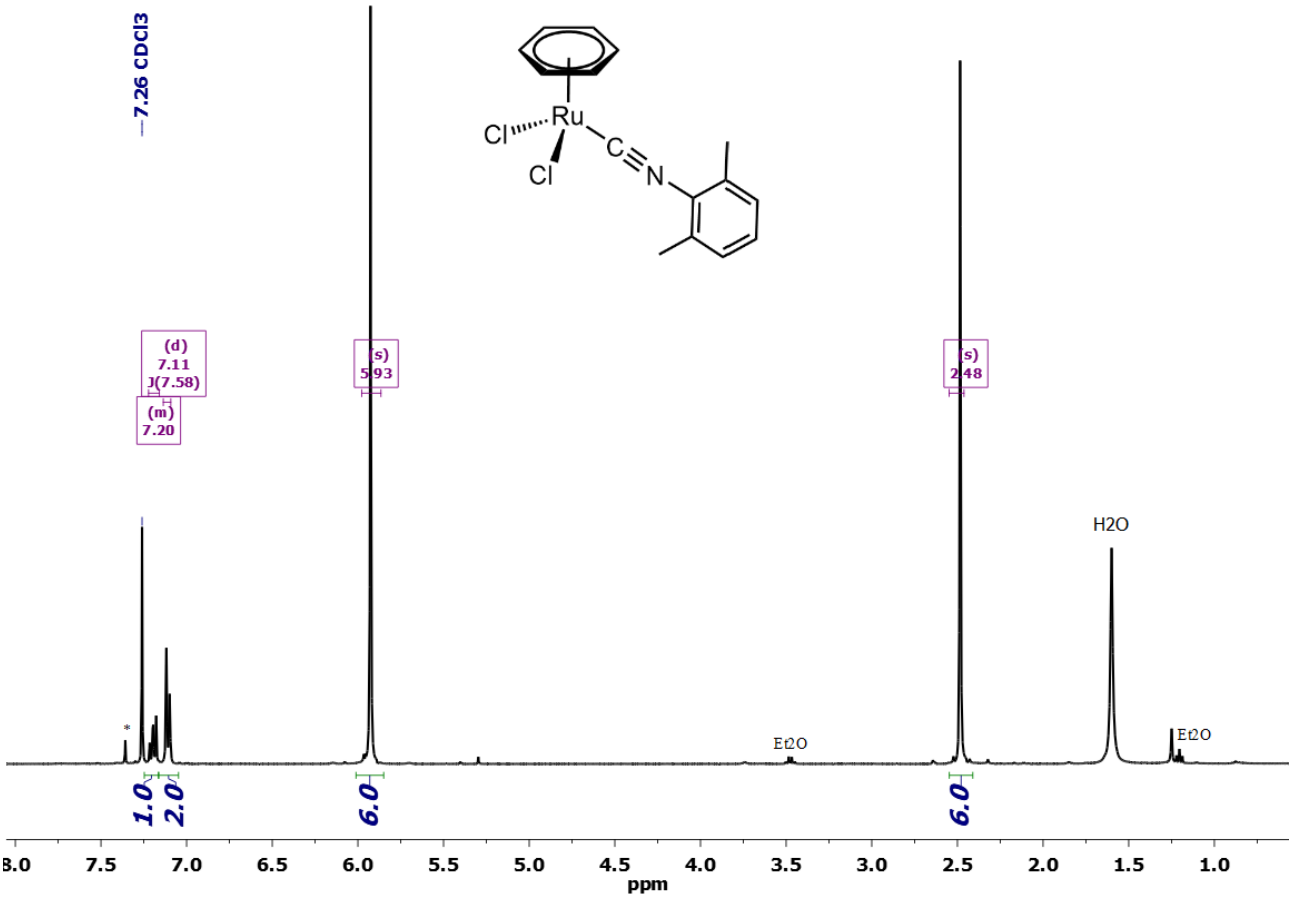

Figure S46. $^{13}C\{^{1}H\}$ NMR spectrum (100 MHz, $CDCl_3$) of **3f**. The asterisk(*) indicates the signal of free C_6H_6.

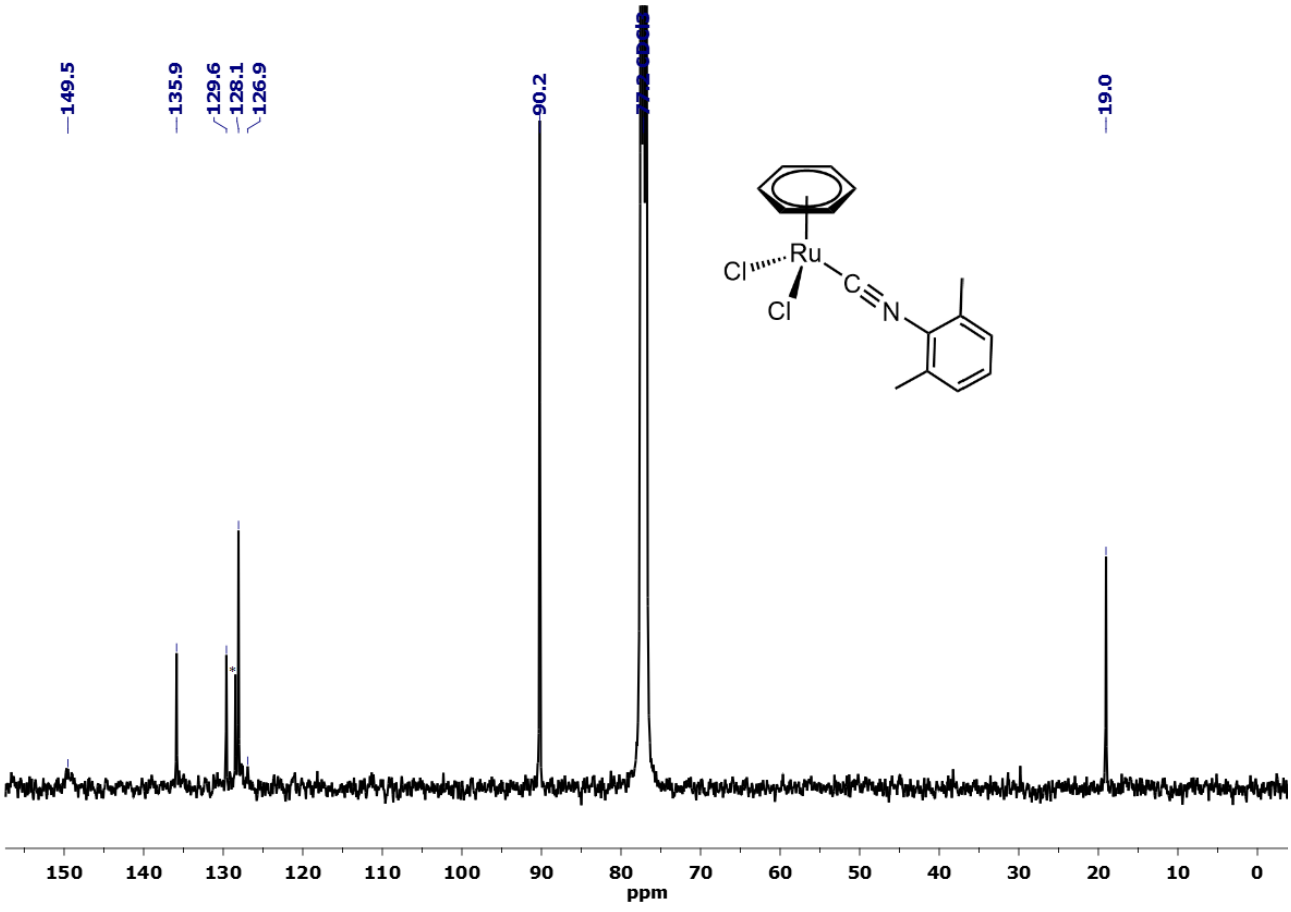

Figure S47. Solvent-subtracted IR spectra (1700-2300 cm^{-1}) of **1a** (orange line), **2a** (blue line) and methyl isocyanide (black dashed line) in CH_2Cl_2. The transmittance of the C≡N stretching peaks is normalized.

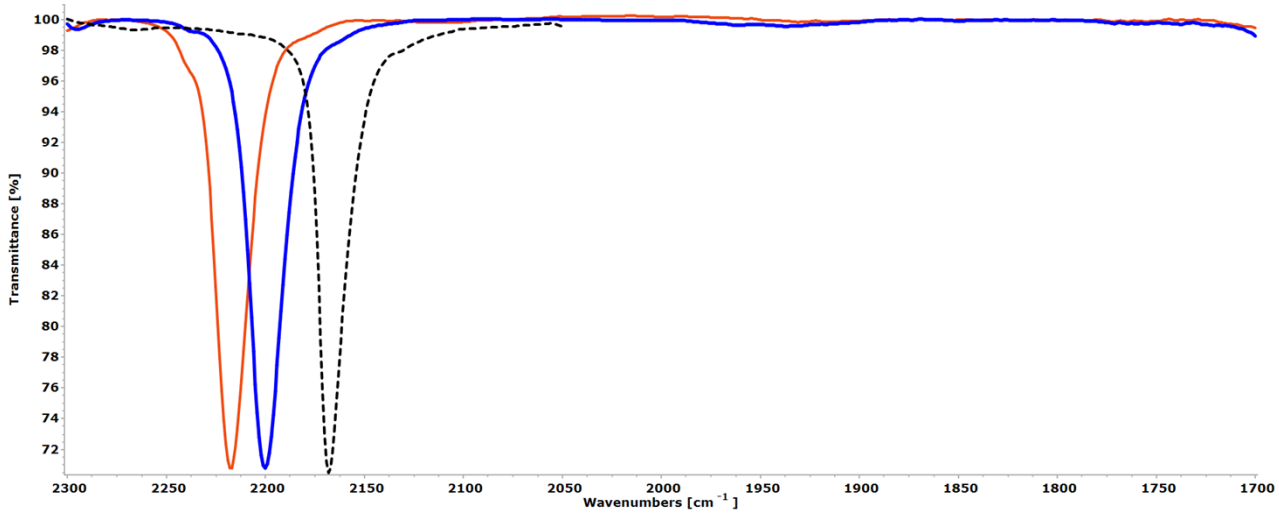

Figure S48. Solvent-subtracted IR spectra (1500-2300 cm^{-1}) of **1b** (orange line), **2b** (blue line), **3b** (red line), **1b-l** (green line) and cyclohexyl isocyanide (black dashed line) in CH_2Cl_2. The transmittance of the C≡N stretching peaks is normalized.

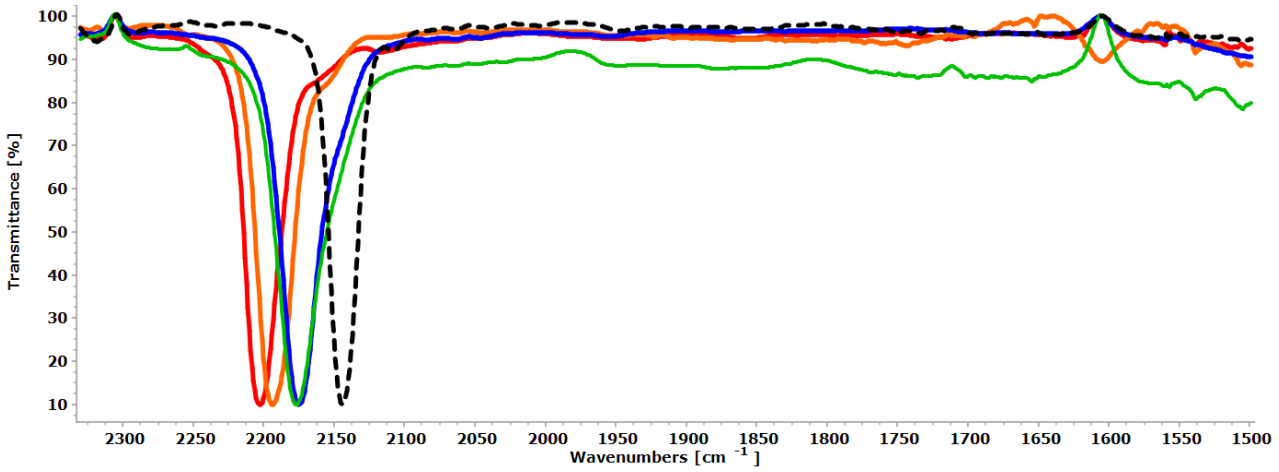

Figure S49. Solvent-subtracted IR spectra (1300-2700 cm^{-1}) of **1c** (orange line), **2c** (blue line) and (*S*)-α-methylbenzyl isocyanide (black dashed line) in CH_2Cl_2. The transmittance of the C≡N stretching peaks is normalized.

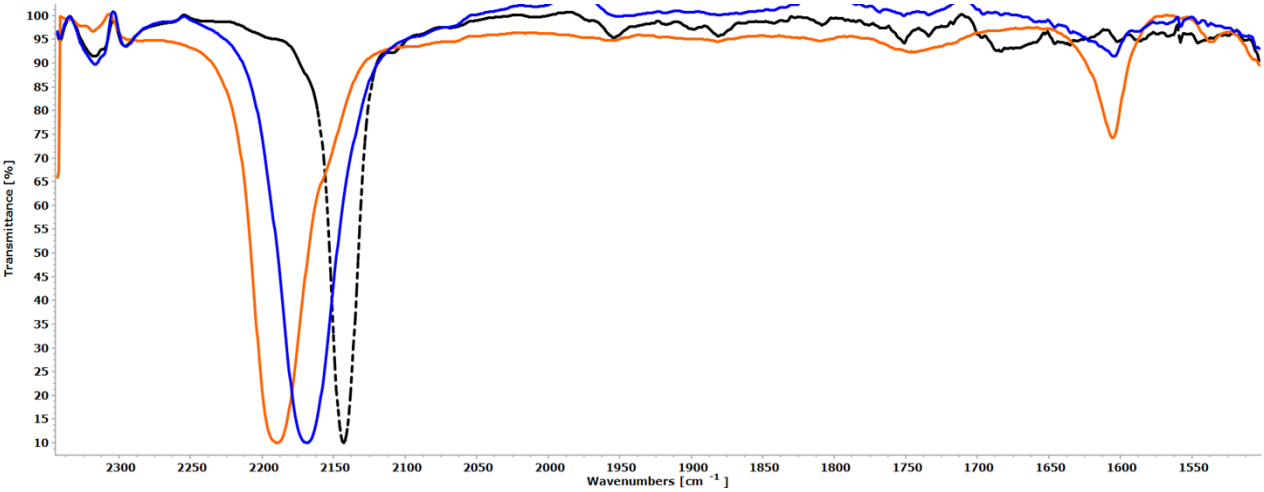

Figure S50. Solvent-subtracted IR spectra (1750-2300 cm^{-1}) of **1d** (orange line), **2d** (blue line), **3d** (red line) and diethyl isocyanomethyl phosphonate (black dashed line) in CH_2Cl_2. The transmittance of the C≡N stretching peaks is normalized.

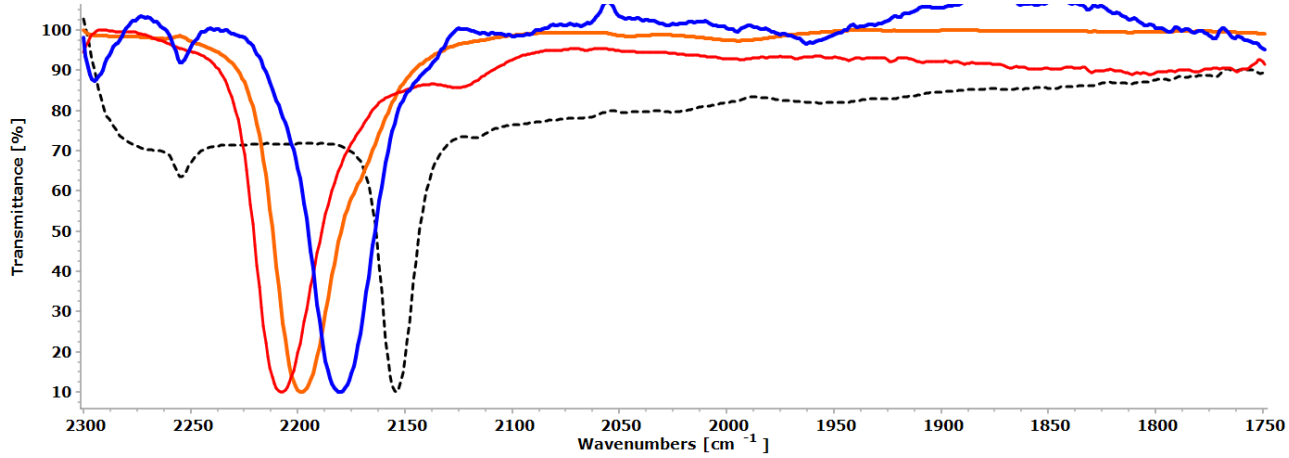

Figure S51. Solvent-subtracted IR spectra (1500-2300 cm^{-1}) of **1e** (orange line) and ethyl isocyanoacetate (black dashed line) in CH_2Cl_2. The transmittance of the C≡N stretching peaks is normalized.

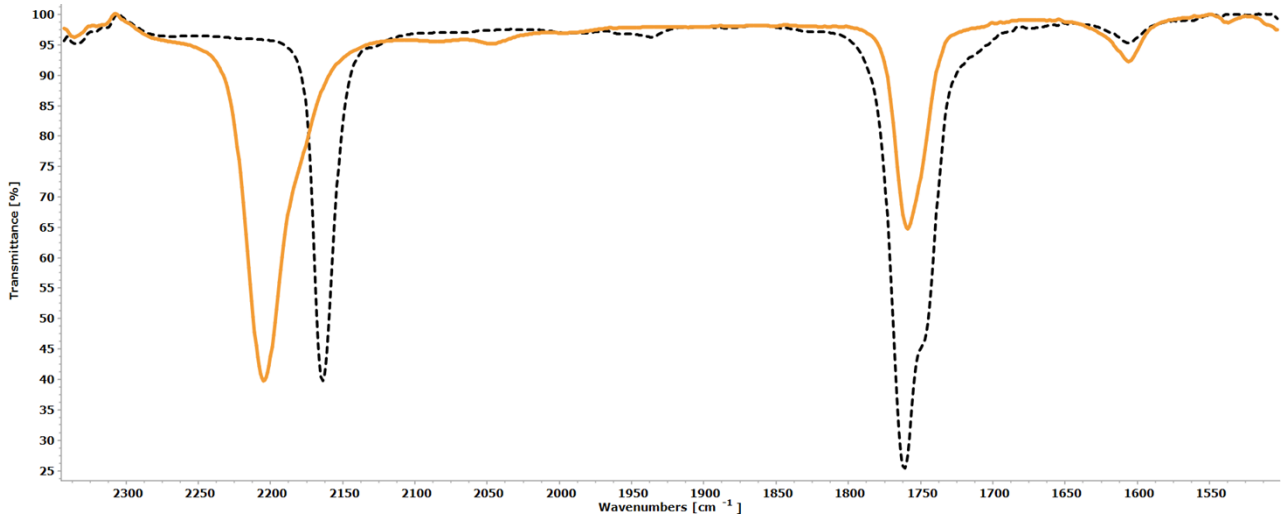

Figure S52. Solvent-subtracted IR spectra (1300-2700 cm^{-1}) of **1f** (orange line), **2f** (blue line), **3f** (red line) and xylyl isocyanide (black dashed line) in CH_2Cl_2. The transmittance of the C≡N stretching peaks is normalized.

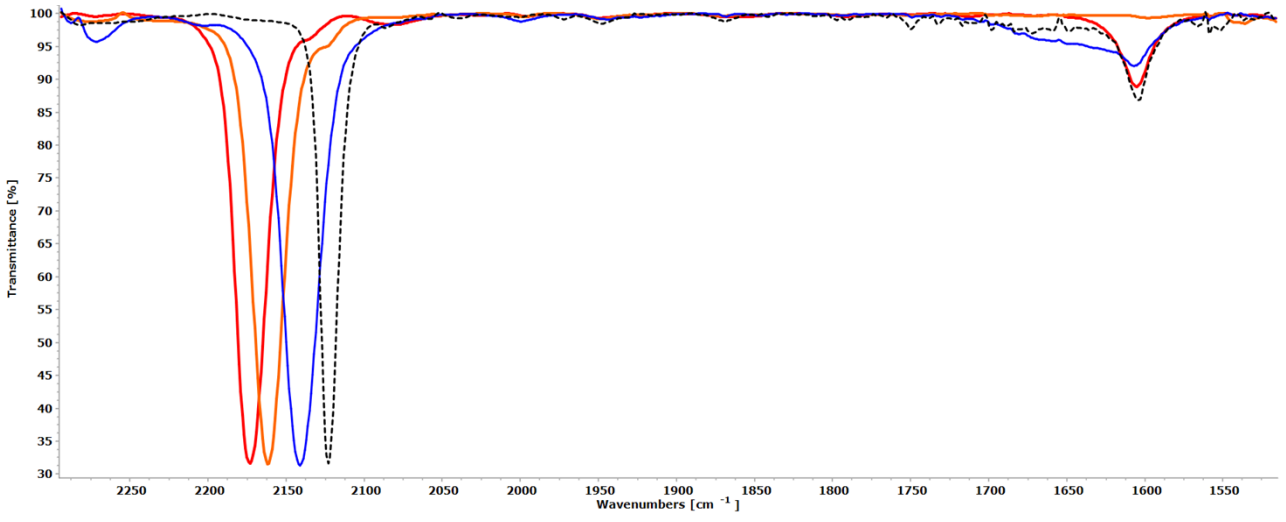

Figure S53. Solvent-subtracted IR spectra (1550-2300 cm^{-1}) of **1g** (orange line) and 4-methoxyphenyl isocyanide (black dashed line) in CH_2Cl_2. The transmittance of the C≡N stretching peaks is normalized.

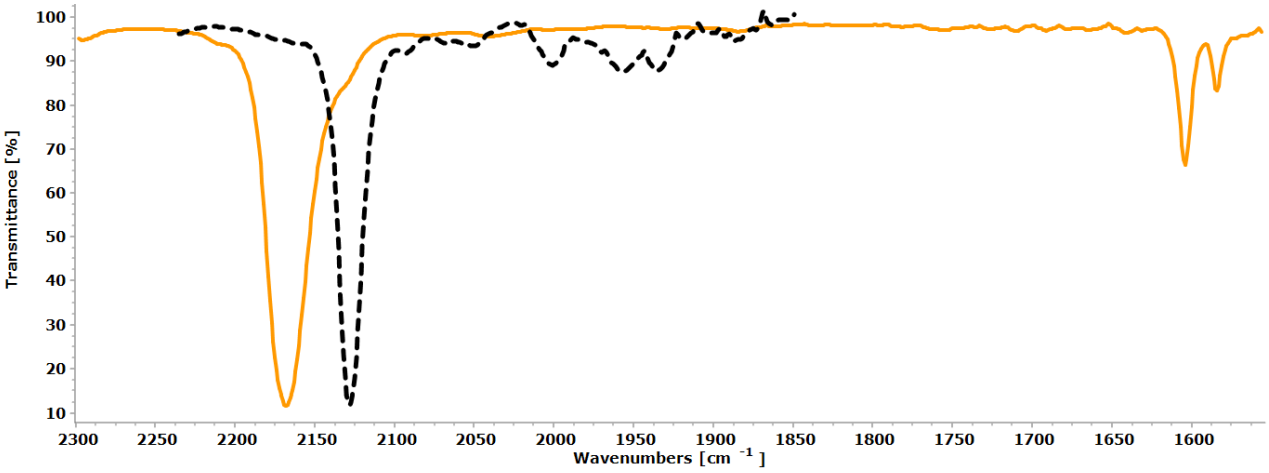

Table S1. Comparison of selected IR and ^{13}C NMR data for $[RuCl_2(CNR)(\eta^6\text{-}p\text{-cymene})]$ (**1**), $[RuI_2(CNR)(\eta^6\text{-}p\text{-cymene})]$ (**1-I**), $[RuCl_2(CNR)(\eta^6\text{-}C_6Me_6)]$ (**2**), $[RuCl_2(CNR)(\eta^6\text{-}C_6H_6)]$ (**3**) complexes and the corresponding isocyanide (CNR). All data are from this work except where otherwise noted. The letters (**a-g**) are given only to the isocyanides investigated in this work. Coordination-induced shifts (Δν or Δδ, for IR and NMR data, respectively - rounded to the first digit) are given in parentheses.

Isocyanide substituent R		**IR: ν(CN) / cm^{-1} (*Δν / cm^{-1}*)[a] in CH_2Cl_2** **^{13}C NMR: δ(CN) / ppm (*Δδ / ppm*)[a] in $CDCl_3$**			
Compound		$R-\overset{+}{N}\equiv C^-$	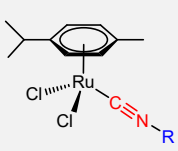 **1**	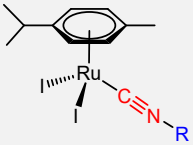 **1-I**	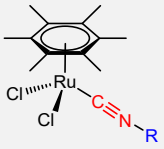 **2**	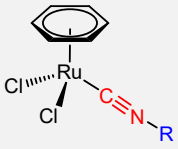 **3**
	**a**	2168 156.0 [b]	2218 (*+50*) 139.2 (*−17*)	*n.r.*	2200 (*+32*) 144.3 (*−12*)	*n.r.*
	**b**	2144 154.0	2194 [c] (*+50*) 138.7 [c] (*−15*)	2177 (*+33*) 136.3 (*−18*)	2175 (*+31*) 143.4 (*−11*)	2203 (*+59*) 136.1 (*−18*)
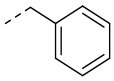		2155 157.7 [b]	2200 [c] (*+45*) 141.3 [c] (*−16*)	*n.r.*	*n.r.*	*n.r.*
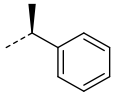	**c**	2143 156.4 [c]	2189 (*+46*) 141.2 (*−15*)	*n.r.*	2169 (*+26*) 146.3 (*−10*)	*n.r.*
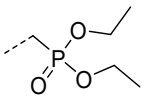	**d**	2154 160.5 [b]	2198 (*+44*) 144.6 (*−16*)	*n.r.*	2180 (*+26*) 149.6 (*−11*)	2208 (*+54*) 142.2 (*−18*)
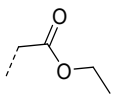	**e**	2164 163.7 [b]	2205 (*+41*) 146.4 (*−17*)	*n.r.*	*2194* (*+30*) [d] 149.0 (*−15*) [d]	*n.r.*
		2139 152.6 [b]	2186 [c] (*+47*) 137.9 [c] (*−15*)	2169 [c] (*+30*) 135.8 [c] (*−17*)	*2174* (*+35*) [d] 142.7 (*−10*) [d]	*n.r.*
	**f**	2123 167.6	2162 [c] (*+ 39*) 151.7 [c] (*−16*)	*2144* (*+ 21*) [e] 149.1 (*−19*) [e]	2141 (*+ 18*) 157.3 (*−10*)	2172 (*+ 49*) 149.5 (*−18*)
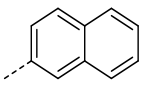		2127 [f] 164.3 [b]	2160 [c,f] (*+33*) 149.5 [c] (*−15*)	*n.r.*	*n.r.*	*n.r.*
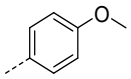	**g**	2128 162.6 [b]	2168 (*+40*) 147.4 (*−15*)	*n.r.*	*n.r.*	*n.r.*

[a] Coordination-induced shift (Ru-CNR minus free CNR). [b] Taken from the literature.[8,9,10,11,12,13,14,15] [c] Taken from our previous work.[16] [d] Taken from the literature; IR data refer to solid state (KBr).[17] [e] Taken from the literature; IR data refer to solid state (ATR).[18] [f] Only the major IR band is reported. *n.r* = the compound has not been reported either in this work or in the literature.

Figure S54. Molecular structure of **1c**. Displacement ellipsoids are at the 50 % probability level.

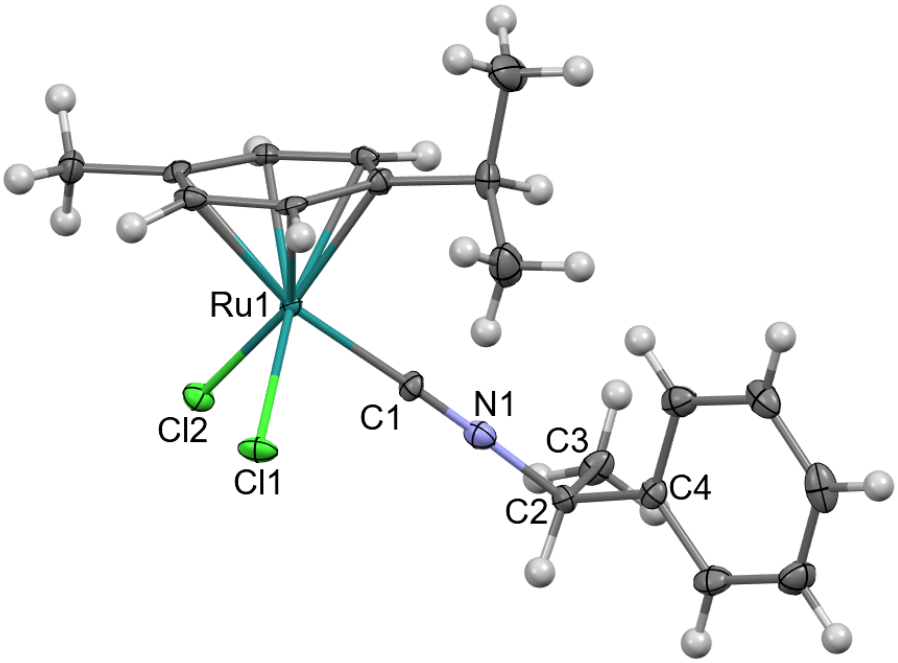

Figure S55. Molecular structure of **1e** in **1e**·CH_2Cl_2. Displacement ellipsoids are at the 50 % probability level.

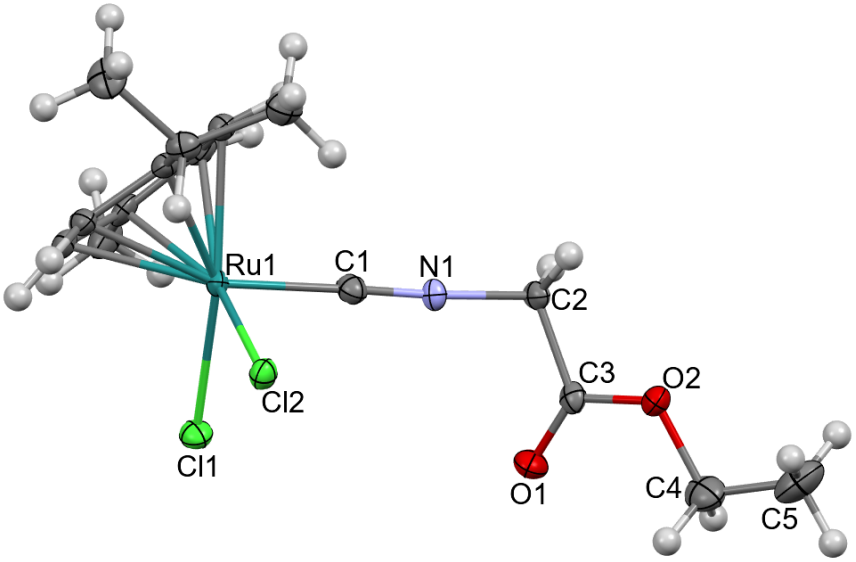

Figure S56. Molecular structure of **1g** in **1g**·$CHCl_3$. Displacement ellipsoids are at the 50 % probability level.

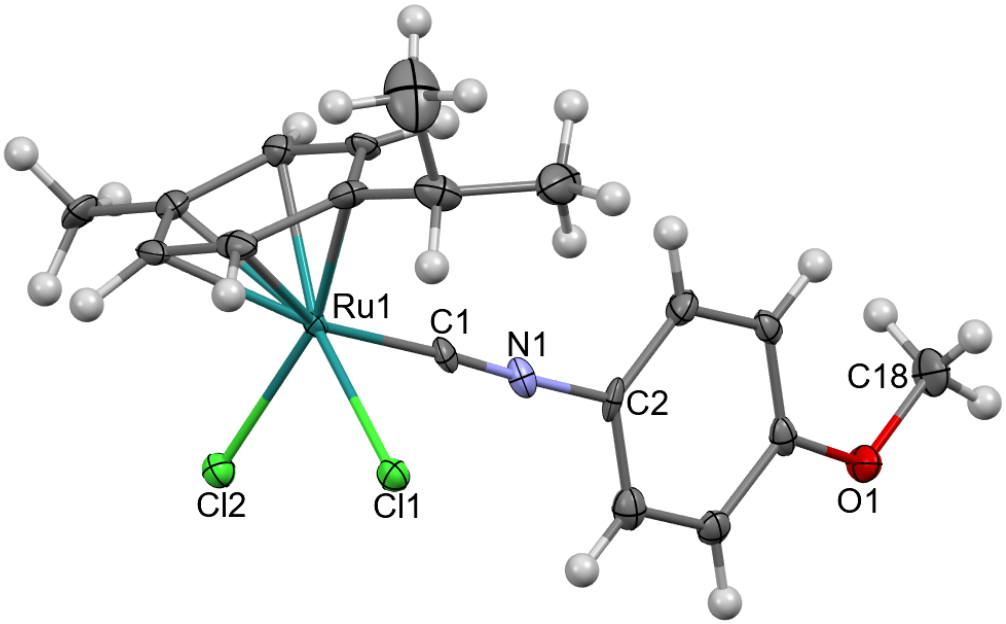

Table S2. Main bond distances (Å) and angles (°) of **1a, 1c, 1e, 1g**, **2c** and **1b-l.**

	1a	**1c**	**1e**·½CH_2Cl_2	**1g**·$CHCl_3$	**2c**·H_2O	**1b-l**
Ru1-C(arene)$_{av}$	2.20(2)	2.210(17)	2.215(12)	2.20(2)	2.224(7)	2.221(10)
Ru1-X1*	2.416(2)	2.4074(17)	2.4000(13)	2.399(2)	2.4136(8)	2.7148(4)
Ru1-X2*	2.411(2)	2.4008(15)	2.4067(12)	2.404(2)	2.4190(7)	2.7134(4)
Ru1-C1	1.981(10)	1.969(6)	1.960(5)	1.954(8)	1.961(3)	1.962(4)
C1-N1	1.209(15)	1.150(8)	1.172(10)	1.156(11)	1.151(4)	1.142(5)
N1-C2	1.459(17)	1.441(8)	1.446(12)	1.404(10)	1.457(4)	1.453(5)
X1-Ru1-X2*	87.85(9)	87.52(6)	86.63(4)	88.17(8)	87.55(3)	89.357(12)
X1-Ru1-C1*	84.6(3)	84.94(19)	87.20(15)	85.5(3)	87.15(9)	84.32(12)
C1-Ru1-X2*	88.9(3)	85.3(2)	87.01(16)	84.8(2)	87.85(8)	86.00(12)
Ru1-C1-N1	165.7(12)	178.3(7)	172.7(8)	177.2(8)	176.1(3)	176.2(4)
C1-N1-C2	174.8(19)	178.2(7)	176.5(18)	176.7(10)	178.6(3)	173.2(4)

* X = Cl for **1a, 1c, 1e, 1g**, **2c**; X = I for **1b-l.**

Figure S57. Solid-state IR spectrum (650-4000 cm^{-1}) of [RuCl(CCPh)(CNCy)(η^6-C_6Me_6)], **4b**.

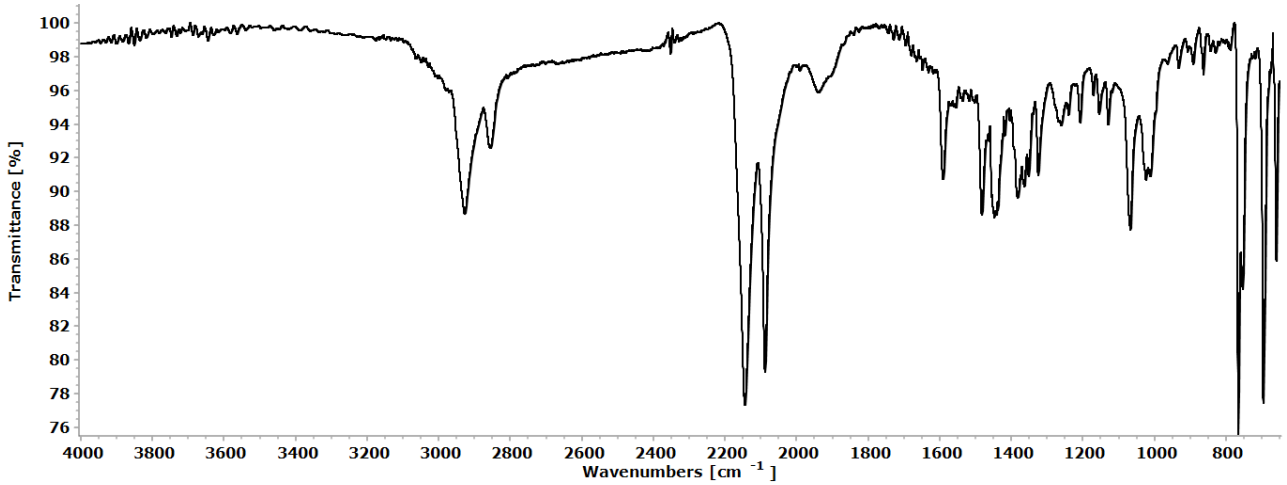

Figure S58. Solvent-subtracted IR spectra (1600-2300 cm^{-1}) of **4b** (green line), **2b** (red line) and cyclohexyl isocyanide (black dashed line) in CH_2Cl_2. The transmittance of the C≡N stretching peaks is normalized.

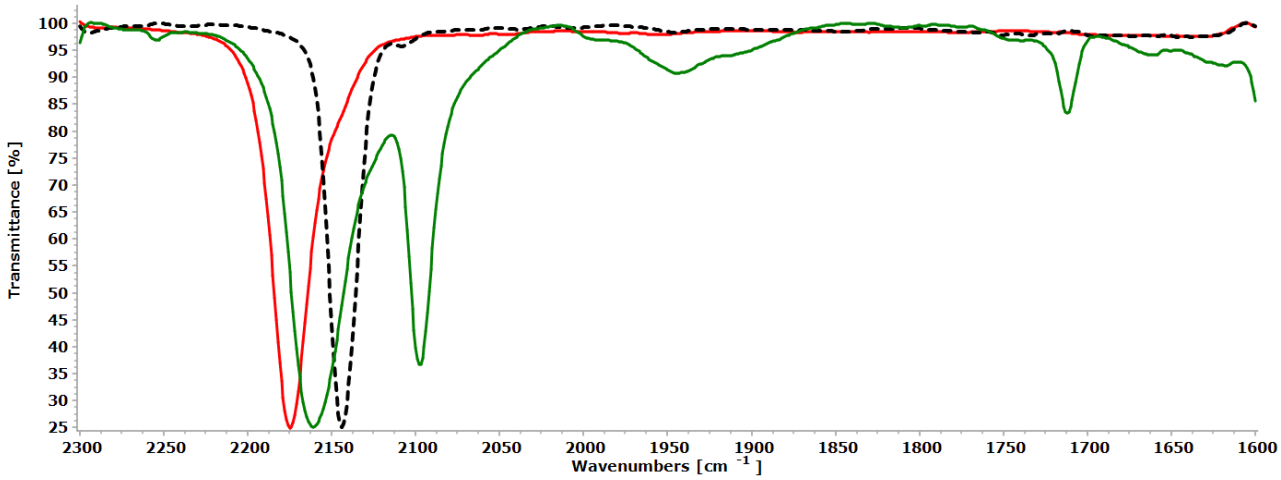

Figure S59. ^{1}H NMR spectrum (400 MHz, $CDCl_3$) of **4b.**

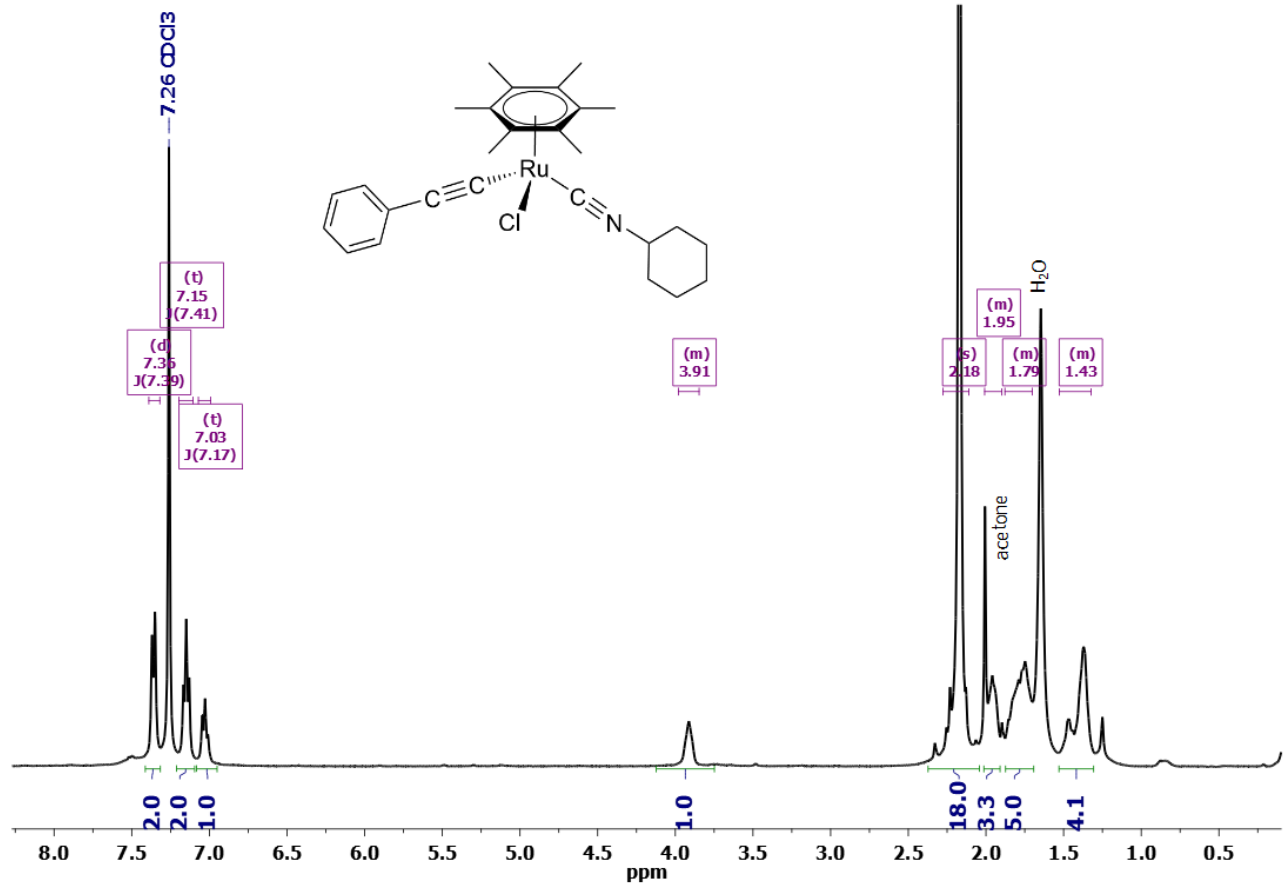

Figure S60. $^{13}C\{^{1}H\}$ NMR spectrum (100 MHz, $CDCl_3$) of **4b**.

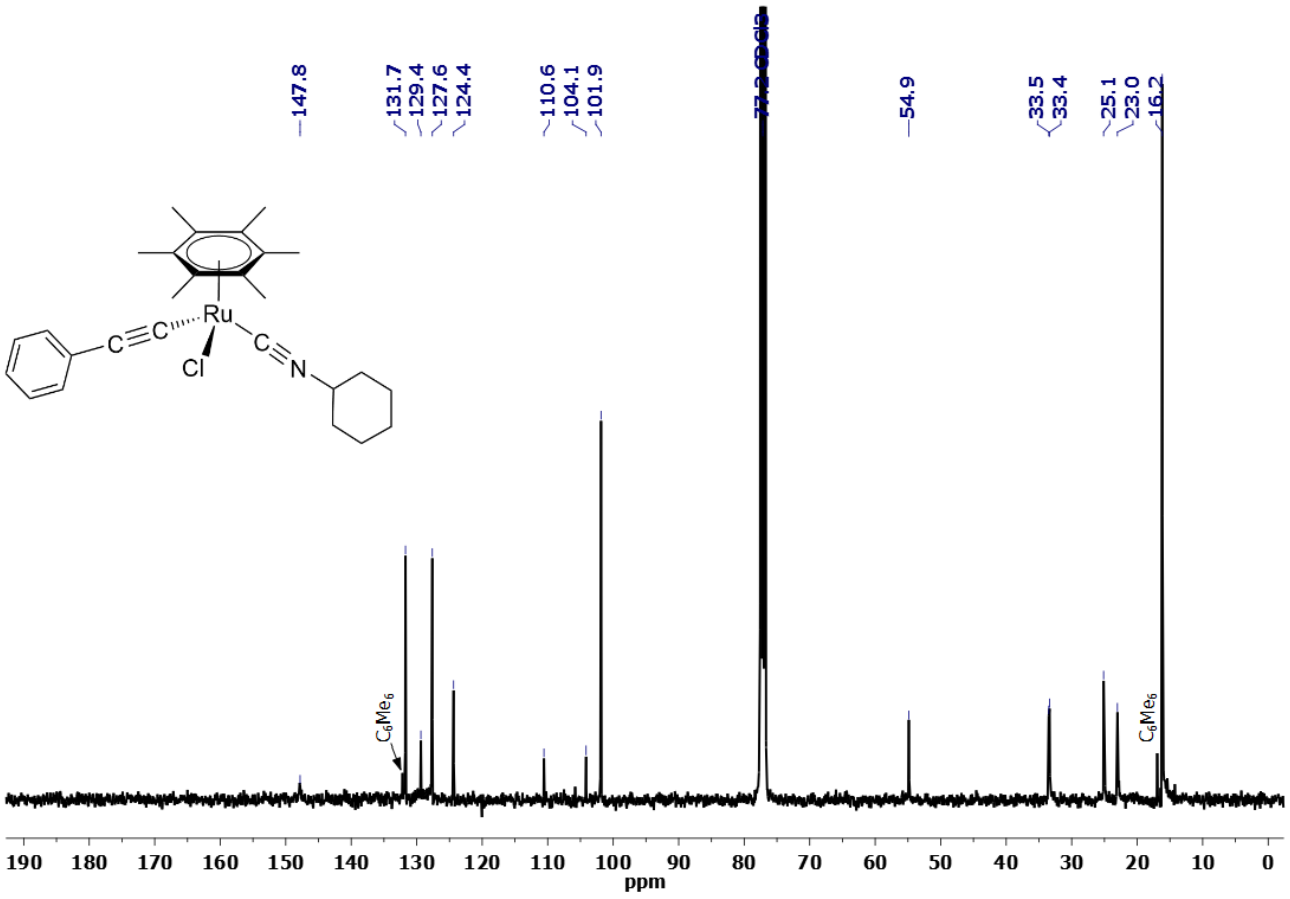

Figure S61. Solid-state IR spectrum (650-4000 cm^{-1}) of [RuCl(CCPh)(CNXyl)(η^6-C_6Me_6)], **4f**.

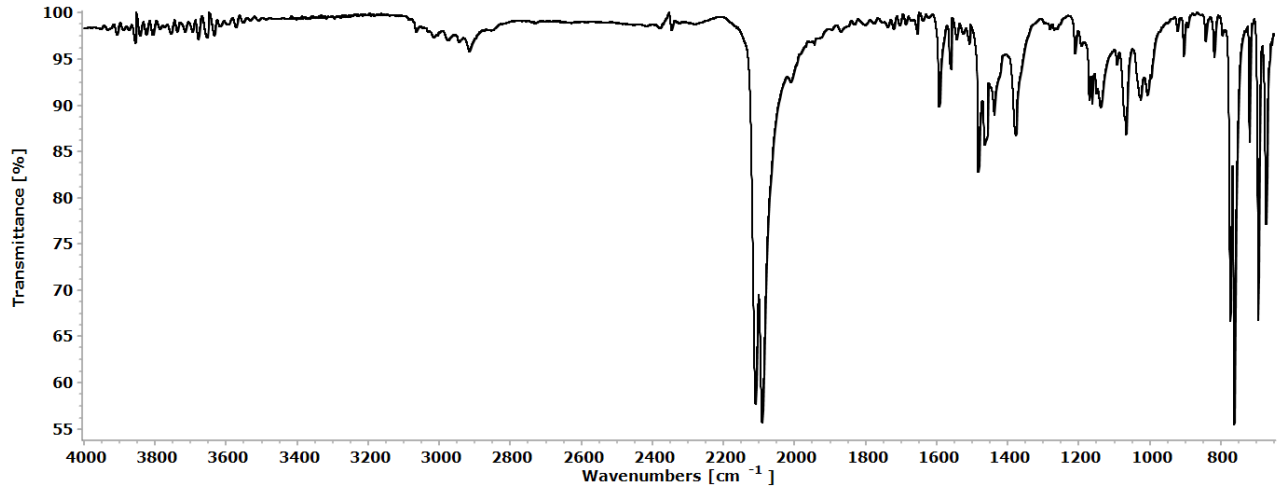

Figure S62. Solvent-subtracted IR spectra (1500-2300 cm^{-1}) of **4f** (green line), **2f** (red line) and xylyl isocyanide (black dashed line) in CH_2Cl_2. The transmittance of the C≡N stretching peaks is normalized.

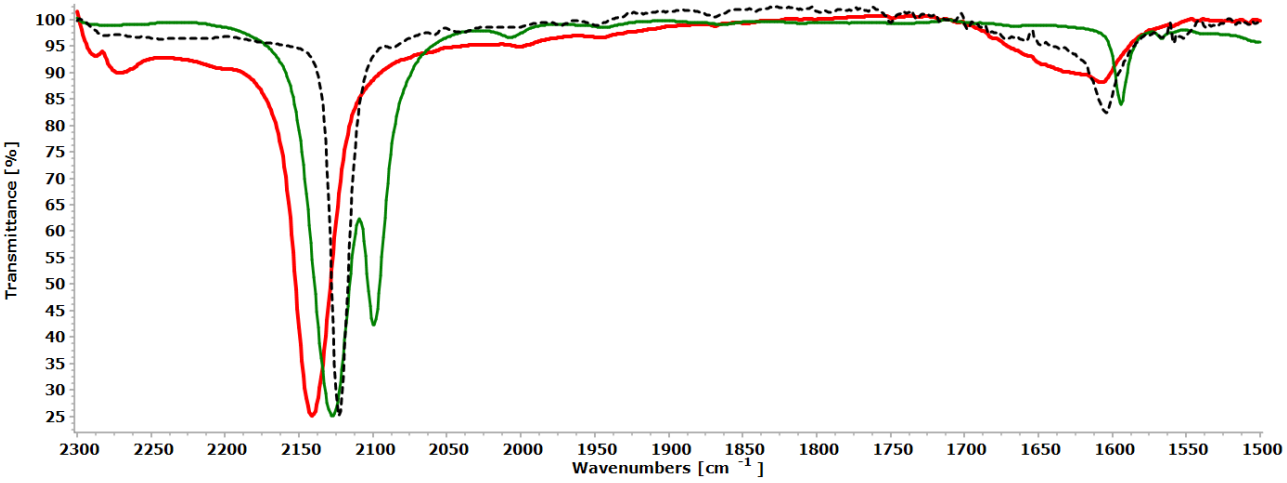

Figure S63. ^{1}H NMR spectrum (400 MHz, $CDCl_3$) of **4f.**

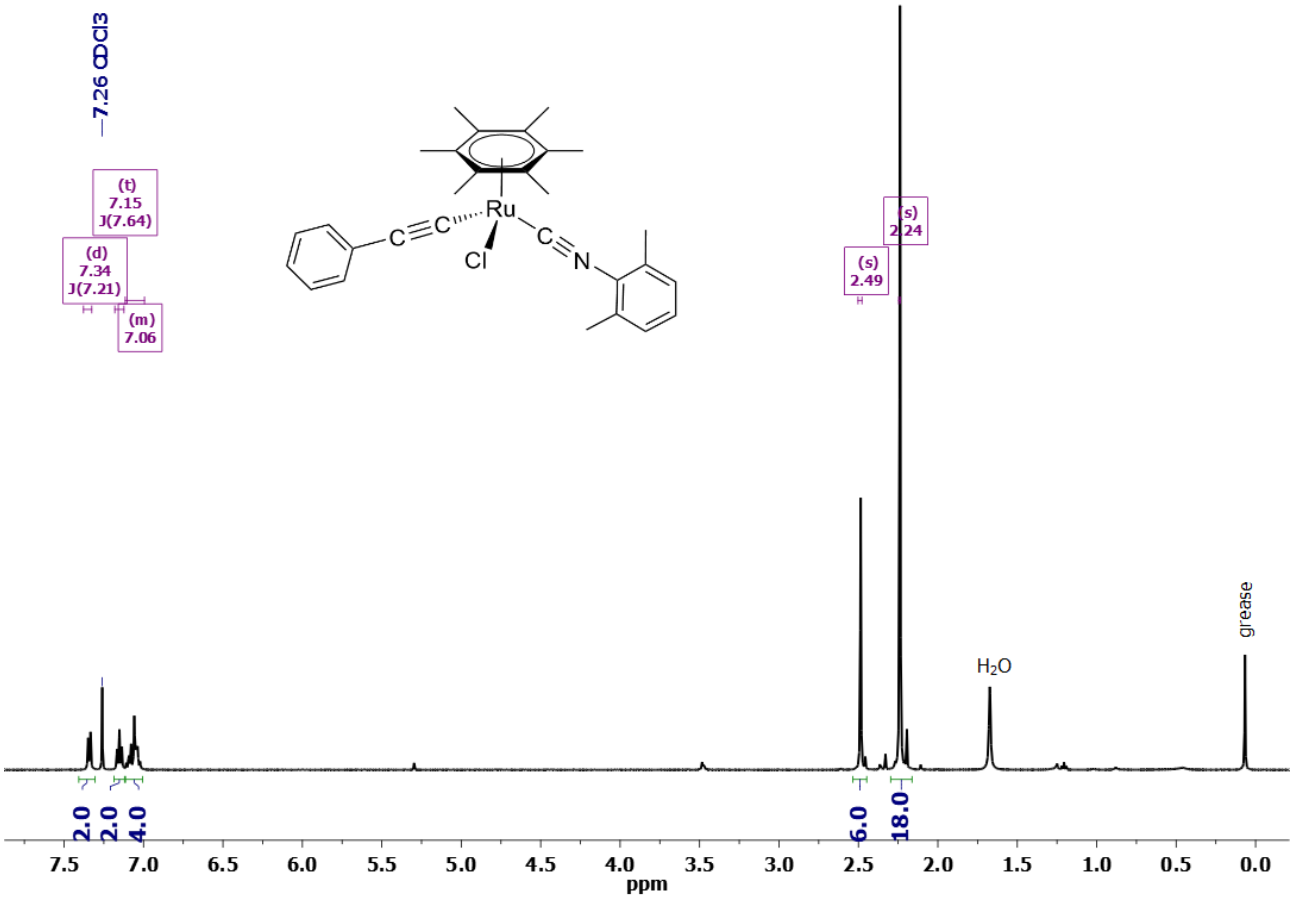

Figure S64. $^{13}C\{^{1}H\}$ NMR spectrum (100 MHz, $CDCl_3$) of **4f**.

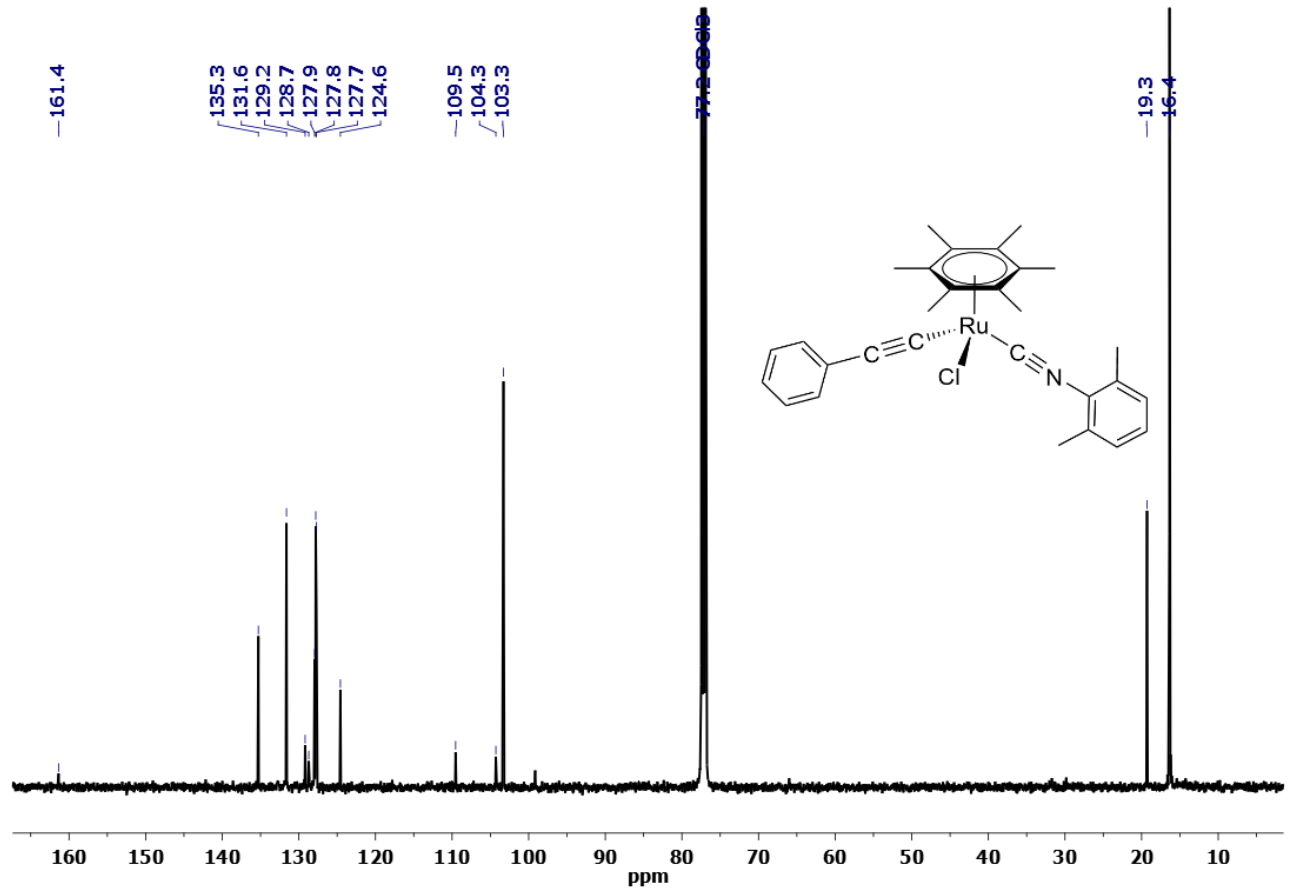

Figure S65. Solid-state IR spectra (650-4000 cm^{-1}) of $[RuCl_2(MeCN)_3(CNCy)]$, **5b** (original sample, black line) and the solid recovered from a CD_3CN solution of **5b** kept for 24h at 50 °C (red line). The transmittance of the main isocyanide stretching peak is normalized.

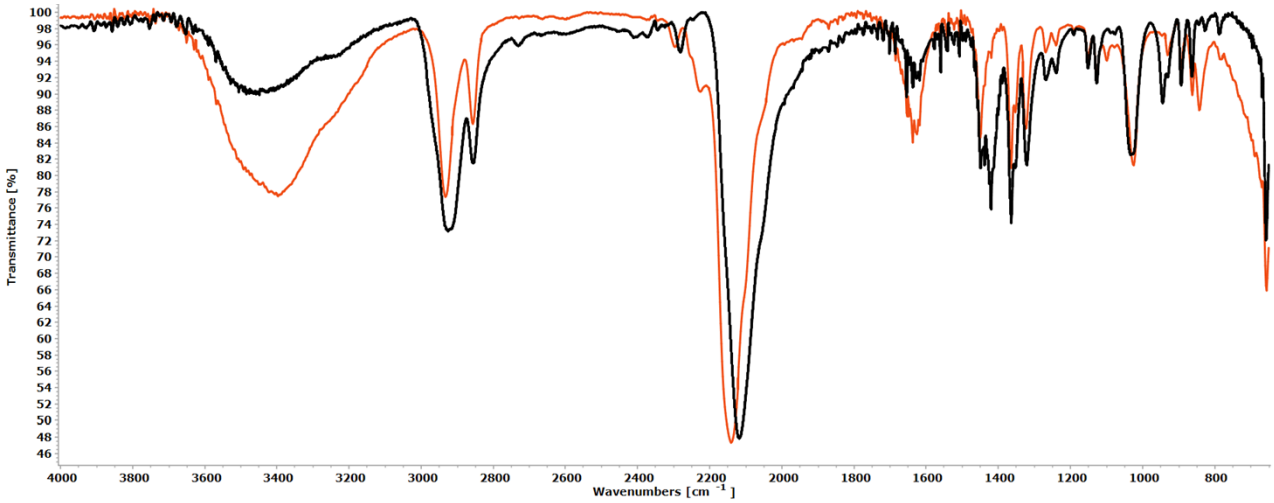

Figure S66. Solvent-subtracted IR spectra (1500-2500 cm^{-1}) of **5b** (violet line) and cyclohexyl isocyanide (black dashed line) in CH_2Cl_2.

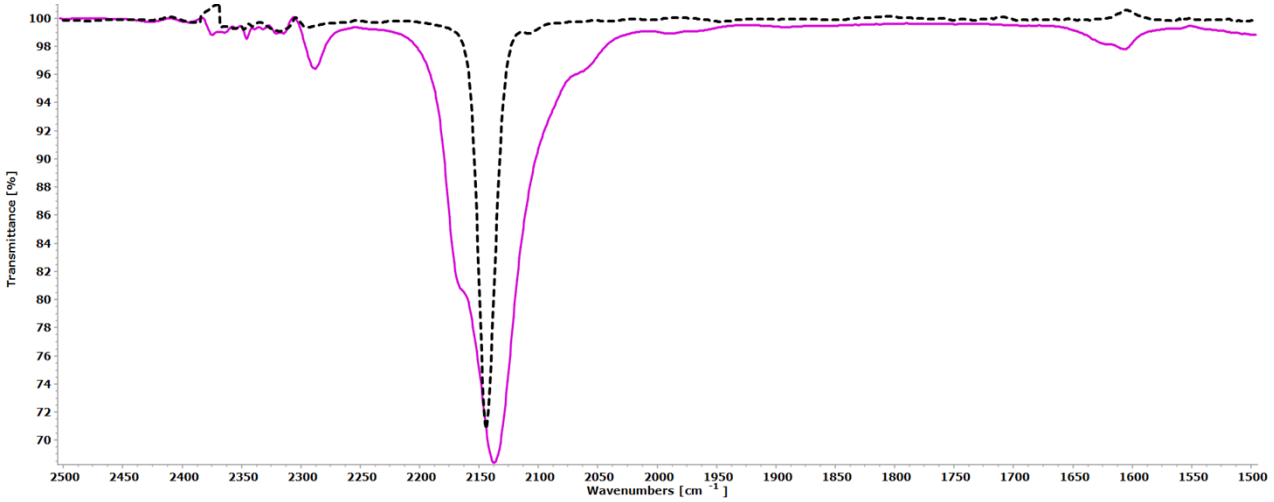

Figure S67. ^{1}H NMR spectrum (400 MHz, CD_3CN) of **5b** (mixture of isomers; freshly-prepared solution).

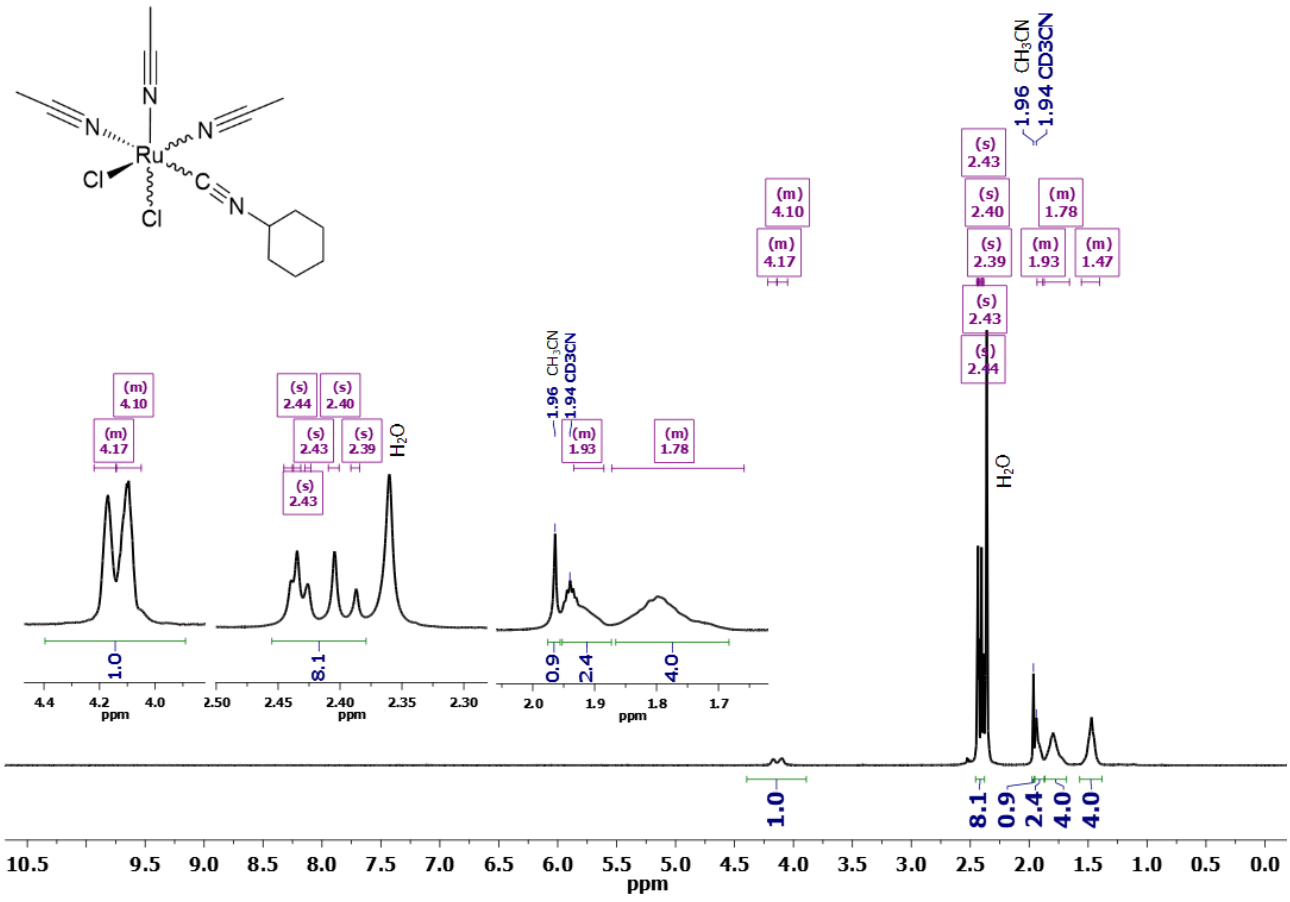

Figure S68. Changes in the ^{1}H NMR spectrum (400 MHz, CD_3CN; 1.85-2.60 and 3.90-4.50 ppm) of **5b** over time: freshly-prepared solution (top, violet line); after 30' at room temperature (cyan line); after 14 h at room temperature (yellow-ochre line) - identical after several days; after 24 h at 50 °C (bottom, red line).

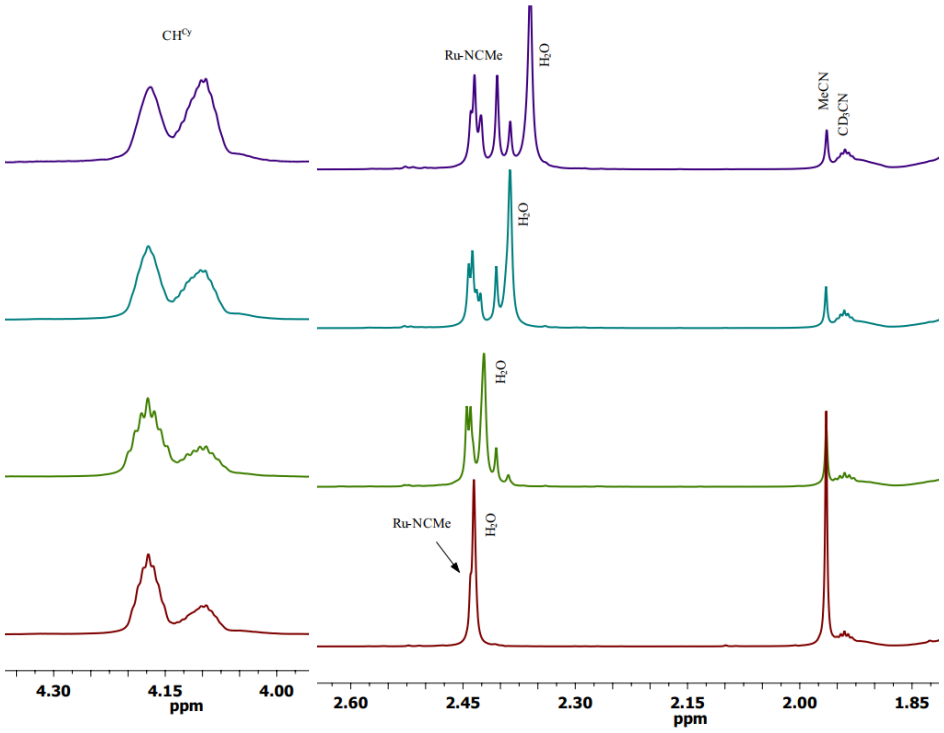

Figure S69. $^{13}C\{^{1}H\}$ NMR spectrum (100 MHz, CD_3CN) of **5b** (mixture of isomers)

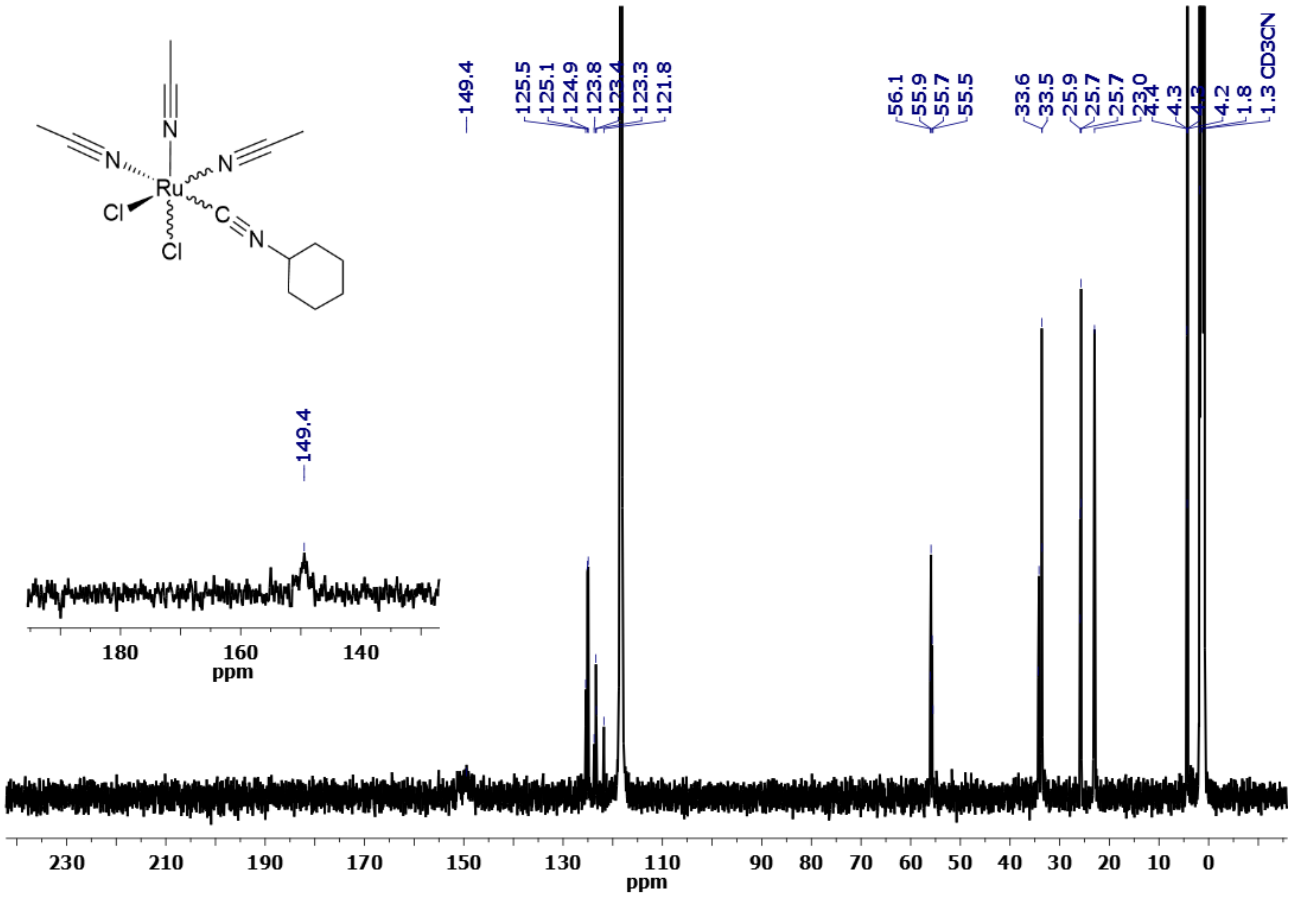

Figure S70. Solid-state IR spectra (650-4000 cm^{-1}) of $[RuCl_2(MeCN)_3(CNXyl)]$, **5f** (original sample, black line) and the solid recovered from a CD_3CN solution of **5f** kept for 24h at 50 °C (red line). The intensity of the main isocyanide stretching peak is normalized.

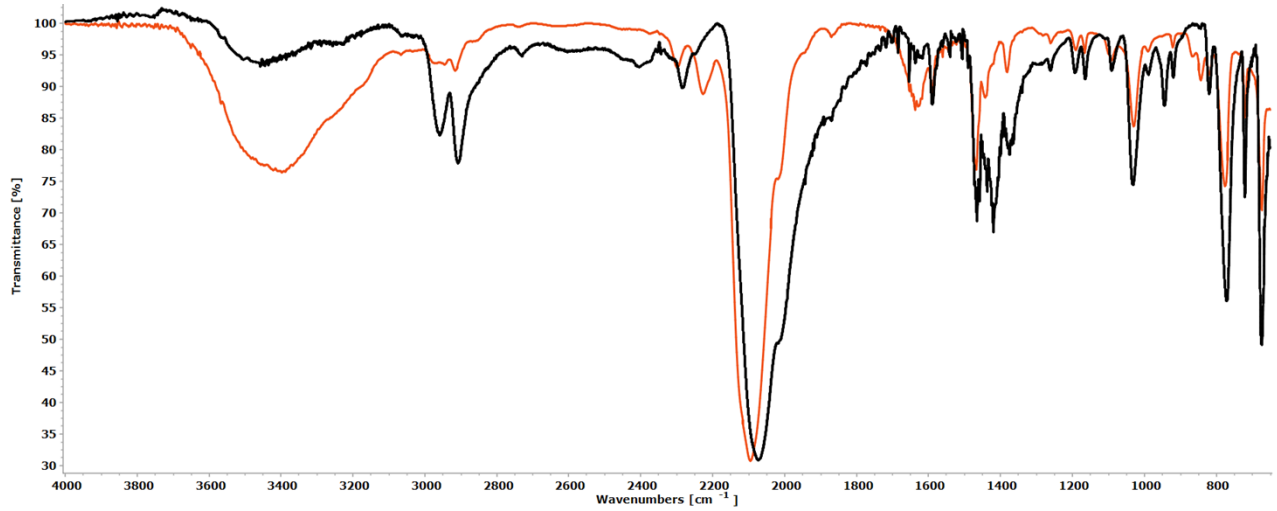

Figure S71. Solvent-subtracted IR spectra (1300-2500 cm^{-1}) of **5f** (violet line) and xylyl isocyanide (black dashed line) in CH_2Cl_2.

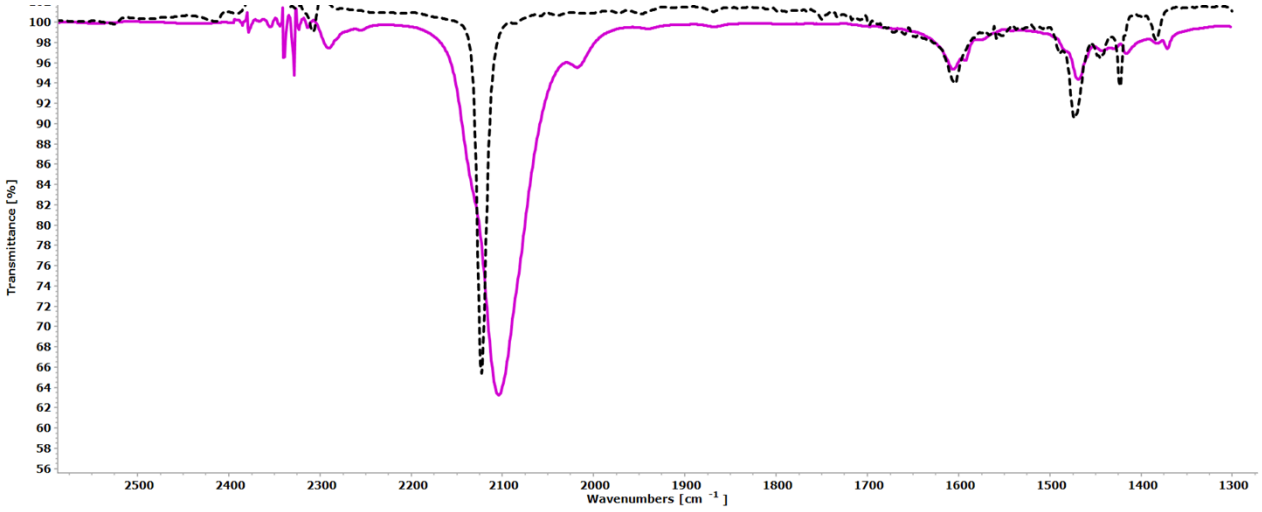

Figure S72. ^1H NMR spectrum (400 MHz, CD_3CN) of **5f** (mixture of isomers; freshly-prepared solution).

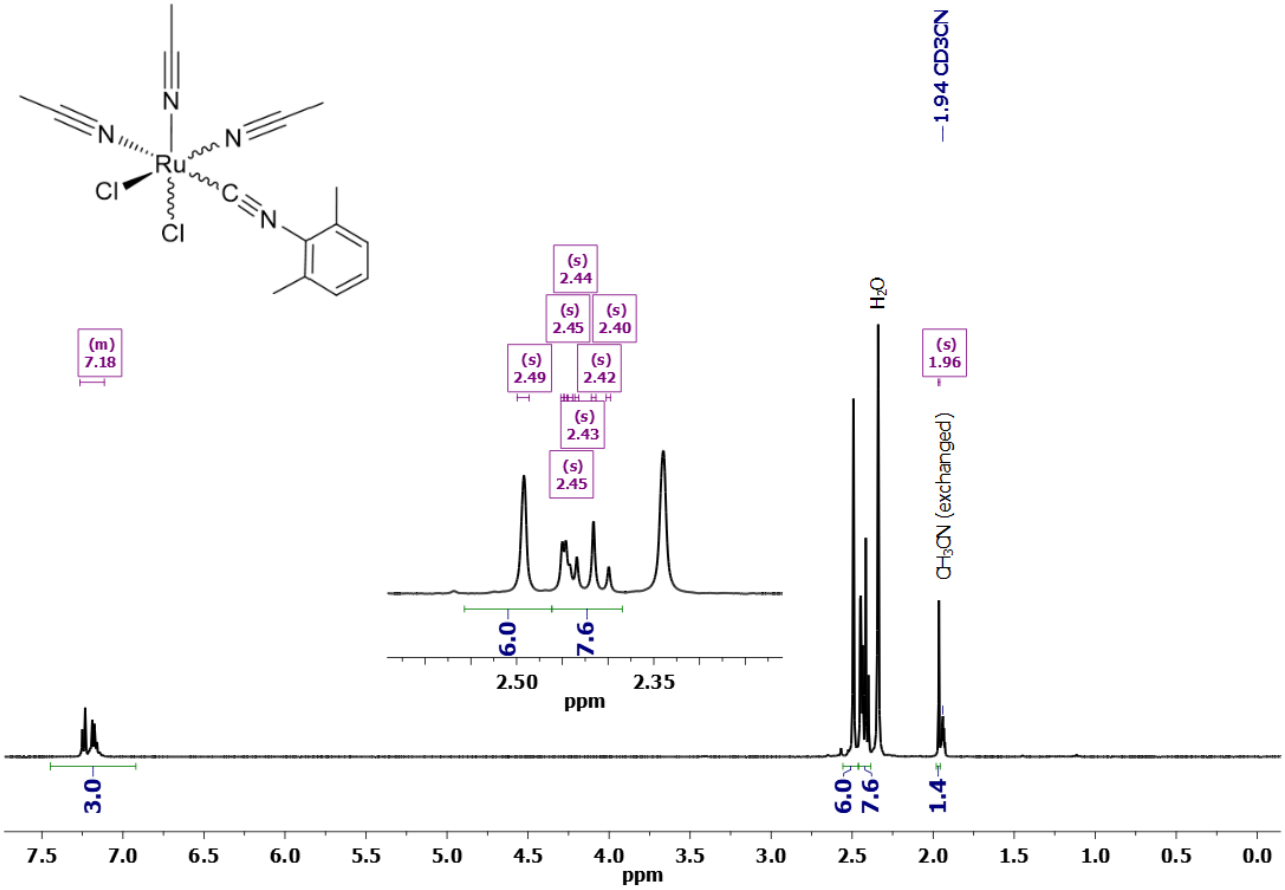

Figure S73. Changes in the ^{1}H NMR spectrum (400 MHz, CD_3CN; 1.85-2.60 ppm) of **5f** over time: freshly-prepared solution (top, violet line), after 14 h at room temperaure (cyan line), after 10 days at room temperature (bottom, olive green line), after 24 h at 50 °C (bottom, red line).

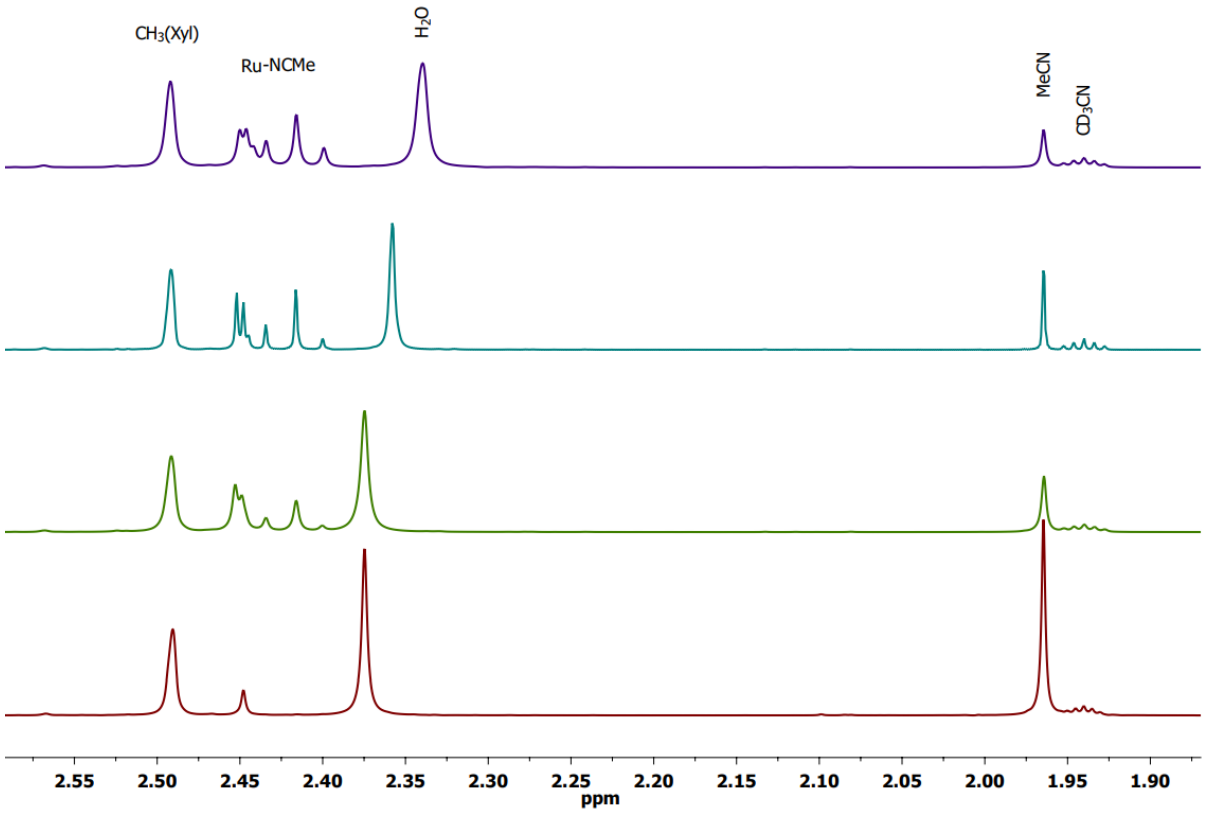

Figure S74. $^{13}C\{^{1}H\}$ NMR spectrum (100 MHz, CD_3CN) of **5f** (mixture of isomers).

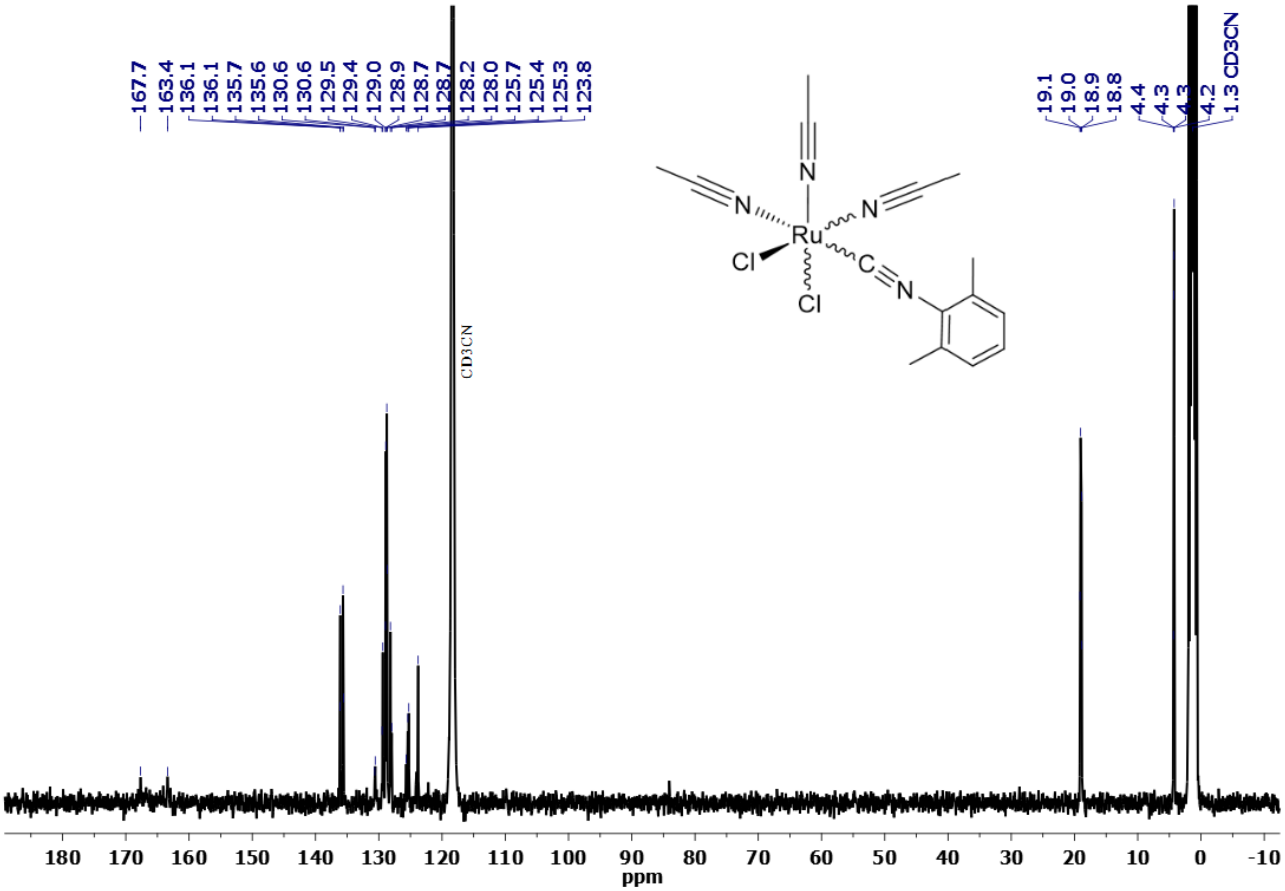

Table S3. Main bond distances (Å) and angles (°) of **4b** and **4f**.

	4b	**4f**
Ru1-C(arene)$_{av}$	2.254(7)	2.256(10)
Ru1-Cl1	2.4093(7)	2.4067(10)
Ru1-C1	1.931(3)	1.929(4)
Ru1-C11	2.020(3)	2.025(4)
C1-N1	1.156(4)	1.152(5)
N1-C2	1.446(4)	1.402(5)
C11-C12	1.208(4)	1.170(6)
C12-C13	1.443(4)	1.459(6)
Cl1-Ru1-C1	88.85(8)	87.47(11)
Cl1-Ru1-C11	91.06(8)	88.28(11)
C1-Ru1-C11	83.15(11)	84.70(15)
Ru1-C1-N1	178.0(3)	179.3(4)
C1-N1-C2	169.4(3)	165.6(4)
Ru1-C11-C12	171.1(3)	176.9(4)
C11-C12-C13	172.6(3)	176.6(5)

Catalytic studies

Figure S75. GC-MS chomatogram of the reaction of dimerization/trimerization of phenylacetylene. Conditions: acetonitrile, phenylacetylene (1.0 mmol), Na_2CO_3 (100 μmol), **1b** (25 μmol), 80 °C, 24 h.

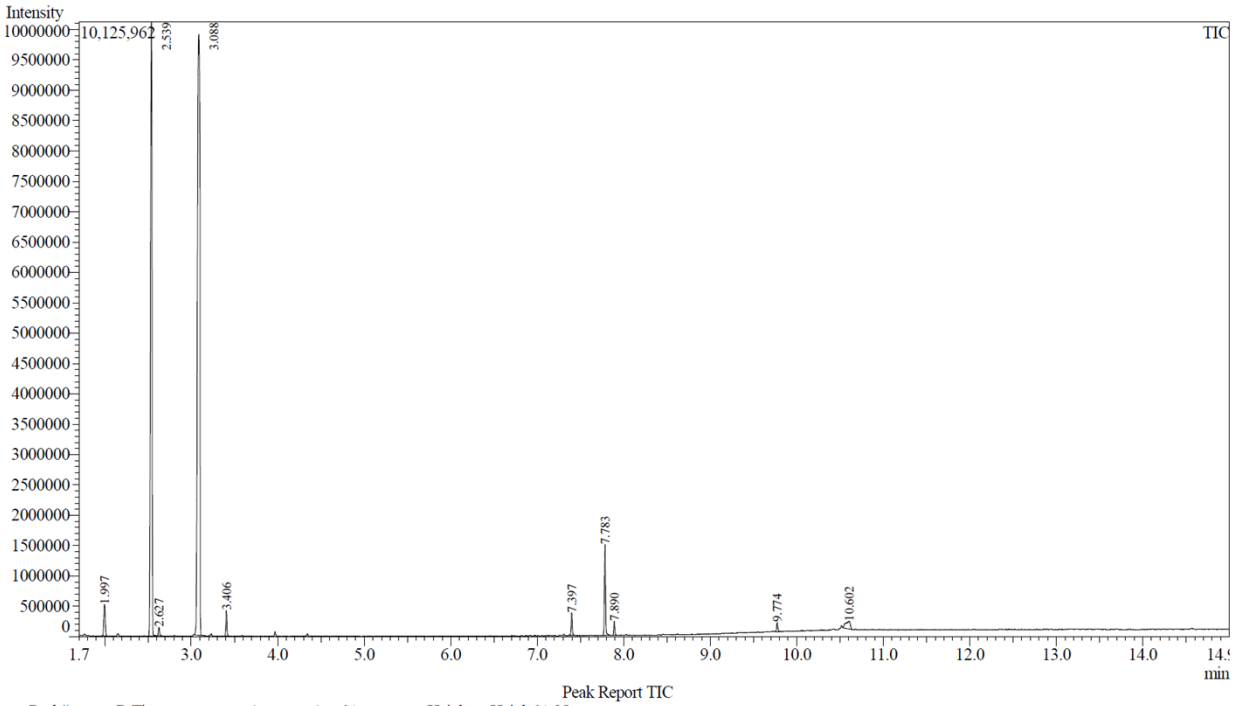

Peak Report TIC

Peak#	R.Time	Area	Area%	Height	Height%	Name
1	1.997	605511	1.74	518722	2.21	Toluene
2	2.539	12569315	36.10	10113587	43.13	Phenylethyne
3	2.627	132131	0.38	137471	0.59	Styrene
4	3.088	18724543	53.78	9897107	42.20	Benzene, 1,2,3-trimethyl-
5	3.406	342416	0.98	421395	1.80	o-Cymene
6	7.397	321852	0.92	371907	1.59	Dibenzo[a,e]cyclooctene
7	7.783	1341625	3.85	1489779	6.35	Dibenzo[a,e]cyclooctene
8	7.890	179940	0.52	225622	0.96	Benzene, 1,1'-(1,3-butadiyne-1,4-diyl)bis-
9	9.774	138308	0.40	150357	0.64	1,1':2',1"-Terphenyl, 4'-phenyl-
10	10.602	459356	1.32	125085	0.53	1,4-Methanonaphthalene, 9-(diphenylmethyler
		34814997	100.00	23451032	100.00	

<< Target >>
Line#:5 R.Time:3.405(Scan#:342) MassPeaks:346
RawMode:Averaged 3.400-3.410(341-343) BasePeak:119.05(120300)
BG Mode:Calc. from Peak Group 1 - Event 1 Scan

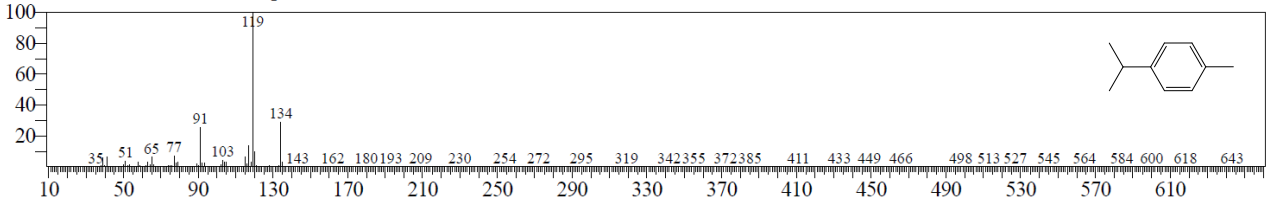

Line#:6 R.Time:7.395(Scan#:1140) MassPeaks:365
RawMode:Averaged 7.390-7.400(1139-1141) BasePeak:204.05(59275)
BG Mode:Calc. from Peak Group 1 - Event 1 Scan

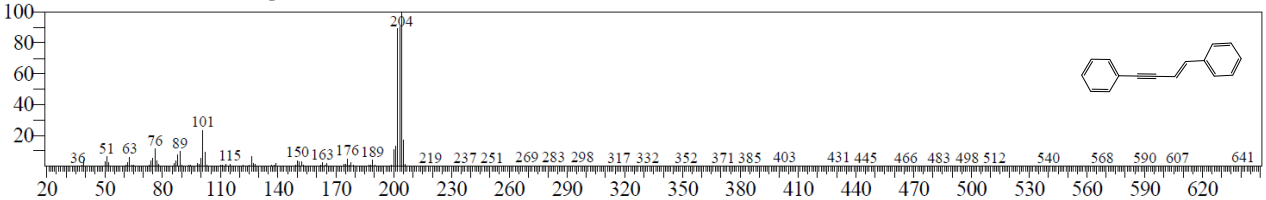

Line#:7 R.Time:7.785(Scan#:1218) MassPeaks:363
RawMode:Averaged 7.780-7.790(1217-1219) BasePeak:204.05(238711)
BG Mode:Calc. from Peak Group 1 - Event 1 Scan

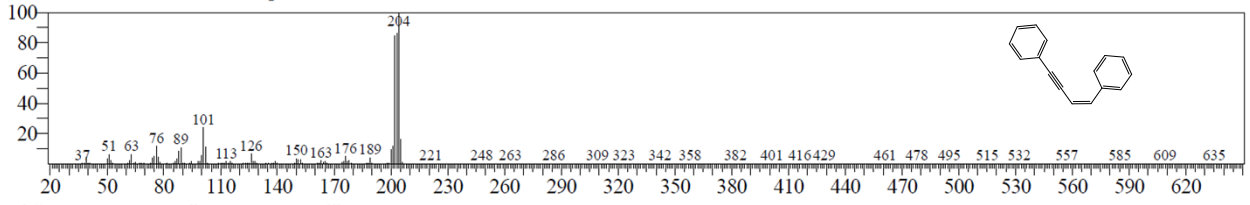

<< Target >>
Line#:8 R.Time:7.890(Scan#:1239) MassPeaks:388
RawMode:Averaged 7.885-7.895(1238-1240) BasePeak:202.00(64340)
BG Mode:Calc. from Peak Group 1 - Event 1 Scan

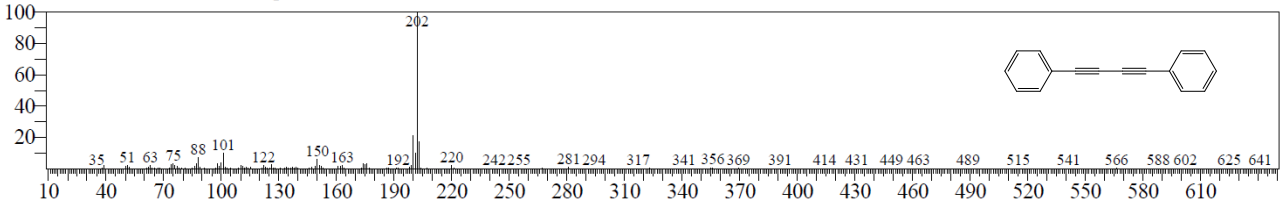

Line#:9 R.Time:9.775(Scan#:1616) MassPeaks:405
RawMode:Averaged 9.770-9.780(1615-1617) BasePeak:306.10(26706)
BG Mode:Calc. from Peak Group 1 - Event 1 Scan

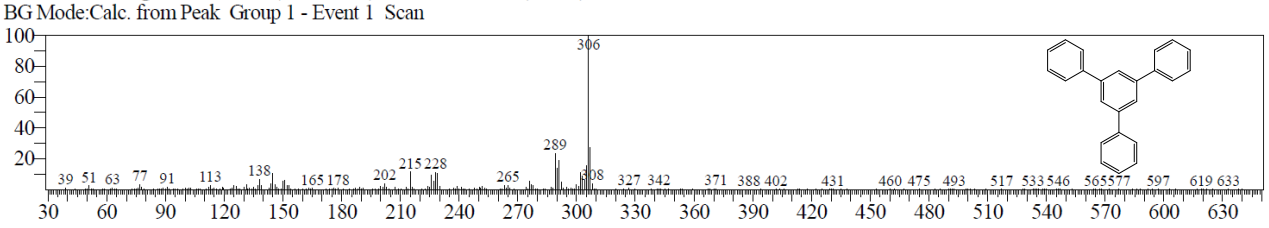

Line#:10 R.Time:10.600(Scan#:1781) MassPeaks:381
RawMode:Averaged 10.595-10.605(1780-1782) BasePeak:306.10(11656)
BG Mode:Calc. from Peak Group 1 - Event 1 Scan

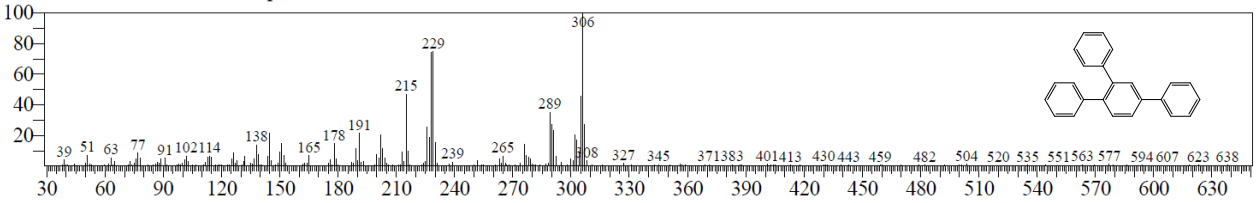

Reactivity with phenylacetylene and Na_2CO_3 in catalytically relevant conditions

Table S4. IR and ^{1}H NMR analyses of the solids obtained from the mixtures of selected [$RuCl_2$(CNR)(η^6-arene)] complexes (arene = *p*-cymene, **1**, C_6H_6, **2**, C_6Me_6, **3**; R = Cy, **b**, Xyl, **f**), Na_2CO_3, PhCCH (1:1:10 molar ratio) in MeCN at 80 °C for 2 h.

Starting material	IR (CH_2Cl_2):[a] ũ/cm^{-1} and assignment	^{1}H NMR ($CDCl_3$): identified species [b]
1b	2192s-sh (**1b**); 2173s, 2147s (Ru-CNCy); 2100m-sh (Ru-CCPh); 1966s, 1949s (Ru-CO)	**1b** (50 %) as the only Ru(*p*-cymene) complex, *p*-cymene (50 %) PhC(H)=C(H)-C≡CPh (*E*/*Z* ratio: 6)
1f	2158s-sh (**1f**), 2120-2110s-br (Ru-CNXyl); 2079s-sh (Ru-CCPh); 2017w, 1972m, 1955m (Ru-CO)	**1f** (30 %), **1f-X** (14 %), *p*-cymene (56 %) PhC(H)=C(H)-C≡CPh (*E*/*Z* ratio: 6.7)
2b	2174sh (**2b**); 2160s, 2097m (**4b**); 1967w-br (Ru-CO)	**2b** (24 %), **4b** (63 %), C_6Me_6 (13 %) PhC(H)=C(H)-C≡CPh (*E*/*Z* ratio: 3.6)
2f	2140s (**2f**); ≈ 2150-sh, 2101w-sh (**4b**); 1994-1974w-br (Ru-CO)	**2f** (79 %), **4f** (14 %), C_6Me_6 (7 %) PhC(H)=C(H)-C≡CPh (*E*/*Z* ratio: 2)
3b	2161s-sh, 2143s-br, 2119s-sh (Ru-CNCy); 2088m-sh (Ru-CCPh); 1951m-br (Ru-CO)	No trace of **3b** or any other benzene species PhC(H)=C(H)-C≡CPh (*E*/*Z* ratio: 6.6)
3f	2128s-sh (Ru-CNXyl), 2097s, 2079s (Ru-CCPh); 2016w, 1957w-br (Ru-CO)	No trace of **3f** or any other benzene species PhC(H)=C(H)-C≡CPh (*E*/*Z* ratio: 4.4)

[a] In each case there is agreement between the IR spectrum of the final solution (MeCN) and that recorded after volatiles removal under vacuum and re-dissolution in CH_2Cl_2. [b] The percentage amount refers only to arene (*p*-cymene, hexamethylbenzene) species.

PhC(H)=C(H)-C≡CPh. ^{1}H NMR ($CDCl_3$): δ/ppm = 7.05, 6.39 (d, $^3J_{HH}$ = 16 Hz) for the *E* isomer; 6.69, 5.93 (d, $^3J_{HH}$ = 12 Hz) for the *Z* isomer.

***p*-cymene**. ^{1}H NMR ($CDCl_3$): δ/ppm = 7.14 (d, *J* = 8.5 Hz, 2H), 7.12 (d, *J* = 8.5 Hz, 2H), 2.89 (hept, *J* = 6.9 Hz, 1H), 2.33 (s, 3H), 1.25 (d, *J* = 6.9 Hz, 6H).

C_6Me_6. ^{1}H NMR ($CDCl_3$): δ/ppm = 2.23 (s).

1f-X, unknown Ru(*p*-cymene)(CNXyl) species. ^{1}H NMR ($CDCl_3$): δ/ppm = 5.35 (d, *J* = 6.1 Hz, 1H), 5.32 (d, *J* = 5.9 Hz, 1H), 5.13 (d, *J* = 5.8 Hz, 1H), 2.77 (m, *J* = 6.9 Hz, 1H), 2.50 (s, 6H), 2.40 (s, 3H), 1.24 (d, *J* = 6.9 Hz, 3H), 1.18 (d, *J* = 6.9 Hz, 3H).

Figure S76. Solvent-subtracted IR spectra (CH_2Cl_2, 1800-2300 cm^{-1}) of **1b** (orange line) and the solid obtained from the reaction of **1b**, Na_2CO_3, PhCCH (1:1:10 molar ratio) in MeCN at 80 °C for 2 h (green line).

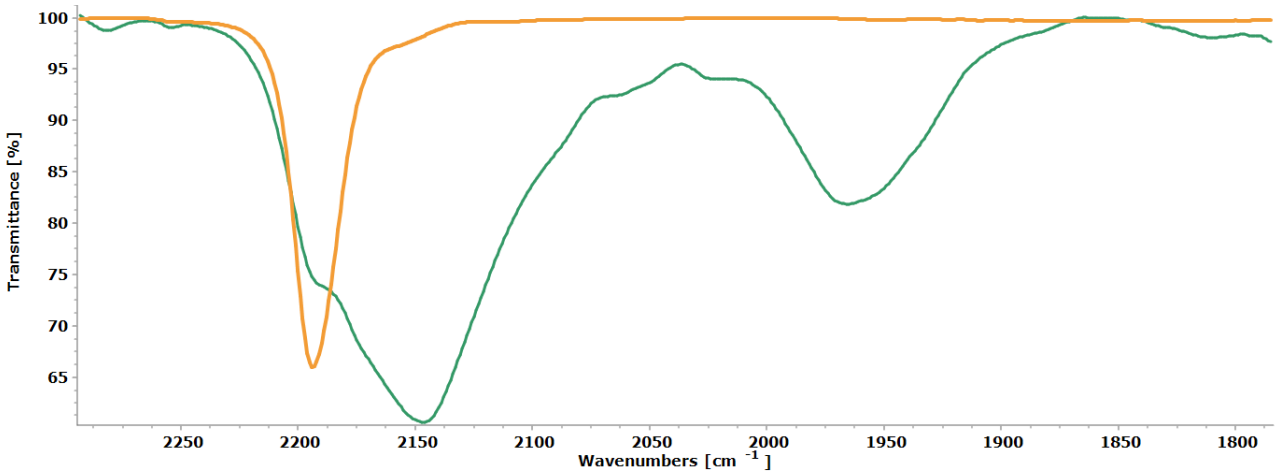

Figure S77. Solvent-subtracted IR spectra (CH_2Cl_2, 1750-2250 cm^{-1}) of **1f** (orange line) and the solid obtained from the reaction of **1f**, Na_2CO_3, PhCCH (1:1:10 molar ratio) in MeCN at 80 °C for 2 h (green line).

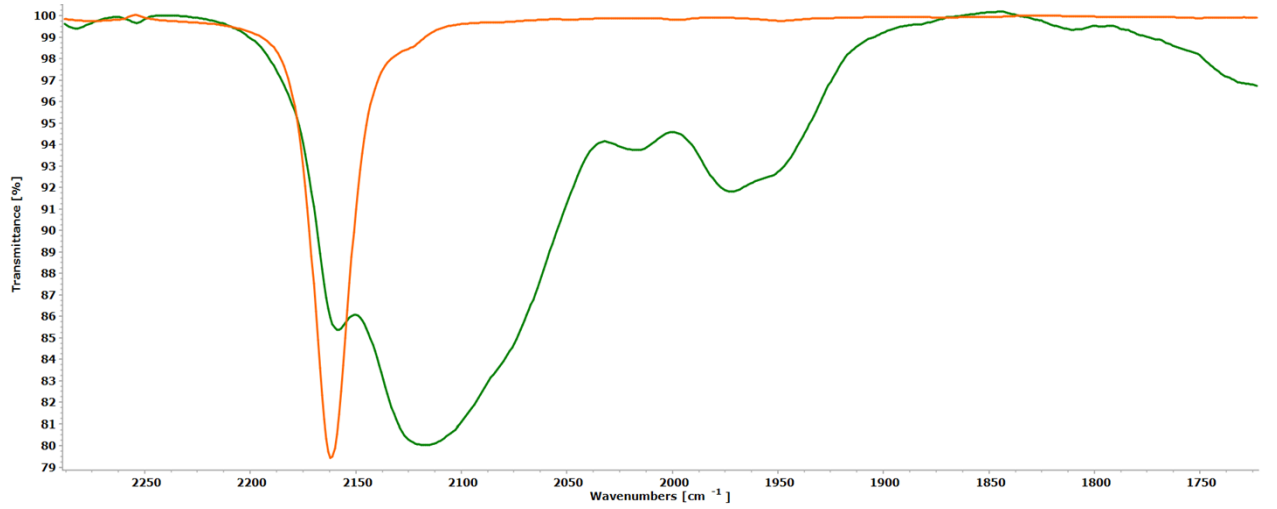

Figure S78. Solvent-subtracted IR spectra (CH_2Cl_2, 1800-2300 cm^{-1}) of **2b** (yellow line), **4b** (red line) and the solid obtained from the reaction of **2b**, Na_2CO_3, PhCCH (1:1:10 molar ratio) in MeCN at 80 °C for 2 h (green line).

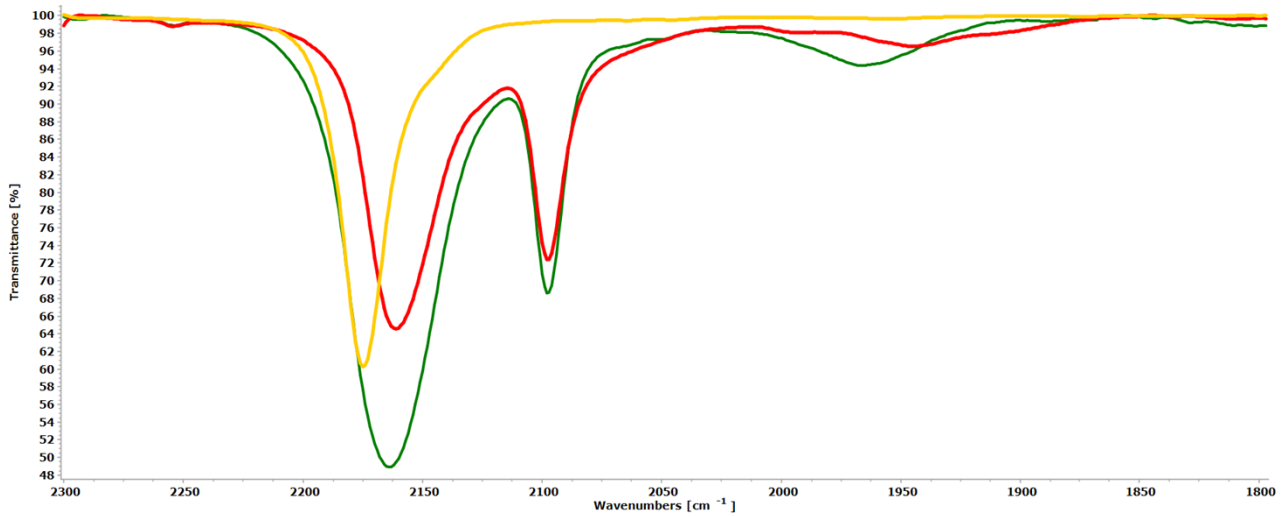

Figure S79. Solvent-subtracted IR spectra (CH_2Cl_2, 1800-2250 cm^{-1}) of **2f** (yellow line), **4f** (red line) and the solid obtained from the reaction of **2f**, Na_2CO_3, PhCCH (1:1:10 molar ratio) in MeCN at 80 °C for 2 h (green line).

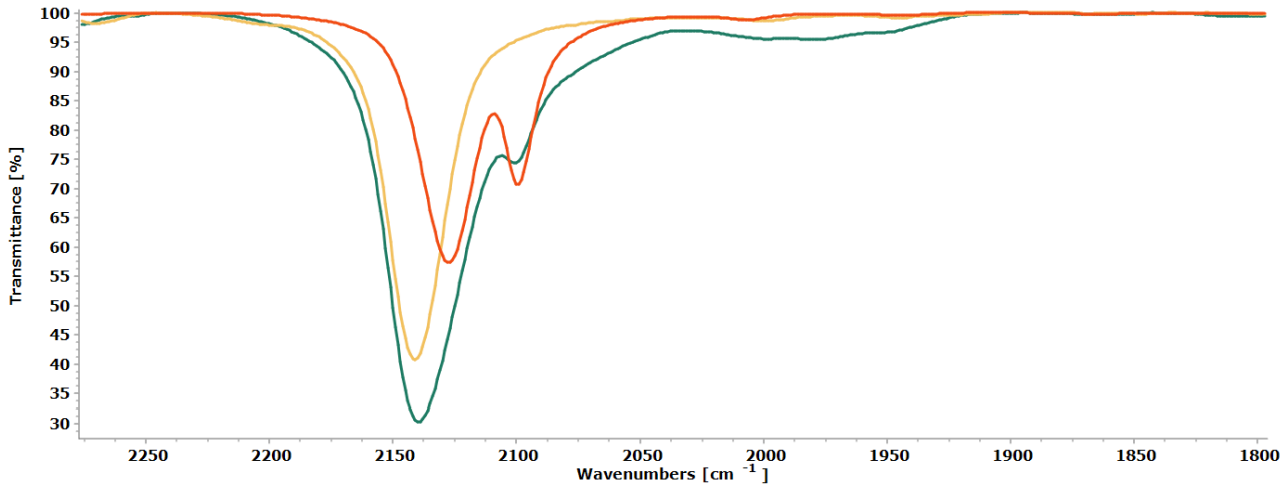

Figure S80. Solvent-subtracted IR spectra (CH_2Cl_2, 1850-2300 cm^{-1}) of **3b** (orange line) and the solid obtained from the reaction of **3b**, Na_2CO_3, PhCCH (1:1:10 molar ratio) in MeCN at 80 °C for 2 h (green line).

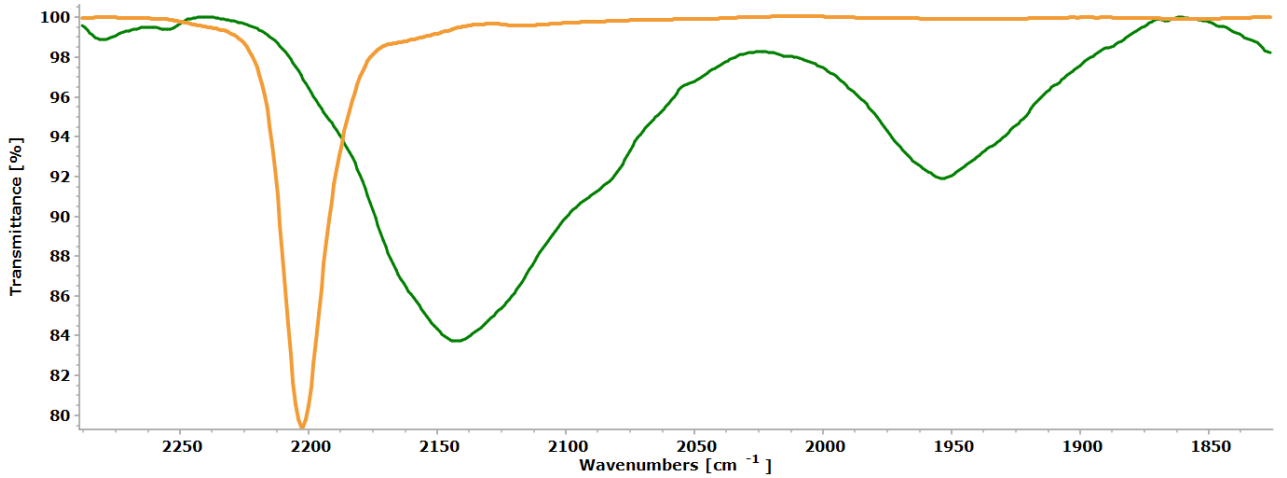

Figure S81. Solvent-subtracted IR spectra (CH_2Cl_2, 1850-2300 cm^{-1}) of **3f** (orange line) and the solid obtained from the reaction of **3f**, Na_2CO_3, PhCCH (1:1:10 molar ratio) in MeCN at 80 °C for 2 h (green line).

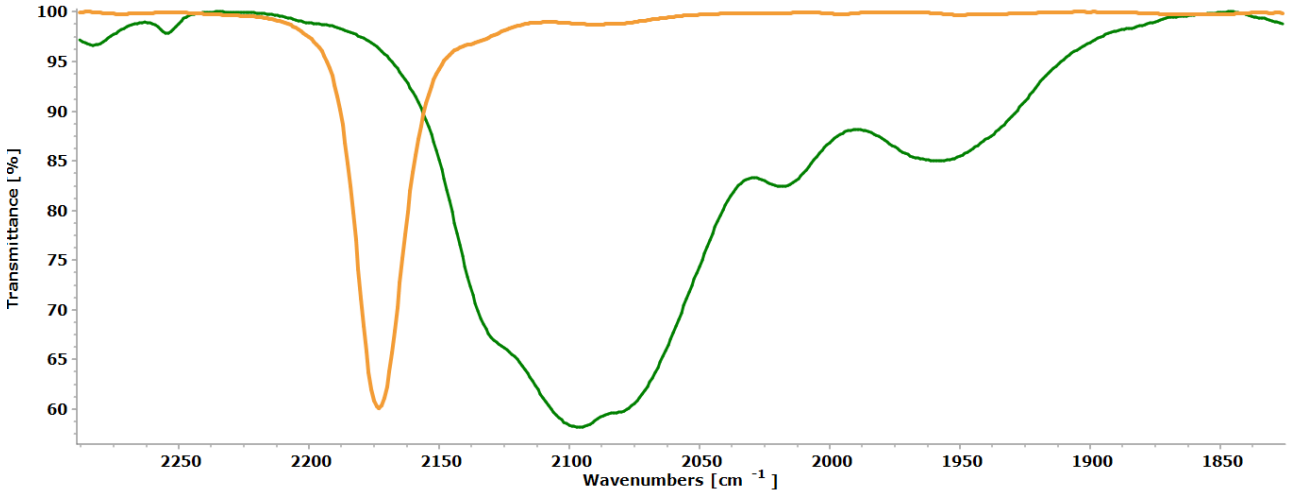

Figure S82. Solvent-subtracted IR spectra (CH_2Cl_2, 1850-2275 cm^{-1}) of aliquots of the reaction of **1b**, Na_2CO_3, PhCCH (1:10:100 molar ratio) in MeCN at 55 °C at different times, normalized for the intensity at 2180 cm^{-1}. Colour gradient: red (initial spectrum) to yellow to green to blue (final spectrum). The absorption at 2254 cm^{-1} is due to PhCCH. Below: difference spectrum with respect to **1b** (red line).

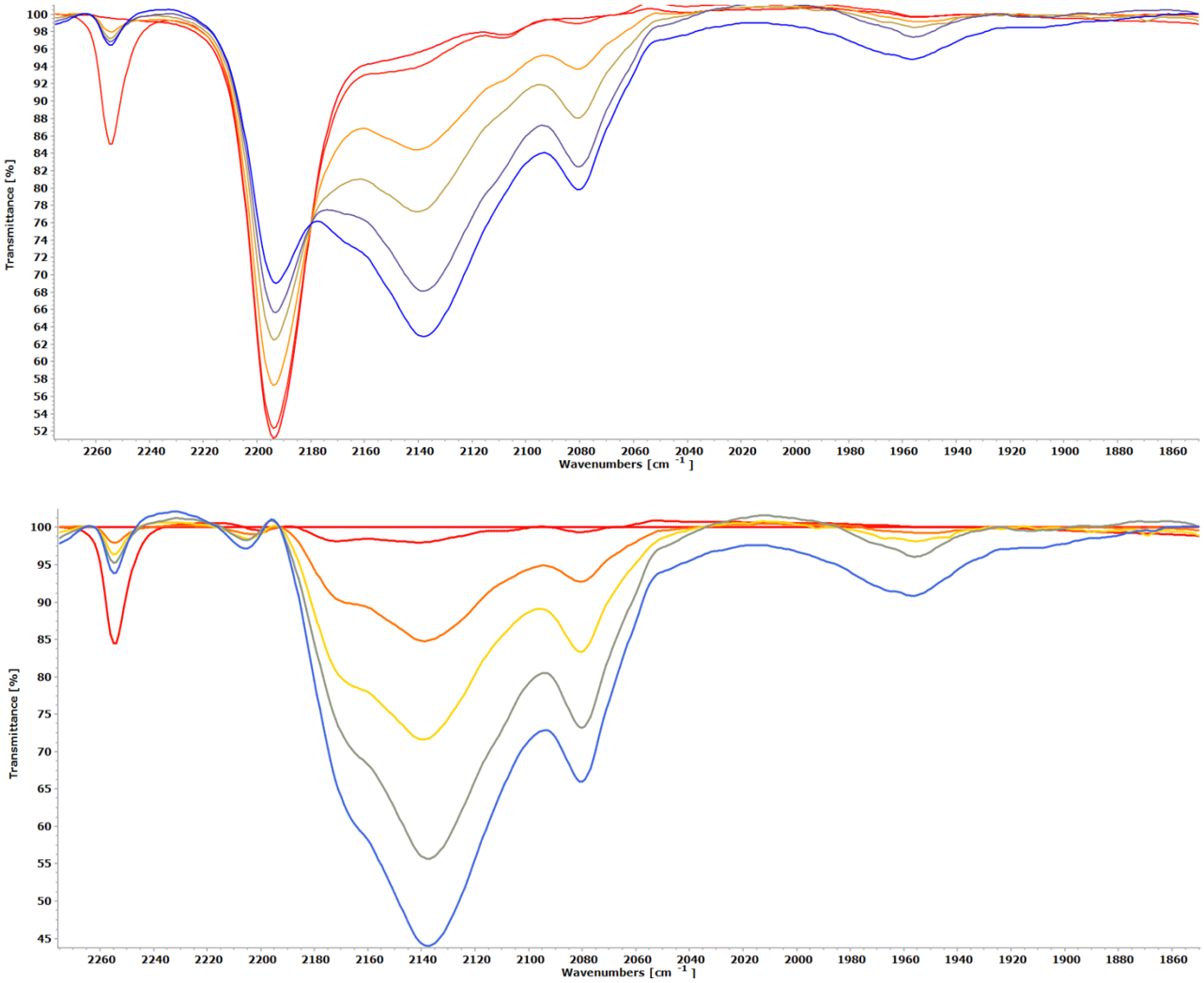

Table S5. IR analysis of aliquots of the reaction of **1b**, Na_2CO_3 and PhCCH (1:10:100 molar ratio) in MeCN at 55 °C at different times (Figure S82). Colour shade qualitatively reflects the relative intensity of the associated IR band(s). *NMR and MS analyses performed at this time-point.

IR band / cm^{-1}	Assignment	Reaction time (hours)						
		0	0.5	1.5	2.5	3.5	4.5	5.5 *
2193	**1b**							
2167sh, 2139 ≈ 2120sh	Ru-C≡N-Cy							
2080	Ru-C≡C-Ph							
≈ 1956	Ru-C≡O							

$^{1}H/^{13}C$ NMR ($CDCl_3$): δ/ppm = 5.57(d), 5.40(d), 2.29(m)/87-107, 1.28(d)/22-31-107 for **1b**; 3.94(m) for another unidentified CyNC complex; 2.52(m), 2.39(s), 0.85(m) for other unidentified species.

ESI-MS (MeOH, base peak of main clusters): m/z = 415.043 for **1b**; 438.037; 461.148; 505.170; 557.141; 643.193, 745.241, 847.285, 949.335 for Ru(*p*-cymene)$(PhCCH)_x$ species.

Figure S83. Solvent-subtracted IR spectra (CH_2Cl_2, 1850-2275 cm^{-1}) of aliquots of the reaction of **1b**, Na_2CO_3, PhCCH (1:10:100 molar ratio) in MeCN at 80 °C at different times, normalized for the intensity at 2175 cm^{-1}. Colour gradient: red (initial spectrum) to orange to green to blue (final spectrum). The absorption at 2254 cm^{-1} is due to PhCCH.

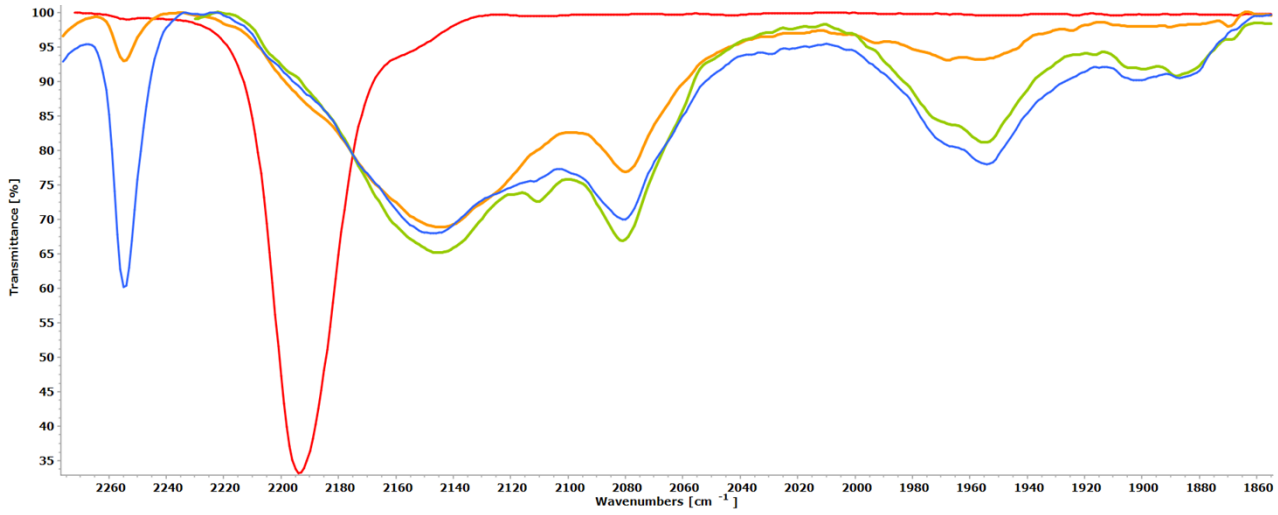

Table S6. IR analysis of aliquots of the reaction of **1b**, Na_2CO_3 and PhCCH (1:10:100 molar ratio) in MeCN at 80 °C at different times (Figure S83). Colour shade qualitatively reflects the relative intensity of the associated IR band(s). *NMR and MS analyses performed at this time-point.

IR band / cm^{-1}	Assignment	Reaction time (hours)			
		0	1	3	4 *
2193	**1b**				
≈ 2165sh, 2144 2080	Ru-C≡N-Cy Ru-C≡C-Ph				
1969 1955	Ru-C≡O				

^{1}H NMR ($CDCl_3$): neither **1b** nor other *p*-cymene complex is present in the mixture.

Figure S84. Solvent-subtracted IR spectra (CH_2Cl_2, 1850-2300 cm^{-1}) of aliquots of the reaction of **2b**, PhCCH, Na_2CO_3 (1:10:100 molar ratio) in MeCN at 60 °C at different times, normalized for the intensity at 2160 cm^{-1} (isocyanide stretching band of **4b**). Colour gradient: red (initial spectrum) to yellow to green to blue (final spectrum).

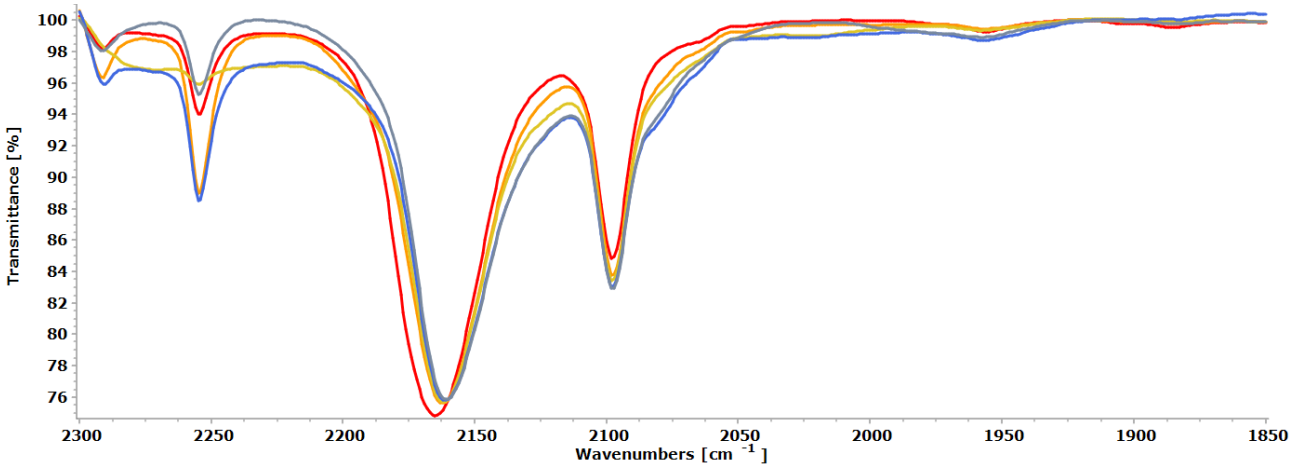

Table S7. IR analysis aliquots of the mixture of **2b**, Na_2CO_3, PhCCH (1:10:100 molar ratio) in MeCN at 60 °C at different times (Figure S84). Colour shade qualitatively reflects the relative intensity of the associated IR band(s). *NMR analyses performed at this time-point.

IR band / cm^{-1}	Assignment	Reaction time (hours)					
		0	4	6	8	10	12 *
2174	**2b**			-	-	-	
2161, 2097	**4b**						
2080sh	Ru-C≡C-Ph						
1954	Ru-C≡O				?		

$^{1}H/^{13}C$ NMR ($CDCl_3$): δ/ppm = 3.91, 2.17/102 ppm for **4b**; 2.23/133 for C_6Me_6; 2.20, 2.01 for other unknown species.

Figure S85. Solvent-subtracted IR spectra (CH_2Cl_2, 1850-2250 cm^{-1}) of aliquots of the reaction of **2b**, Na_2CO_3 and PhCCH (1:10:100 molar ratio) in MeCN at 80 °C at different times, normalized for the intensity at 2160 cm^{-1} (isocyanide stretching band of **4b**). Colour gradient: red (initial spectrum) to yellow to green to blue (final spectrum). Below: difference spectrum with respect to **4b** (dashed purple line).

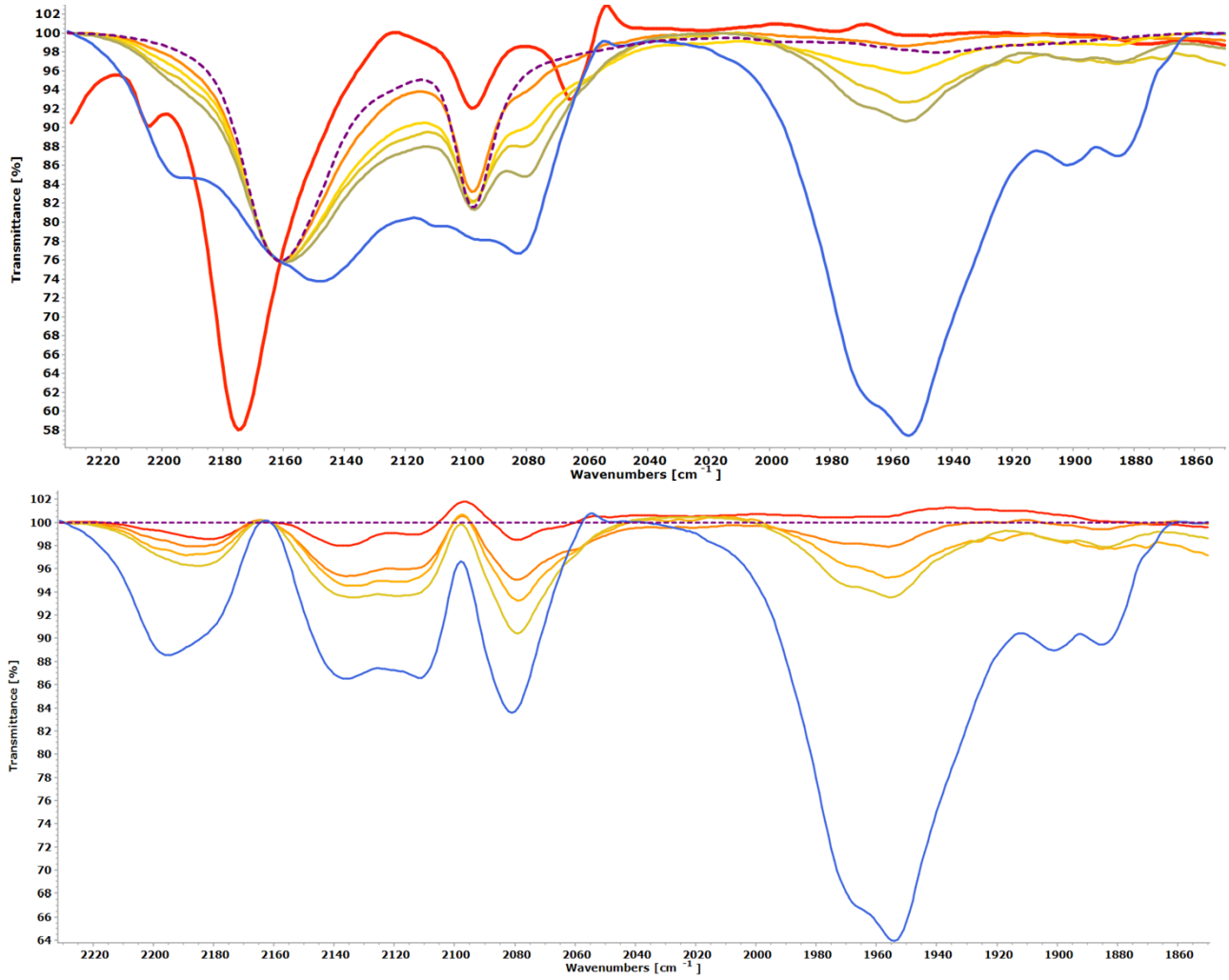

Table S8. IR analysis of aliquots of the reaction of **2b**, Na_2CO_3 and PhCCH (1:10:100 molar ratio) in MeCN at 80 °C at different times (Figure S85). Colour shade qualitatively reflects the relative intensity of the associated IR band(s). *NMR analyses performed at this time-point.

IR band / cm^{-1}	Assignment	Reaction time (hours)					
		0	1.5	3	4.5	6	7.5 *
2174	**2b**		-	-	-	-	
2161, 2097	**4b**						
2195, 2181 2137, ≈ 2120	C-C≡C-Ph ? Ru-C≡N-Cy						
2111, 2080	Ru-C≡C-Ph						
1968, 1954	Ru-C≡O						

$^{1}H/^{13}C$ NMR ($CDCl_3$): δ/ppm = 3.92, 2.17/102 ppm for **4b**; 2.23 for C_6Me_6; 2.62, 2.13 for other unknown species.

Figure S86. Solvent-subtracted IR spectra (CH_2Cl_2, 1850-2250 cm^{-1}) of aliquots of the reaction of **2f**, Na_2CO_3 and PhCCH (1:10:100 molar ratio) in MeCN at 80 °C at different times, normalized for the intensity at 2127 cm^{-1} (isocyanide stretching band of **4f**). Colour gradient: red (initial spectrum) to orange to olive green to blue (final spectrum). Below: difference spectrum with respect to **4f** (dashed purple line).

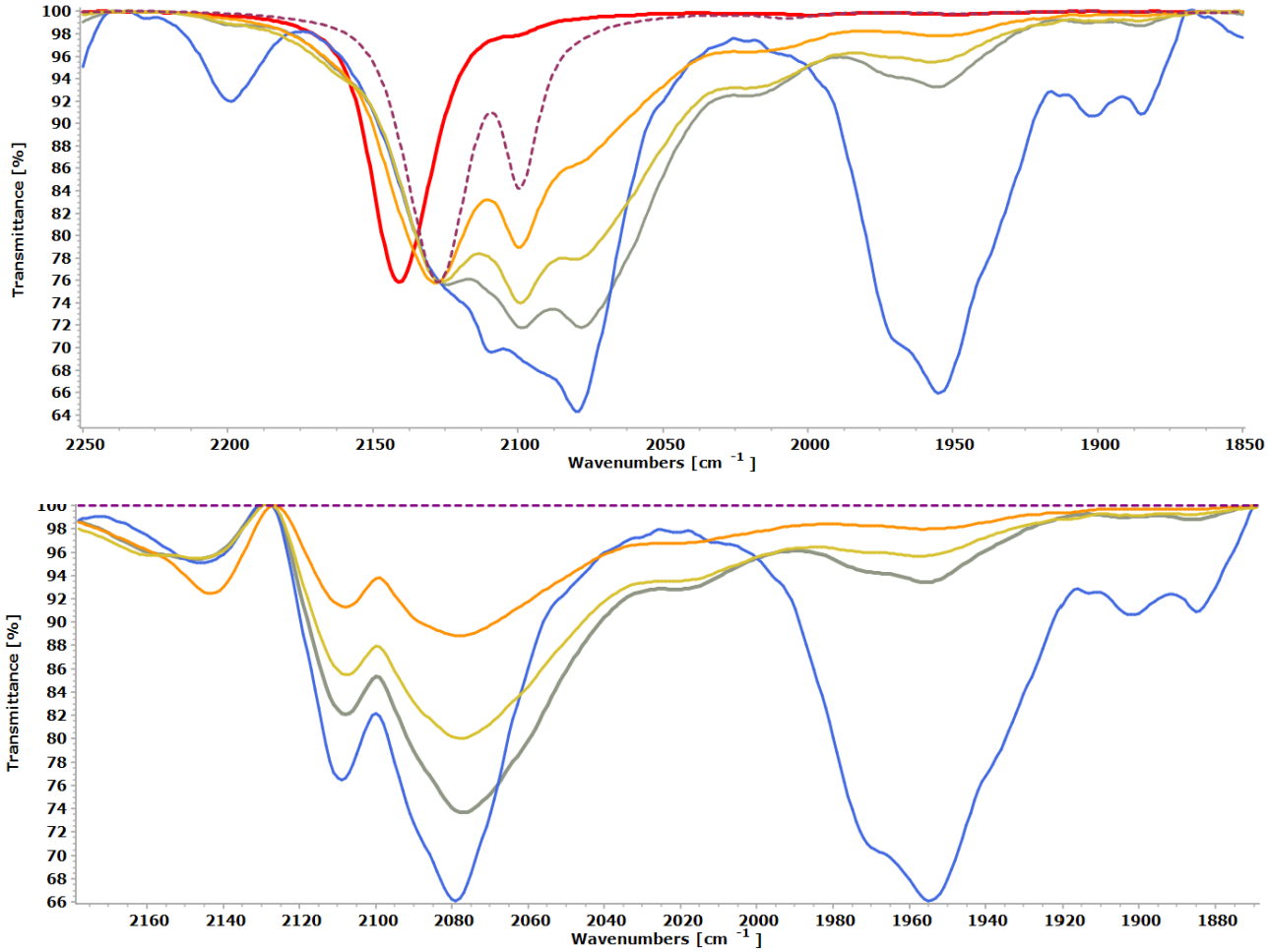

Table S9. IR analysis of aliquots of the reaction of **2f**, Na_2CO_3, PhCCH (1:10:100 molar ratio) in MeCN at 80 °C at different times (Figure S86). Colour shade qualitatively reflects the relative intensity of the associated IR band(s). *NMR and MS analyses performed at this time-point.

IR band / cm^{-1}	Assignment	Reaction time (hours)				
		0	1.5	3.0 *	4.5	22
2140	**2f**		*sh*			
2128, 2100	**4f**					
2108 2089sh 2078	Ru-C≡N(Xyl) Ru-C≡C-Ph Ru-C≡C-Ph					
2199	C-C≡C-Ph ?		-	-	-	
1954 1971	Ru-C≡O					

$^{1}H/^{13}C$ NMR ($CDCl_3$): δ/ppm = 2.49/128,129,136, 2.24/104 for **4f**; 2.23/136 for C_6Me_6; 2.07/97.5, 1.92/98, 1.89/102, 1.84/97, 1.81/94, 1.75/97, 1.73/106, 1.66/107, 1.52/104, 1.47/104 for unknown Ru(C_6Me_6) complexes; 2.35/129.6,138.8 for unknown Xyl species; 3.07, 2.00 for other species. ESI-MS (MeOH, base peak of main clusters): m/z = 408.102 for a {RuCl(MeCN)$_2$} species; 474.172 for a {Ru(MeCN)$_2$(PhCC)} species; 532.131 for **4f**; 1041.280 (Ru_1Cl_1+PhCCH species).

Figure S87. Solvent-subtracted and intensity-normalized IR spectra (CH_2Cl_2, 1300-2500 cm^{-1}) of aliquots of the freshly prepared mixture of **1b** and Na_2CO_3 (1:10 mol. ratio) in MeCN (blue line) and after 2 h at 55 °C (orange line), showing the probable formation of a {Ru(CNCy)(CO_3)} complex (2145m-sh, 1450s-br).

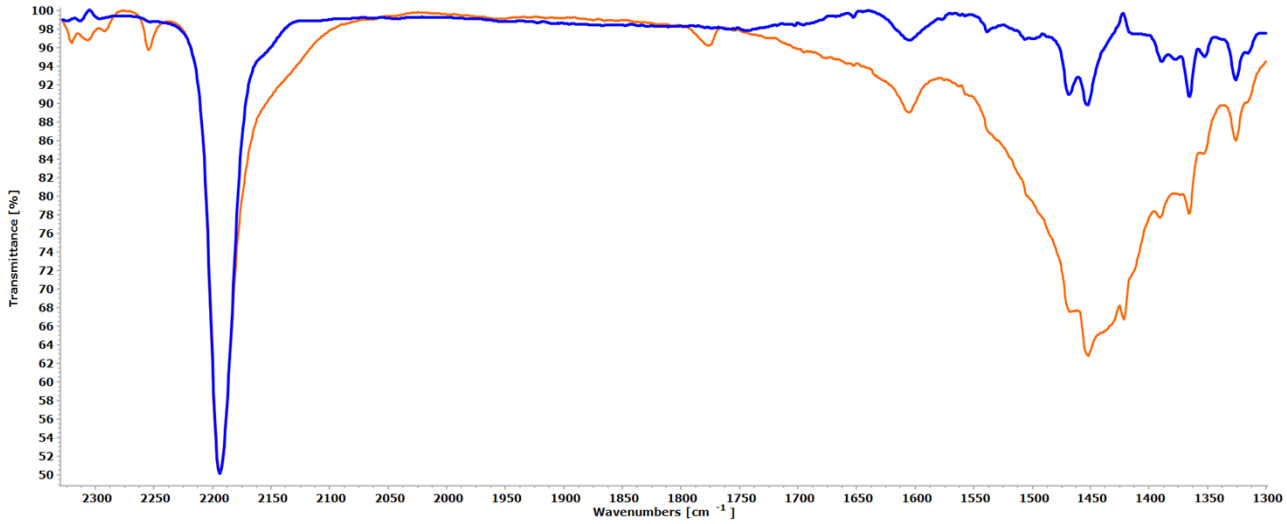

Figure S88. Solvent-subtracted and intensity-normalized IR spectra (CH_2Cl_2, 1300-2400 cm^{-1}) of aliquots of the freshly prepared mixture of **2b** and Na_2CO_3 (1:10 mol. ratio) in MeCN (blue line), after 2.5 h at 80 °C (orange line) and after 7 h at 80 °C (green line). The last spectrum shows the probable formation of a {Ru(CNCy)(CO_3)} complex (2145m-sh, 1436s-br) and Ru-carbonyl species (1960-1940w-br).

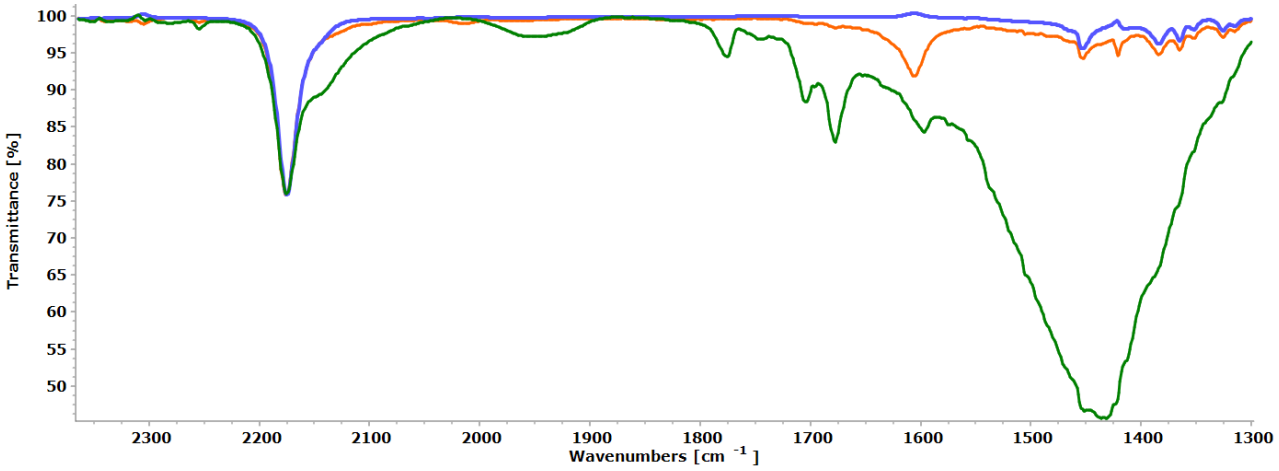

Figure S89. Solvent-subtracted and intensity-normalized IR spectra (CH_2Cl_2, 1300-2600 cm^{-1}) of aliquots of the freshly prepared mixture of **2f** and Na_2CO_3 (1:10 mol. ratio) in MeCN (blue line) and after 3 h at 80 °C (orange line).

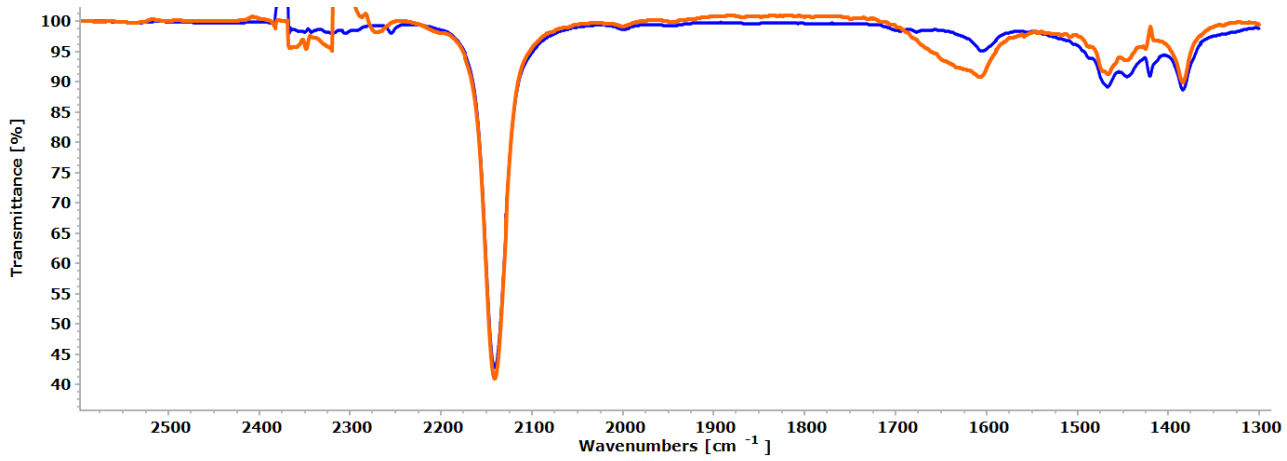

Figure S90. Solvent-subtracted IR spectra (CH_2Cl_2, 1850-2275 cm^{-1}) of aliquots of the reaction of **1b**, Na_2CO_3, PhCCH (1:10:100 molar ratio) in EtOH at 80 °C at different times, normalized for the intensity at 2180 cm^{-1}. Colour gradient: red (initial spectrum) to yellow to orange to blue (final spectrum). The dotted green line corresponds to the reaction profile for the same reacting mixture in MeCN after 4 h.

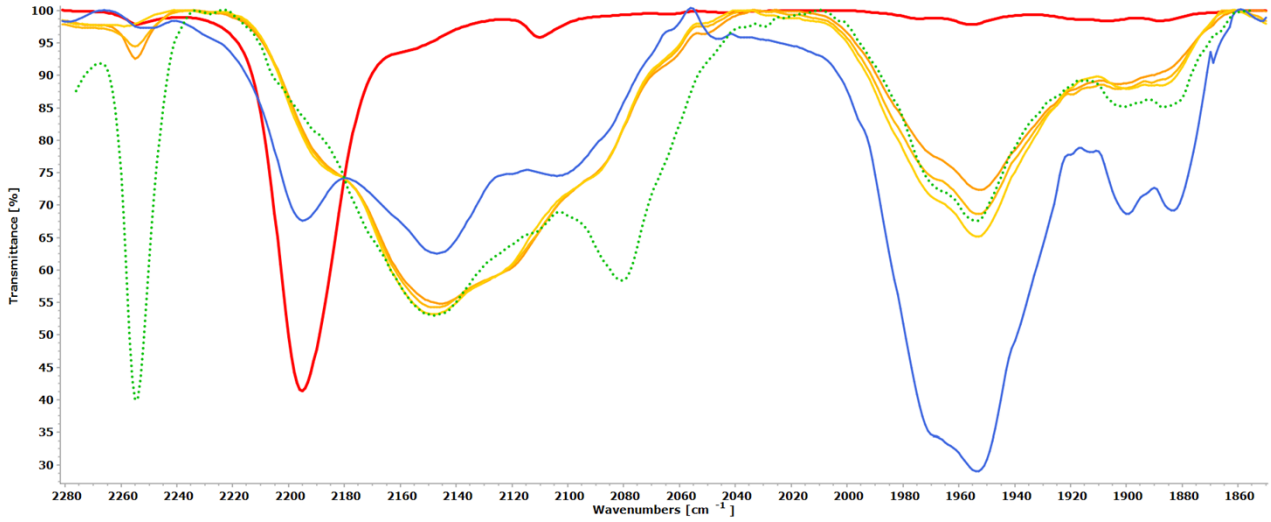

Table S10. IR analysis of aliquots of the reaction of **1b**, Na_2CO_3 and PhCCH (1:10:100 molar ratio) in EtOH at 80 °C at different times (Figure S90). Colour shade qualitatively reflects the relative intensity of the associated IR band(s).

IR band / cm^{-1}	Assignment	Reaction time (hours)				
		0	2	4	6	24
2193	**1b**		?	?	?	
2120	Ru-C≡N-Cy					
2150 2090	Ru-C≡N-Cy Ru-C≡C-Ph					
1970 1953	Ru-C≡O					
2195	Ru-C≡N-Cy					

Figure S91. Solvent-subtracted IR spectra (CH_2Cl_2, 1850-2250 cm^{-1}) normalized for the intensity at 2180 cm^{-1} of **1b** (red line), the organic-soluble species recovered from the reaction of **1b**, Na_2CO_3 and PhCCH (1:10:100 molar ratio) in water/mesitylene after 1 h at 55 °C (yellow line), after 2 h at 55 °C (green line) or after 1.5 h at room temperature (blue line). The corresponding spectra of the species recovered from the aqueous solution is represented by the dotted lines.

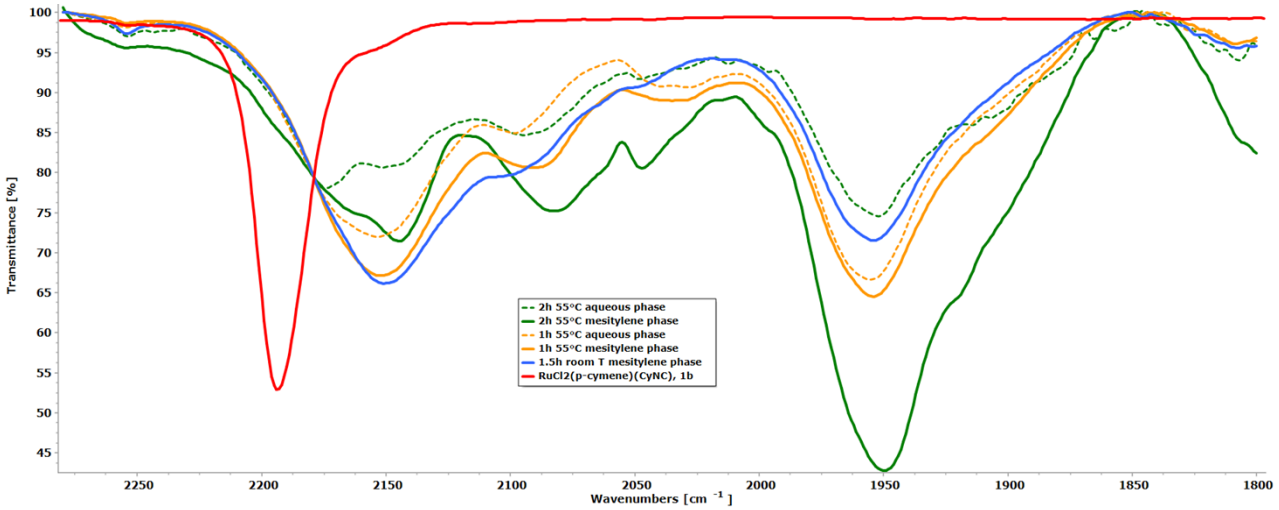

Figure S92. Solvent-subtracted IR spectra (CH_2Cl_2, 1850-2250 cm^{-1}) of the organic-soluble species recovered from the reaction of **2f**, Na_2CO_3 and PhCCH (1:10:100 molar ratio) in water/mesitylene at 80 °C at different times, normalized for the intensity of the isocyanide band at 2130-2140 cm^{-1}. Colour gradient: red (initial spectrum) to yellow to blue (final spectrum). The dotted yellow line is the IR spectrum (CH_2Cl_2) of the fraction recovered from the aqueous phase. The dashed purple line is the spectrum of **4f**.

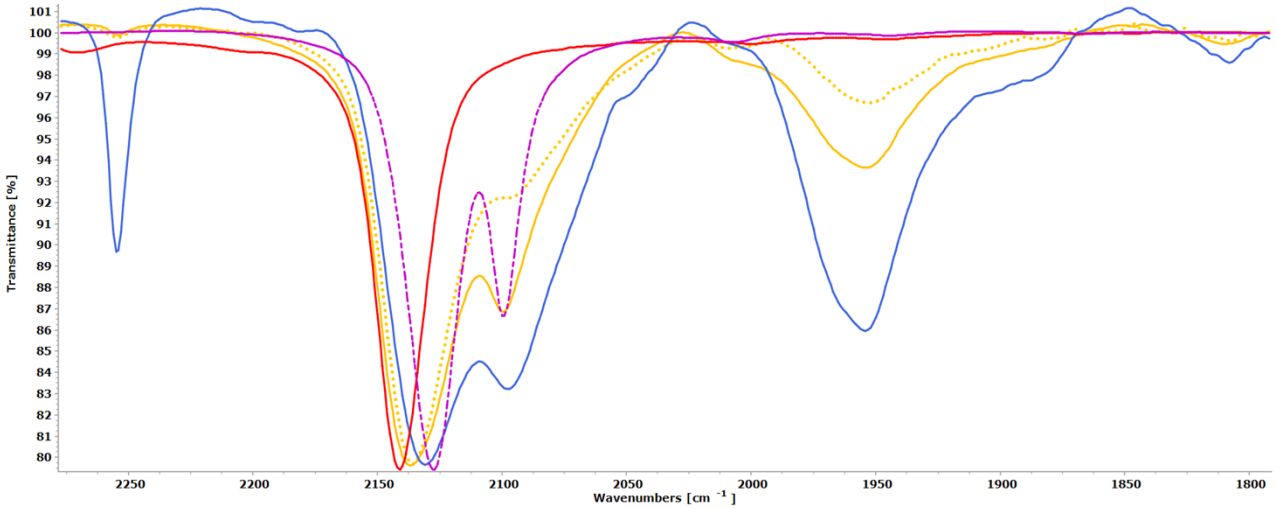

Table S11. IR analysis of the mesitylene-soluble species recovered from the reaction of **2f**, Na_2CO_3, PhCCH (1:10:100 molar ratio) in water/mesitylene at 80 °C after different times (Figure S89). Colour shade qualitatively reflects the relative intensity of the associated IR band(s).

IR band / cm^{-1}	Assignment	Reaction time (hours)		
		0	1	3
2140	**2f**			
2130, 2097	**4f**			
1969sh 1955	Ru-C≡O			

References

1 (a) T. Arthur, T. A. Stephenson, T. A., Synthesis of triple halide-bridged arene complexes of ruthenium(II) and osmium(II), *J. Organomet. Chem*. **1981**, 208, 369-87; (b) Y.N. Vashisht Gopal, Neelima Konuru, and Anand K. Kondapi, Topoisomerase II antagonism and anticancer activity of coordinated derivatives of $[RuCl_2(C_6H_6)(dmso)]$, *Archiv. Biochem. Biophys*. **2002**, 401, 53–62 (no characterization data is reported)

2 D. R. Robertson, T. A. Stephenson, T. Arthur, Cationic, neutral and anionic complexes of ruthenium(II) containing η6-arene ligands, *J. Organomet. Chem*. **1978**, 162, 121-36

3 (a) M. Gaye, B. Demerseman, P. H. Dixneuf, (Dialkylsulfide)(arene) ruthenium(II) derivatives, J. Organomet. Chem., **1991**, 411, 263-270; (b) G. Sanchez, J. Garcia, J. Perez, G. Garcia, G. Lopez, G. Villora, Thermal study of areneruthenium(II) derivatives, *Thermochim. Acta* **1997**, 293, 153-161

4 E. Hodson, S. J. Simpson, Synthesis and characterisation of [(g6-cymene)Ru(L)X2] compounds: single crystal X-ray structure of [(η6-cymene)Ru(P{OPh}3)Cl2] at 203 K, *Polyhedron* **2004**, 23, 2695–2707

5 H. Werner, R. Werner, Die Vorstufen zur Synthese der Metall-Basen, $ArM(PR_3)_2$ und $ArM(PR_3)L$ (M = Ru, Os), *Chem. Ber.* **1982**, 115, 3766-3780.

6 K. Roder, H. Werner, Darstellung neutraler und kationischer Aren(carbony1)metall-Komplexedes Rutheniums und Osmiums mit C_6Me_6Ru und C_6H_6Os als Baueinheiten, *Chem. Ber.* **1989**, 122, 833-840

7 (a) D. A. Tocher, R. O. Gould, T. A. Stephenson, M. A. Bennett, J. P. Ennett, T. W. Matheson, L. Sawyer, V. K. Shah, Areneruthenium(II) carboxylates: reactions with ligands and the X-ray structure of the p-cymene pyrazine complex $[Ru(η\text{-}p\text{-}MeC_6H_4CHMe_2)Cl(pyz)_2]PF6$, *J. Chem. Soc., Dalton Trans*., **1983**, 1571-1581. (b) D. L. Davies, O. Al-Duaij, J. Fawcett, M. Giardiello, S. T. Hilton, D. R. Russella, Room-temperature cyclometallation of amines, imines and oxazolines with [MCl2Cp*]2 (M = Rh, Ir) and $[RuCl_2(p\text{-cymene})]_2$, *Dalton Trans*., **2003**, 4132-4138 (c) M. Melchart, A. Habtemariam, S. Parsons, S. A. Moggach, P. J. Sadler, Ruthenium(II) arene complexes containing four- and five-membered monoanionic O,O-chelate rings, *Inorg. Chim. Acta* **2006**, 359, 3020-3028

8 **2-Naphthyl isocyanide**: X. Yan, S. Zhang, P. Zhang, X. Wu, A. Liu, G. Guo, Y. Dong, X. Li, [Ph3C][B(C6F5)4]: A Highly Efficient Metal-Free Single-Component Initiator for the Helical-Sense-Selective Cationic Copolymerization of Chiral Aryl Isocyanides and Achiral Aryl Isocyanides, *Angew. Chem. Int. Ed.* **2018**, 57, 8947-8952

9 **Benzyl isocyanide**: T. M. El Dine, D. Evans, J. Rouden, J. Blanchet, Formamide Synthesis through Borinic Acid Catalysed Transamidation under Mild Conditions, *Chem. Eur. J*. **2016**, 22, 5894-5898

10 **Tert-butyl isocyanide**: N. Liu, F. Chao, M.-G. Liu, N.-Y. Huang, K. Zou, L. Wang, Odorless Isocyanide Chemistry: One-Pot Synthesis of Heterocycles via the Passerini and Postmodification Tandem Reaction Based on the in Situ Capture of Isocyanides, *J. Org. Chem.* **2019**, 84, 2366–2371.

11 **4-methoxyphenyl isocyanide**: S. Kamijo, T. Jin, Y. Yamamoto,Novel Synthetic Route to Allyl

Cyanamides: Palladium-Catalyzed Coupling of Isocyanides, Allyl Carbonate, and Trimethylsilyl Azide, *J. Am. Chem. Soc.* **2001**, 123, 38, 9453–9454

12 **Diethyl isocyanomethyl phosphonate:** C.-P. Yu, Y. Tang, L. Cha, S. Milikisiyants, T. I. Smirnova, A. I. Smirnov, Y. Guo, Wei-chen Chang, Elucidating the Reaction Pathway of Decarboxylation-Assisted Olefination Catalyzed by a Mononuclear Non-Heme Iron Enzyme, *J. Am. Chem. Soc*. **2018**, 140, 15190–15193

13 **Methyl isocyanide**. J. J. Cappon, K. D. Witters, J. Baart, P. J. E. Verdegem, A. C. Hoek, *Recueil des Travaux Chimiques des Pays-Bas*, **1994**, 113, 318-328

14 **α-methylbenzyl isocyanide**. P. Cmoch, J. Jaźwiński, NMR studies on interaction of rhodium(II) tetratrifluoroacetate with the ligands containing nitrile, isonitrile, isothiocyanate or isocyanate functional groups, *J. Mol. Struct.* **2009**, 919, 348-355

15 **Ethyl isocyanoacetate.** L. Yang, Z. Zhang, B. Cheng, Y. You, D. Wu & C. Hong, Two tandem multicomponent reactions for the synthesis of sequence-defined polymers, *Science China Chemistry* **2015**, 58, 1734–1740

16 L. Biancalana, N. Di Fidio, D. Licursi, S. Zacchini, A. Cinci, A. M. Raspolli Galletti, F. Marchetti, C. Antonetti, New ruthenium(II) isocyanide catalysts for the transfer hydrogenation of ethyl levulinate to γ-valerolactone in C2-C6 alcohols, *J. Catal*. **2024**, 439, 115761

17 R. Dussel, D. Pilette, P. H. Dixneuf, W. P. Fehlhammer, Isocyanide arene-ruthenium(II) complexes and activation of alkenylacetylenes: synthesis and characterization of isocyanide carbene- and mixed carbene-ruthenium compounds, *Organometallics* **1991**, 10, 3287-3291.

18 A. P. Walsh, W. W. Brennessel, J. D. Jones, Synthesis and characterization of a series of rhodium, iridium, and ruthenium isocyanide complexes, *Inorg. Chim. Acta* **2013**, 407, 131-138.